TÉCNICO LISBOA

Prediction and Simulation of Trajectories of Drifting Objects off the Coast of Portugal

José Correia Pires Pinto Gago

Thesis to obtain the Master of Science Degree in

Naval Architecture and Ocean Engineering

Supervisor: Prof. Ângelo Manuel Palos Teixeira

Examination Committee

Chairperson: Prof. Carlos Guedes Soares

Supervisor: Prof. Ângelo Palos Teixeira

Member of the Committee: Prof. Roberto Vettor

September 2018

Acknowledgements

I would like to thank everyone that directly or indirectly took part of this milestone of my academic life, in particular to:

- Professor Ângelo Manuel Palos Teixeira of the *Instituto Superior Técnico*, *Universidade de Lisboa*, for accepting to be my advisor and for let me work on a very interesting subject for me. He allowed me to have freedom to work on my own but stepped on whenever he felt I needed and was always available to give me an advice in case I had some obstacle in the development of the dissertation;

- the researcher Knut-Frode Dagestad of the *Research and Development* Department at the *Norwegian Meteorological Institute*, for the time he spent helping me to fully understand the capabilities of the Opendrift software developed by Knut-Frode himself, and for the kindness he revealed when answering all my questions;

- Comandante José António Velho Gouveia, director of *Instituto de Socorros a Náufragos*, for meeting me and dispensing some of his precious time to give me an inside view of the structure behind the search and rescue operations in Portuguese waters and for helping me understand the *Instituto de Socorros a Náufragos* role in that structure;

- my parents for everything they invested in my education, giving me everything I needed to succeed and for their patience dealing with me, even though I know sometimes it was a hard task;

- my brother and sister for being the best role models I could possibly get in my life and for always having the right advices to give me when I needed the most;

- Joana for being there for me every day to help me never give up no matter how big the obstacle in my path was. With her it feels like everything is possible;

- my University colleagues for making this journey meaningful not only inside the campus but specially outside. Not only to the ones that started this adventure with me but also to the ones that made this objective possible. They made this cycle very enlightening for me both professionally and personally;

- my roller hockey team mates and staff over the years in Parede Foot-ball Clube, for understanding that some days it was hard for me to be completely focused on our team goals and for making me believe I can always do better.

Resumo

O objetivo desta dissertação é desenvolver uma ferramenta de previsão e simulação da trajetória de objetos à deriva para apoio às operações de busca e salvamento e comparar os resultados com programas existentes. Inicialmente descrevem-se as operações de Busca e Salvamento em águas Portuguesas, assim como a Legislação nacional e internacional em vigor. Apresenta-se a formulação de modelos de deriva simples para diferentes tipos de objetos. São identificados e descritos dois exemplos de programas utilizados atualmente na previsão da localização de objetos à deriva. Descrevem-se os principais tipos de padrões de busca utilizados no mar e suas vantagens e desvantagens. Apresenta-se a ferramenta desenvolvida para a previsão e simulação da deriva de diferentes tipos de objetos sob a ação do vento e da corrente marítima, tendo em conta as incertezas associadas ao processo utilizando Simulação de Monte Carlo. Quatro cenários diferentes são analisados e comparados com as previsões do software *Opendrift* e com formulações empíricas. Os resultados das simulações mostram-se coerentes com o os obtidos pela ferramenta de comparação, validando assim o modelo desenvolvido. Por fim, é adotado um modelo Gaussiano misto bivariado (Gaussian Mixture Model) para a modelação probabilística da localização final do objeto calculada usando a ferramenta desenvolvida e simulação de Monte Carlo. Este modelo probabilístico é então usado para definir a área de procura correspondente a uma probabilidade de 95% de contenção do objeto para cada cenário. É efetuada uma comparação entre diferentes cenários e entre três objetos diferentes ao largo da costa de Portugal.

Palavras Chave: Busca e Salvamento; Dinâmica de Deriva; Simulação de Monte Carlo; Previsão da Trajetória de Objetos à Deriva; Modelação Probabilística.

Abstract

The objective of this dissertation is to develop a tool to predict and simulate the drift of objects at sea to support Search and Rescue operations and compare it with existing software. First the Maritime Search and Rescue operations in Portuguese waters as well as the related National and International Legislation are described. A summary of the formulations associated with basic drifting models is provided according to the type of floating object. Some examples of tools used nowadays for object location prediction at sea are introduced and explained. The most common types of search patterns used are described as well as their vantages and disadvantages. A tool is developed to predict and simulate the trajectory of objects due to the effect of wind and current and taking into account the uncertainties in the process using Monte Carlo Simulation. Four different scenarios are analyzed and compared with the predictions of the *Opendrift* software and with empirical formulations. The simulation results are in line with the ones obtained by the comparing tool, making a good statement for the developed tool reliability. A bivariate Gaussian Mixture Model is adopted for probabilistic modeling of object final locations calculated using the developed tool and by Monte Carlo Simulation. This probability model is then used to define the area corresponding to a 95% probability of object containment for every scenario. A comparison between different scenarios and between three different objects off the Coast of Portugal is carried out.

Keywords: Search and Rescue; Drifting Dynamics; Leeway; Monte Carlo Simulation; Trajectory Prediction of Drifting Objects; Probabilistic Modeling.

List of Contents

List of Figures

List of Acronyms

- AGCS – Allianz Global Corporate & Specialty
- AI – Accident Investigation
- AMN – *Autoridade Marítima Nacional*
- ANPC – *Autoridade Nacional de Proteção Civil*
- CSP – Commence Search Point
- CWL – Crosswind Leeway
- DGS – *Direção Geral de Saúde*
- DWL – Downwind Leeway
- EMCIP – European Marine Casualty Information Platform
- EMSA – European Maritime Safety Agency
- ESV – *Estações Salva-Vidas*
- EU – European Union
- GAMA – *Gabinete de Investigação de Acidentes Marítimos e da Autoridade para a Meteorologia Aeronáutica*
- GCAP – *Grande Capacidade*
- GMM – Gaussian Mixture Model
- GNR – *Guarda Nacional Republicana*
- GPS – Global Positioning System
- GUI - Graphical User Interface
- IAMSAR – International Aeronautical and Maritime Search and Rescue
- ICAO – International Civil Aviation Organization
- ICMSR – International Convention on Maritime Search and Rescue
- IMO – International Maritime Organization
- INEM – *Instituto Nacional de Emergência Médica*
- ISN – *Instituto de Socorros a Náufragos*
- L – Leeway
- LKP – Last Known Position
- MCAP – *Média Capacidade*
- MCS – Monte Carlo Simulation
- MRCC – Maritime Rescue Coordination Center
- MRSC – Maritime Rescue Coordination Sub-Center
- PCAP – *Pequena Capacidade*
- pdf – Probability Density Function
- PIW – Person in Water
- POC – Probability of Containment
- POD – Probability of Detection
- POS – Probability of Success
- PSP – *Polícia de Segurança Pública*

- RWD – Relative Wind Direction
- S – Search Pattern Spacing
- SAR – Search and Rescue
- SBSM – *Serviço de Busca e Salvamento Marítimo*
- SNBSM – *Sistema Nacional para a Busca e Salvamento Marítimo*
- SOG – Speed Over Ground
- SRR – Search and Rescue Region
- SRU – Search and Rescue Unit
- STW – Speed Through Water
- TSS – Traffic Separation Scheme
- UNCLOS – United Nations Convention on the Law of the Sea
- ZA – Sheltered Areas

List of Symbols

- U – Constant Velocity
- O – Object
- W – Wind
- C – Current
- C_D – Drag Coefficient
- A – Projected Area
- ρ – Density
- λ^2 – Force Ratio Between Over and Underwater Object Parts
- f – Leeway Rate
- α – Angle Relative to the Y Positive Axis in Clockwise Direction
- θ – Angle Relative to the X Positive Axis in Counter-Clockwise Direction
- Lat – Latitude
- Lon – Longitude
- c – Probability interval upper limit
- P – Probability
- X – First Cartesian Position Coordinate
- Y – Second Cartesian Position Coordinate
- Z – Third Cartesian Position Coordinate
- V – Velocity
- μ – Mean
- σ – Standard Deviation
- a – Slope Including Associated Uncertainty
- b – Offset Including Associated Uncertainty
- ε – Uncertainty factor
- D – Drift
- Δt – Time Interval
- δ – Angular Distance
- α_b – Bearing Angle
- d – Distance between the initial and final position
- R – Earth Radius
- t_i – Object Location at the Initial Time Instant of Simulation
- $t_f R$ – Right Drifting Object Location at the Final Time Instant of Simulation
- $t_f L$ – Left Drifting Object Location at the Final Time Instant of Simulation

1. Introduction

1.1. Overview

According to IMO and ICAO (1998), “search” is an operation, normally coordinated by a rescue coordination center or rescue sub-center, using available personnel and facilities to locate persons in distress and “rescue” is an operation to retrieve persons in distress, provide for their initial medical or other needs, and deliver them to a place of safety. So, Search and Rescue (SAR) can be defined as a lifesaving operation aiming to assist people in distress or imminent life-threatening situations, normally coordinated by a rescue coordination center. The duty of each country in terms of operating area, coordination and resources used at sea in SAR operations is defined by several international maritime conventions. In SAR operations at sea is key to have a good logistic structure and the means necessary to respond to any required situation, at any time, as fast as possible.

The SAR operations have three main issues to overtake (Kratzke et al., 2010). The first one is the management and coordination required to put into action an operation in the shortest possible time. The acquiring of reliable probability distribution maps of the object location is the second main problem to solve. The third, and last one, is the choice of pattern to use over the defined searching area, to search and find the missing object at sea, according to the means available. This dissertation is focused on the three main issues in maritime SAR operations, paying special attention to the second one: the definition of a probability distribution map of the object location, taking into account the drift of the object and the uncertainties affecting its trajectory.

1.2. Objectives

The objective of this thesis is to provide an overview of SAR operations in Portugal waters and to develop a simple drifting model to obtain the probability distribution maps of the location of floating objects using Monte Carlo Simulation (MCS), taking into account the uncertainties in the drifting process. The *Opendrift* software is used for comparison purposes and to validate the developed tool, through the analysis of four different scenarios of drifting objects off the coast of Portugal.

1.3. Structure

In order to achieve the proposed goal, the thesis document is organized in seven main chapters. After the present introduction, Chapter 2 provides a brief overview of maritime accidents and incidents worldwide and in European and Portuguese waters. A description of the existing international legislation on the maritime search and rescue operations is described in the same chapter, as well as the Portuguese structure created for maritime SAR operations and its organization. This provides a good insight on the international and Portuguese legal SAR framework. As regards to the Portuguese structure, a reference is made to the operating areas, entities involved and means available for the operations and its locations. Chapter 3 presents the basic formulation for trajectory prediction of drifting objects at sea, based on previous research works. The object types used in different models and the

meaning of their parameters are explained. A brief insight is provided on the object location prediction tools used by different countries. In particular, the *Opendrift* software developed by Degestad, Röhrs, Breivik and Ådlandsvik (Dagestad et al., 2018), used for validating the developed tool in Chapter 5, is described in Chapter 3. The main search patterns used to locate the object inside the search area are also described. Chapter 4 presents the implementation of the basic drifting model tool together with a detailed explanation of its conceptualization and output. Chapter 5 presents the assumptions made for each studying scenario created, using the developed tool and the *Opendrift*. Finally, Chapter 6 presents the results and a comparison between the simulated scenarios, as well as a probabilistic modeling of the object location using a bivariate Gaussian Mixture Model.

The main body of this thesis ends up with Chapter 7, that presents the conclusions and a discussion on the present work and also some suggestions for possible future research works in this topic.

2. Search and Rescue Operations at Sea

"International shipping transports approximately 90% of world trade" (AGCS, 2017). This shows the importance of the shipping industry. Commercial ships are getting bigger and bigger and the number of ships circulating is also increasing, and so should be the risk of accidents at sea. However, merchant ships are not the only vehicles at sea. There is a large number of passenger ships, service ships, fishing vessels, pleasure crafts, as well as some aircrafts needing search and rescue operations at sea in case of an accident.

2.1. Casualties and Incidents

The number of accidents has not increased linearly overtime with the number of ships at sea since the means of avoiding accidents are getting more efficient (Guedes Soares and Teixeira, 2001). The time duration of SAR operations is decreasing due to all the new technologies available nowadays as well as the legislation that makes each country responsible for the SAR operations in its respective ocean area, making the number of casualties at sea to decrease when compared with the number of accidents.

Figure 1 clearly shows that the major concern in terms of ship losses over the last decade is located in the South China, Indochina, Indonesia and Philippines maritime region, representing more than a quarter of the total losses in 2016. The losses in the figure consider only ships over 100 gross tons. The second top hotspot in total losses is the East Mediterranean and Black Sea area, with around 65% the total number of losses of the first area mentioned according to AGCS (2017).

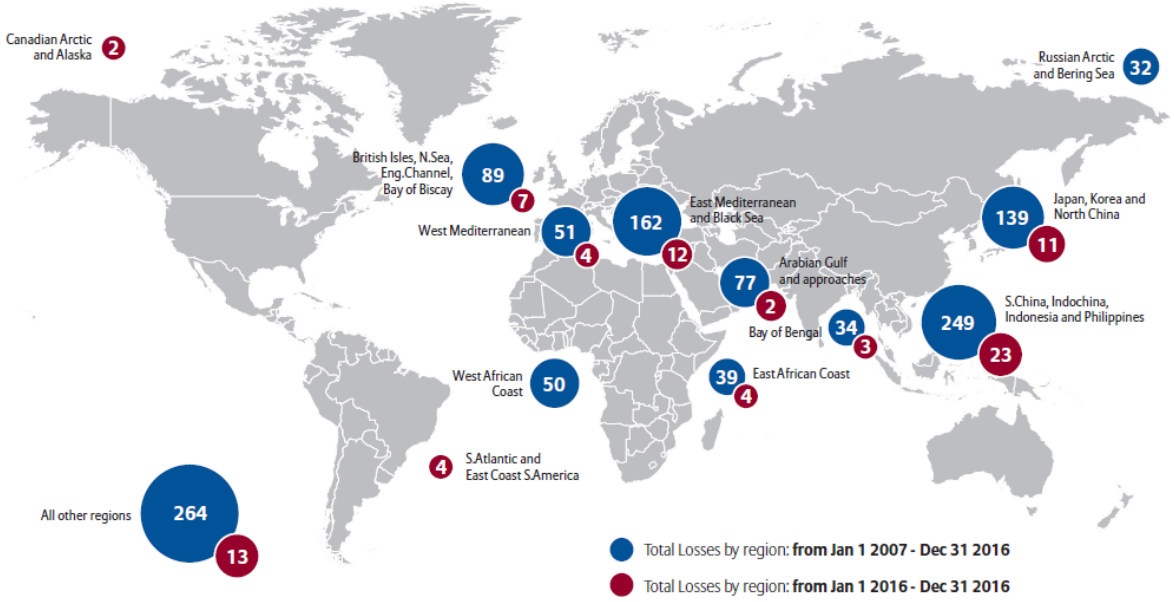

Figure 1 - Total Losses by Region, of ships over 100 gross tons, taken from AGCS (2017)

According to AGCS (2017), from the 25898 casualties registered by AGCS, 1186 were total losses, equivalent to almost 5%. These casualties were mostly caused by machinery damage (32%), Collision (15%) and wrecked/ stranded (15%). As shown in Figure 2, the top location of casualties at sea is the East Mediterranean and Black Sea with 4401 incidents from 2007 to 2017, followed closely by the British Isles, North Sea, English Channel, Bay of Biscay with a total of 4198. In third place is the South China, Indochina, Indonesia and Philippines with around half the casualties of the first two locations.

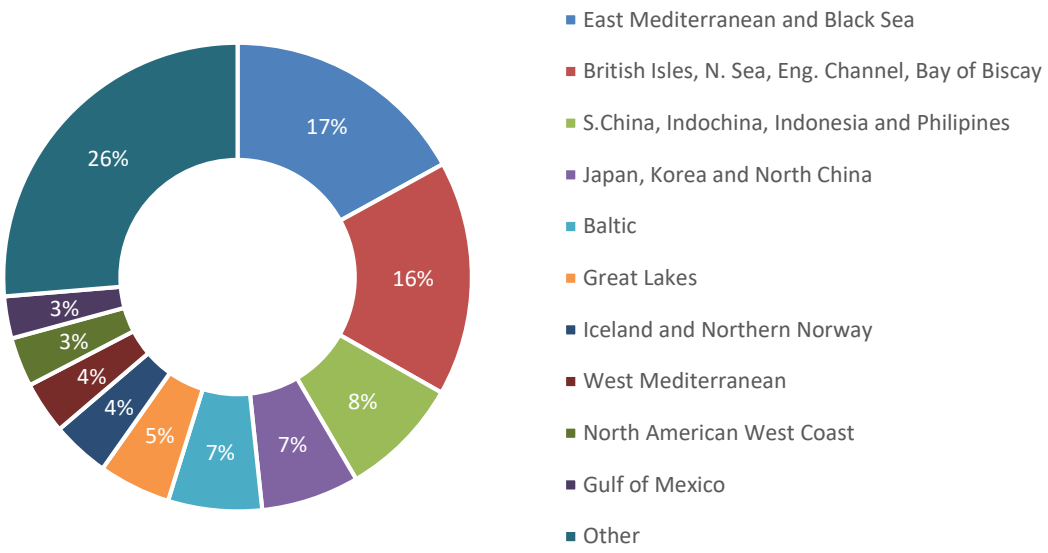

Figure 2 - All Casualties including Total Losses by Region, of ships over 100 gross tons (AGCS, 2017)

At the European level, the Annual Overview of Maritime Casualties and Incidents 2017 report published by the European Maritime Safety Agency (EMSA, 2017) contains statistical data on marine casualties and incidents that: “involve ships flying a flag of one of the European Union (EU) States; occur within EU States’ territorial sea and internal waters as defined in United Nations Convention on the Law of the Sea (UNCLOS); or involve other substantial interests of the EU States.” (EMSA, 2017). The information available in this report was gathered by EMSA in a database called European Marine Casualty Information Platform (EMCIP), where each EU member State stores its own intel. The information studied in this EMSA report includes all types of ships, even ships smaller than 100 gross tons.

There is still a lack in the numbers presented by EMSA due to under-reporting that appears to still exist. However, this under-reporting problem is mainly linked to less serious casualties and incidents.

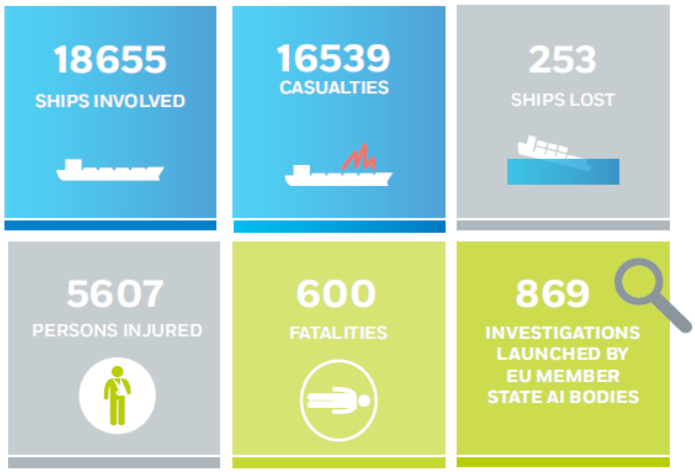

Figure 3 - Overview of Key Figures of Casualties and Incidents in Europe, taken from EMSA (2017)[1]

The key figures presented in Figure 3 illustrate the numbers gathered by EMSA between 2011 and 2016. There were 18655 ships involved in 16539 casualties and incidents and 253 of those ships were lost, which means that around 1.4% of the ships involved were lost. 5607 people got injured and 600 lives were claimed in 6 years, which corresponds to close 935 people injured and 100 fatalities per year.

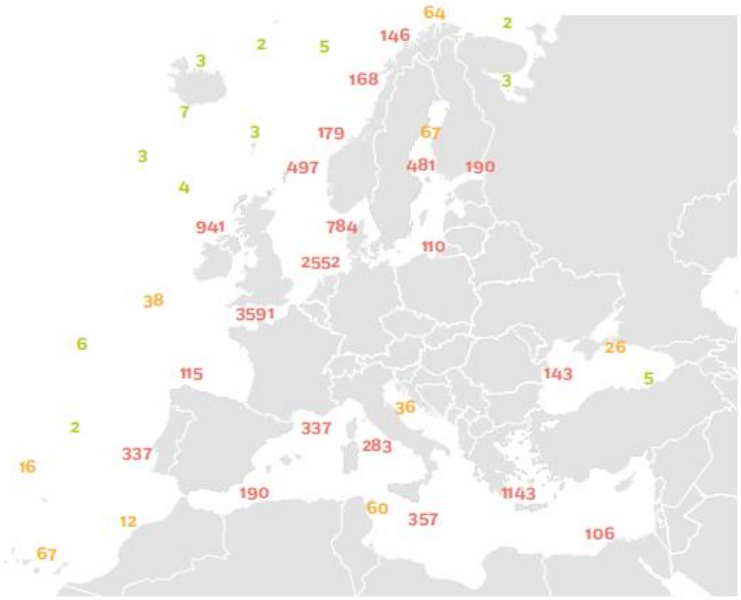

Figure 4 - Distribution of Casualties and Incidents within the Territorial Sea and Internal Waters of EU states 2011-2016, taken from EMSA (2017)

Figure 4 shows the number of casualties and incidents that occurred by region. The British Isles, North Sea, English Channel and Bay of Biscay area are the hottest spots by far, followed by the East Mediterranean and Black Sea region. Although the precise location of the casualties is not available, this figure provides a general idea of an European heatmap. 337 casualties and incidents were

[1] Accident Investigation (AI) bodies are the entities responsible for investigating accidents in each country.

registered close to the Portuguese coast between 2011 and 2016, representing about 2.6% of the total number of casualties and incidents in this EU map and 2% of all the casualties and incidents registered by EMSA.

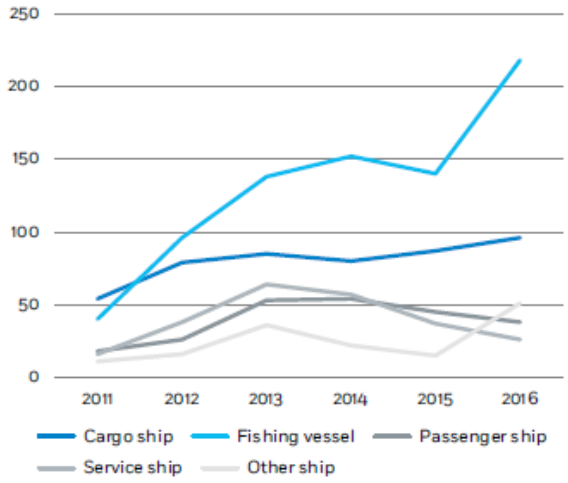

Figure 5 - SAR Operations by type of vessel over the years, taken from EMSA (2017)

According to EMSA (2017), in six years, 1888 ships needed a SAR operation and around 42% of those were fishing vessels. The fishing vessels are the main type of ship requiring SAR operations. Many of the ships lost are related with SAR operations, particularly those that are not close to a port. Figure 5 shows clearly that fishing vessels are in the top. The top two types of vessels involved in SAR operations are fishing and cargo ships, and one of the main reasons for that is that the number of these ships is also higher when compared to the other types.

Figure 6 - Overview of Key Figures of Casualties and Incidents in Portugal, taken from GAMA (2017)

EMSA reports casualties and incidents concerning the EU States that include the ones reported by *Gabinete de Investigação de Acidentes Marítimos e da Autoridade para a Meteorologia Aeronáutica* (GAMA), which is the Portuguese entity responsible for analyzing and codifying the incidents using the

same EMSA taxonomy. The statistical reports provided by GAMA cover accidents involving vessels with the Portuguese flag, as well as any ship in Portuguese waters, regardless its flag.

The overall number of casualties and incidents in 2017 in Portugal are present in Figure 6, using the same type of symbology of Figure 3: 240 casualties and incidents were registered; 13 fatalities occurred; 62 people got injured; 29 ships were lost; 5 casualties caused pollution issues; and 13 investigations were launched. GAMA is making an effort to decrease the number of casualties and incidents that are not notified in order to create a database closer to reality and improve their reports and consequently contribute to EMSA to improve their reports too. That is probably one of the reasons for increasing the notifications over the last three years: 217 in 2015, 238 in 2016 and 240 in 2017.

The number of commercial ships registered with a Portuguese flag sailing all over the world is around 500. Besides these ships, the Portuguese fishing fleet has about 8000 vessels and 90% are shorter than 12m. Portuguese waters have a great density of traffic with most of ships travelling through the Traffic Separation Scheme (TSS), as shown by Silveira et al. (2013).

Most of the casualties and incidents happen within 12 miles off the coast (coastal waters), for which GAMA is the only entity responsible for their investigation. GAMA monitored an average of 5 casualties and incidents per week during 2017.

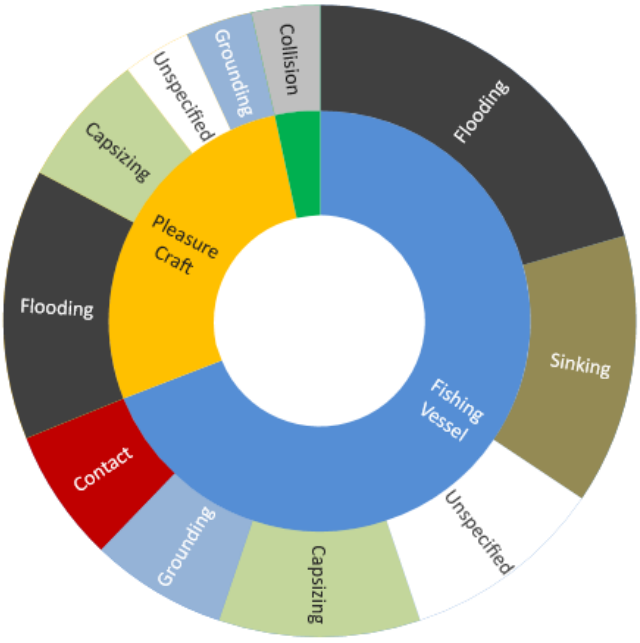

Figure 7 - Total Losses by Type of Ship and by Cause

The core of the ships lost is the fishing industry with 20 vessels lost in 29 (69%). There was also 1 service ship lost and 8 pleasure crafts. The losses of these ships were caused by different casualty events: 10 ships flooded and were loss (6 fishing vessels and 4 pleasure crafts); 1 service ship was declared lost after a collision with a cargo ship; 2 fishing vessels hit stationary objects – contact; 5 vessels capsized (3 fishing vessels and 2 pleasure crafts); 4 fishing vessels sank; and 3 vessels

grounded (2 fishing vessel and 1 pleasure craft), as illustrated in Figure 7. The 4 other total losses have not a cause specified in GAMA (2017) report.

2.2. International Legislation on Maritime SAR

In 1979 there was the need of creating a global SAR plan in a way that there would always be a responsible entity for the SAR operation and coordination, no matter where in the planet the incident took place. For this reason, on April 27, 1979 the International Convention on Maritime Search and Rescue (ICMSR) was adopted in a conference from the International Maritime Organization (IMO), in Hamburg.

This convention has divided the ocean in several areas named Search and Rescue Regions (SRR), where each country is responsible for the SAR operations in its area. Portugal is responsible for an area of approximately 6 million square kilometers, corresponding to nearly 63 times the surface of its land territory, defined in the ICMSR. Inside this area, the Portuguese navy must reply fast and effectively to any incident and cooperate with neighbor countries.

Every SAR operation at sea proceed according to the regulations imposed by IMO and by the International Civil Aviation Organization (ICAO), all defined in the International Aeronautical and Maritime Search and Rescue (IAMSAR) manual (IMO and ICAO, 1998) published in cooperation of both organizations. Its first edition was published in 1998.

The IAMSAR manual is divided in three volumes:

- *Vol.I - Organization and Management*
- *Vol.II - Mission Co-ordination*
- *Vol.III - Mobile Facilities*

In the first volume, the global SAR system concept, establishment and improvement are discussed, as well as co-operation between States. Volume II is an assistance to people planning and co-ordinating SAR operations and exercises. Volume III was created for on-scene practical purpose, intended to be carried by Search and Rescue Units (SRU) to enhance the performance of the mission.

2.3. Portuguese Legislation on Maritime SAR

On the 16th of August 1985, in Portugal, the 1979 ICMSR was approved, in the Decree-Law number 32/85 (Portuguese Government, 1985). This was the first step for the current law in force, published in the Portuguese Republic Official Journal by the National Defense Ministry, in the Decree-Law number 15/94 (Portuguese Government, 1994), on the 22nd of January 1994. In this Decree-Law the "*Sistema Nacional para a Busca e Salvamento Marítimo* (SNBSM)" is defined. SNBSM is the Portuguese system for maritime SAR. The system is operated by the National Defense Minister, as the national authority

responsible for the ICMSR compliance. In 1999 it was decided that a consultive commission would support the Defense minister, in the Decree-Law 399/99 (Portuguese Government, 1999) on the 14th of October. In the SNBSM, the maritime SAR service, known in Portuguese as "*Serviço de Busca e Salvamento Marítimo* (SBSM)", is provided by the Portuguese Navy. The service works twenty-four hours a day and seven days a week and it has responsibility for the actions taken in case of accidents that occur with vessels in the areas of national responsibility. To ensure a fast and efficient response, there is a structure that includes human, material and technological means.

2.4. SAR Operations in Portugal

2.4.1. Portuguese Maritime SAR Area

The area of national responsibility relative to maritime SAR operations is divided in two SRR's: Lisboa and Santa Maria. These two areas are controlled by the Maritime Rescue Coordination Centers (MRCC) of Lisboa and Delgada, respectively. There is also a Maritime Rescue Coordination Sub-Center (MRSC) called MRSC international that coordinates the operations around the Madeira archipelago, being this a sub-region of the Lisboa SRR. The total Portuguese maritime SAR area is shown in Figure 8.

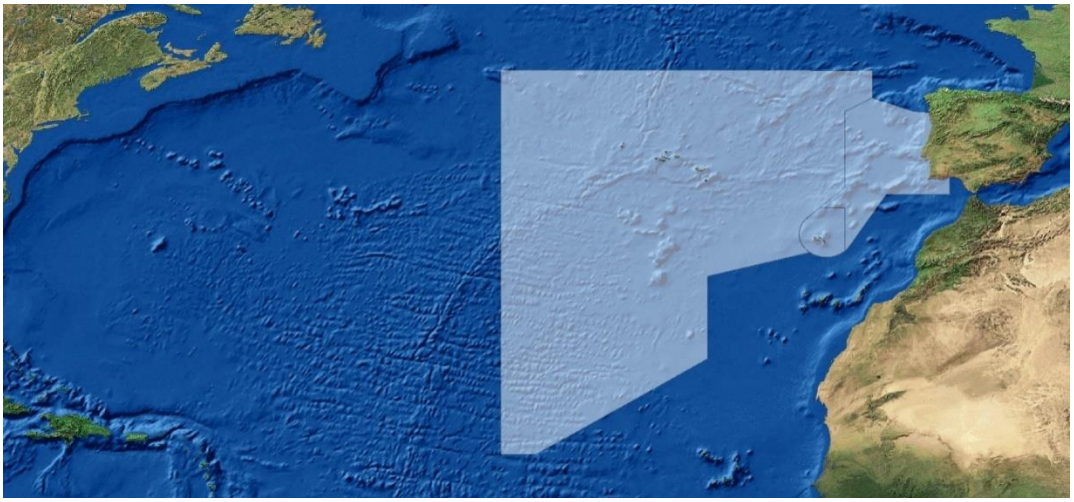

Figure 8 - Portuguese maritime SAR area, taken from Portuguese Navy (2018)

As described by Afonso (2008), the Portuguese Navy, that controls the maritime SAR operations, delegated the coordination work to the Navy Command or in Portuguese the *Comando Naval*, the *Comando da Zona Marítima da Madeira* and the *Comando da Zona Marítima dos Açores* in the respective MRCC Lisboa, MRSC Funchal and MRCC Delgada.

Both Portuguese MRCC's coordinate three types of fundamental units for the maritime SAR operations:

- Coastal Watching Units;
- Search and Rescue Units;
- Search and Rescue Naval Units.

This Coordination Structure is summarized in Figure 9.

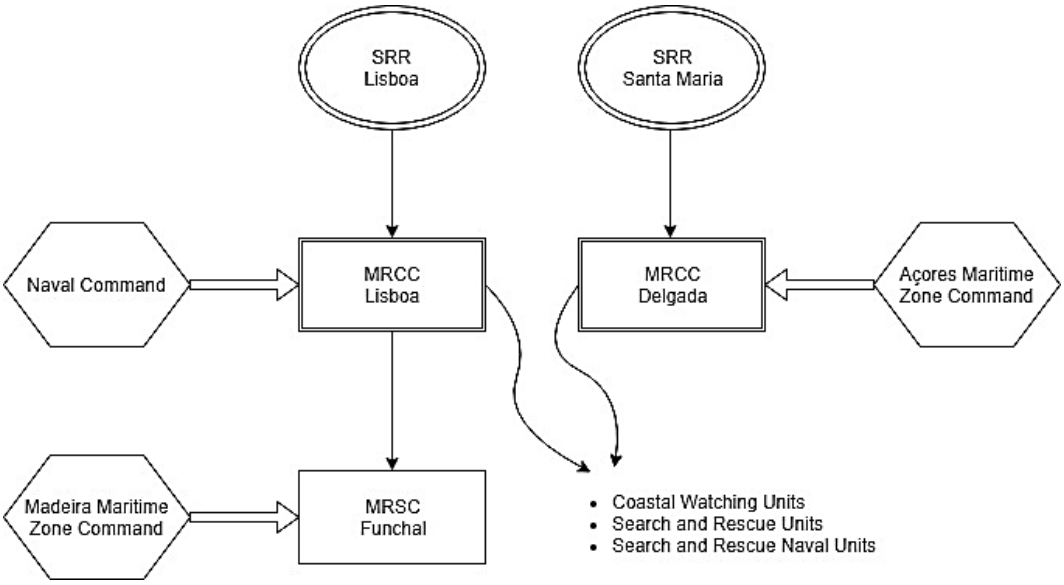

Figure 9 - Portuguese maritime SAR operations structure

The Coastal Watching Units are distributed along the Portuguese coast through the *31* life-saving stations or as called in Portuguese *Estações Salva-Vidas* (ESV) from the *Instituto de Socorros a Náufragos* (ISN), which are responsibility of the respective Ports' Captains.

2.4.2. Entities involved

In order to get a higher rate of success in its mission, the Portuguese Navy gets help from other State departments, such as the Portuguese Airforce, maritime and port administrations, Medical Emergency National Institute (INEM), National Firemen Service, Public Security Police (PSP), Portuguese Red Cross, Health General Direction *(DGS)*, Civil Protection National Authority (ANPC), ANA airports of Portugal and Nacional Republic Guard (GNR). Depending on the situation, every single department can be useful with means or intel information. There is also cooperation between countries when an occurrence takes place close to a border, increasing the probabilities of finding and rescue the missing objects.

2.4.3. ISN means available and its locations along the coast

The ISN is an institute integrated in the Portuguese National Maritime Authority (AMN) with departments oriented for the maritime rescue and assistance to beach users. The ISN is the entity that is in charge of organizing the location of the ESV along the coast and of ensuring they are always ready to answer in case of emergency.

The actual plan of the ESV is organized in order to have the Portuguese coastline well covered by the means available in the stations. According to the means available in each ESV, these are categorized in three types, as shown in Figure 10:

- Type A, represented in grey, are the ESV placed close to high density of maritime traffic and with capacity to operate in the TSS. These ESV have good facilities, more personnel and stronger means to answer the necessities: one great capacity life-saving vessel (GCAP); one medium capacity life-saving vessel (MCAP); one small capacity vessel (PCAP); and one vessel for sheltered areas (ZA).
- Type B, represented in yellow, are the ESV placed around areas with some maritime traffic and do not have the capacity to operate in TSS. These ESV have the same kind of facilities but less personnel and fewer means than the type A ESV: one MCAP life-saving vessel; and one ZA vessel.
- Type C, represented in red, are the ESV placed in areas of less traffic and smaller crafts and do not have the capacity to operate in TSS. These ESV have smaller facilities and less capacity, less personnel and fewer means than Type B ESV: one MCAP or one PCAP life-saving vessel; and one ZA vessel.

Figure 10 - ISN Life-Saving Stations along the Portuguese Coast, taken from Autoridade Marítima Nacional (2018)

3. Trajectory Prediction of Drifting Objects

3.1. Basic Drifting Model

Given the importance of the search and rescue operations worldwide, there has been a great improvement in probabilistic methods to predict the drifting of an object at sea, especially with the technology available nowadays to study the wind and current phenomena, as well as the computing power available. In the last fifteen years, the Portuguese navy handled more than 11000 search and rescue operations (Portuguese Navy, 2018). This emphasizes the importance of developing a drifting model applied to Portuguese coastal waters.

Injuries or casualties, environmental pollution and material losses are the main consequences when dealing with marine accidents like collisions, sinkings, groundings, explosions, etc (Guedes Soares and Teixeira, 2001;Zhang et al., 2013). That is a risk inherent to the maritime transportation in general.

The spreading of oil spills has been studied through a model that takes in consideration the most typical processes that the oil particles are involved in (Sebastião and Guedes Soares, 1995). Also, the uncertainty of the predictions of oil spills trajectories both in coastal areas (Sebastião and Guedes Soares, 2006) and in open sea (Sebastião and Guedes Soares, 2007) have been studied.

The computation and information system required to support and planning fast and efficient SAR operations are defined by Vettor and Guedes Soares (2015) with a special detail on the Portuguese coasts. All the existing probabilistic computational models for predicting trajectories of drifting objects at sea are based on simple drifting mathematical expressions that take into consideration the vectors of wind and current. The wave effects can also be considered, but these are usually ignored because the Stokes[2] drift is mostly downwind, and it is hard to separate them from the direct wind effects on a floating object. Wind and surface currents are defined by Fitzgerald et al. (1993) as wind from the surface level up to 10 meters high and currents from 0.3 to 1.0 meters below the surface. These currents are mainly induced by the wind and not by deep water currents, unless the wind velocity has a low value. Following the definition of Hodgins and Mak (1995), Leeway (L) is the drift of a floating object subject to wind forces alone. Any object drifting on the sea surface is in contact with two different density fluids: air and water. Each fluid exerts a force on the object, which depends on the object shape and dimensions. Both of those forces can be decomposed into drag and lift components. According to Richardson (1997) the drag and lift components of the wind result from the asymmetrical shape of the overwater body area. The drag component is aligned with the relative downwind direction, and the lift component is perpendicular to that direction. So, according to the shape of the object floating and its position, the lift will make the object move to one side or another in the crosswind direction. The hydrodynamic lift component will balance the aerodynamic one, avoiding the object to roll, according to Breivik and Allen

[2] "The Stokes drift is a downwave drift induced by the orbital motion that water particles undergo under the influence of a wave field." (Breivik and Allen, 2008)

(2008). In this study it is also proved by experimental data that the probability of the object drift right or left of the downwind direction is the same.

In order to fully understand the drifting dynamics model, Zhang et al. (2017) consider a floating object with a constant velocity, U_O, or as usually called speed over ground (SOG), subjected to a field, with a constant wind velocity, U_W, and a constant current velocity, U_C. Consequently, the velocities $(U_W - U_O)$ and $(U_O - U_C)$ are the apparent wind velocity and the apparent current velocity, respectively.

Following Ni et al. (2010) formulation development and considering a steady drift and according to Newton's laws of motion, the sum of the forces acting on a body equals zero. For this reason, using the expression of forces applied by fluids, the drifting object motion can be represented by equation 1:

$$\frac{1}{2}\left(C_{D_1}.A_1.\rho_1\right).|U_W - U_O|.(U_W - U_O) = \frac{1}{2}\left(C_{D_2}.A_2.\rho_2\right).|U_O - U_C|.(U_O - U_C) \quad (1)$$

where, C_D is the drag coefficient, A is the cross-sectional area exposed to the respective fluid and ρ is the fluid density. Both C_D and A variables are a characteristic of the type of the floating object. The subscripts 1 and 2 represent the air and water fluids respectively.

Defining a parameter λ as represented by equation 2:

$$\frac{C_{D_1}.A_1.\rho_1}{C_{D_2}.A_2.\rho_2} \equiv \lambda^2 \quad (2)$$

The model can be simplified as given by equation 3:

$$\lambda\,.(U_W - U_O) = U_O - U_C \quad (3)$$

Then, the object velocity can be represented as function of U_W and U_C by equation 4:

$$U_O = \frac{\lambda}{1+\lambda}.U_W + \frac{1}{1+\lambda}.U_C \quad (4)$$

The leeway drift velocity U_L, or as usually called speed through water (STW), can be obtained as a function of U_W and U_C, as in equation 5:

$$U_L = U_O - U_C = \frac{\lambda}{1+\lambda}.U_W - \frac{\lambda}{1+\lambda}.U_C \tag{5}$$

Assuming now the concept of leeway rate, f, expressed in equation 6, the leeway velocity and the velocity of the object are given by equations 7 and 8, respectively:

$$\frac{\lambda}{1+\lambda} \equiv f \tag{6}$$

$$U_L = f.(U_W - U_C) \tag{7}$$

$$U_O = U_C + U_L = U_C + f.(U_W - U_C) \tag{8}$$

The leeway velocity vector can be decomposed in two projections parallel and perpendicular to the wind velocity vector, respectively: Downwind Leeway (DWL) and Crosswind Leeway (CWL), given by equations 9 and 10, respectively:

$$\begin{aligned} DWL &= \left[U_L.\frac{U_W}{|U_W|}\right].\frac{U_W}{|U_W|} = \left[f.(U_W - U_C).\frac{U_W}{|U_W|}\right].\frac{U_W}{|U_W|} \\ &= f.\left[|U_W| - U_C.\frac{U_W}{|U_W|}\right].\frac{U_W}{|U_W|} \end{aligned} \tag{9}$$

$$\begin{aligned} CWL &= U_L - DWL = f.(U_W - U_C) - f.\left[|U_W| - U_C.\frac{U_W}{|U_W|}\right].\frac{U_W}{|U_W|} \\ &= -f.U_C + f.\left(U_C.\frac{U_W}{|U_W|}\right).\frac{U_W}{|U_W|} \end{aligned} \tag{10}$$

The leeway angle, L_α, is independent from the leeway rate, f, and it can be calculated by equation 11 as:

$$\tan L_\alpha = \frac{|CWL|}{|DWL|} = \frac{\left|-U_C + \left(U_C.\frac{U_W}{|U_W|}\right).\frac{U_W}{|U_W|}\right|}{\left||U_W| - U_C.\frac{U_W}{|U_W|}\right|} \tag{11}$$

To maintain the convention already adopted in previous works, the leeway angle is said to be positive when the object drifts to the right side of the downwind direction and negative to the left, as shown in

Figure 11, adapted from Allen and Plourde (1999). The Relative Wind Direction (RWD) has also a different sign when the object is drifting right or left.

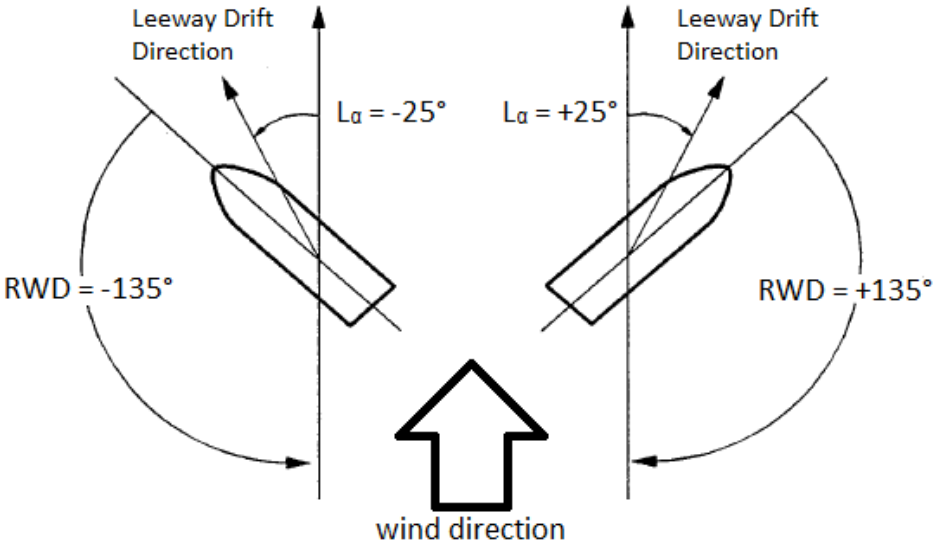

Figure 11 - Leeway Angle Signal Convention, adapted from Allen and Plourde (1999)

3.2. Object Types

Allen and Plourde (1999) have created a new data base of ninety-five leeway target types. The target list includes forty life rafts, fourteen small craft (mostly outboards) and ten fishing vessels. Other leeway target types studied include person in water (PIW), surfboards, sailboats, life capsules, Cuban refugee rafts, fishing vessel boating debris, and medical / sewage waste (Allen and Plourde, 1999). The list can be found in ANNEX A, and each object is defined in terms of three parameters in the calculations:

- Leeway Slope [%];
- Leeway Y-intersect [cm/s];
- Leeway angle [deg].

These variables are explained in detail in Chapter 4.

The table of objects used by *Opendrift,* presented in ANNEX B, results from a study by Breivik et al. (2011), which is an upgrade of the previous work by Allen and Plourde (1999). The new list of objects divides the leeway vector into downwind leeway and crosswind leeway, in which the crosswind vector can have different values for right or left drifts, according to the position of the object in relation to the wind direction. For each of the three components (downwind, right and left) there is a value for the slope, offset and standard deviation, that reflect the errors associated from the type of object and from the wind velocity and direction. Each component follows a normal distribution. The nine parameters that characterize the object were initially introduced by Allen (2005). So, the nine variables introduced by the object type are:

- Downwind Slope [%];
- Downwind Offset [cm/s];
- Downwind Standard Deviation [cm/s];
- Right Crosswind Slope [%];
- Right Crosswind Offset [cm/s];
- Right Crosswind Standard Deviation [cm/s];
- Left Crosswind Slope [%];
- Left Crosswind Offset [cm/s];
- Left Crosswind Standard Deviation [cm/s].

These parameters are explained in further detail in Chapter 4.

3.3. Object Location Prediction Tools

Several software tools have been developed and are currently used in SAR operations for object location prediction. The goal of a drifting simulation model software is to determine the searching area for a floating object on the ocean surface. The models run a large number of simulations, different from each other to represent the uncertainty on the model parameters. Theoretically, the grater the number of simulations, the better. However, in real life situations, every SAR operation is conducted a small-time window given the life-threatening situation of the people lost at sea, which means the number of simulations must be reduced to find a compromise between the quality of the defined area and the time of simulation. This type of software can help shortening the time to locate an object lost at sea and therefore, the number of human lives lost at sea every year.

3.3.1. Opendrift

Opendrift is an open source program developed by Dagestad et al. (2018). The software itself is very generic, working as a base for many different applications in which each user can edit the scrips, being able to use it for the intended purpose.

The *Opendrift* drifting model determines a search and rescue area from several variables: the last known position of the object, the time since when the last known position of the object was determined, the type of object, the wind speed and the current speed on the sea surface. This software is also capable of running backwards, i.e. knowing the position where an object was found *Opendrift* is able to find out where the object came from, determining the possible trajectory down to the moment it was found.

These functionalities of Opendrift are only part of its range of operability. The software was created to simulate trajectories for SAR missions, but also for some other interesting studies like oil drifting, larvae propagation, etc.

The software has the possibility to run via a Graphical User Interface (GUI) which is very simple to use, but consequently lacking many of the features available in the software.

The *Leeway Model* from *Opendrift* was implemented in *Python* programing language and has been upgraded by the research scientist Knut-Frode Dagestad working for the Department of Research and Development in the Norwegian Meteorological Institute, following up the initial work of (Breivik, 2008) from the same institute. The *Leeway Model* is explained in detail in that document and together with some other models resulted in the *Opendrift* software, which is also explained in a recent paper Dagestad et al. (2018).

A tutorial of the software installation and running developed for the present dissertation is presented in Annex C.

3.3.2. Oversee

Oversee is an internationally awarded software system created by *Critical Software* compliant with IAMSAR guidelines and SAR best practice. *Oversee Search and Rescue* is a high-end information system for MRCCs, designed in close cooperation with maritime professionals. Oversee is an intuitive program that enhances the efficiency of an operation in terms of time of response and coordination of the means available.

A trajectory prediction tool is part of the *Oversee* software and its goal is the determination of the search area as well as the pattern of search to use. It is an important tool for the Portuguese MRCC in order to organize the whole operation system. *Critical Software* is a Portuguese company that has already exported this software to foreign countries.

Besides the trajectory prediction tool, the software is also a logistics powerful tool used to concatenate and organize many different information from distinct sources and determine which available means should be activated in each situation according to the retrieved data.

3.4. Search Patterns

The main goal of the drift models is to determine the most probable area where the search will take place, depending on different unknowns that need to be quantified.

The probability of success (POS) of a SAR operation is what is intended to be maximized according to Breivik and Allen (2008) and it is defined as the product of the probability of detection (POD) and the probability of containment (POC), as shown in equation 12:

$$POS = POD \times POC \tag{12}$$

The probability of containment is the probability of the missing object being inside the defined searching area. The probability of detection depends on the resources available for the search of the floating

object, on the dimensions, shape and color of that object and on the procedure used to locate the drifting object.

Once the searching area is determined, it is necessary to plan a systematic search for the target. Numerous factors can influence the planning: meteorological conditions; life-saving vessel or aircraft speed; aircraft altitude; detectability range; dimensions of the missing object, time available for the search, among others. Therefore, the distance between the SRU and the floating object is highly important.

With that said and according to Zhang et al. (2016) it is possible to describe POD as a function of the distance between the SRU and the target, using a model with two parameters that are assigned depending on several variables like the weather conditions and the SRU detection capability.

The selection of the search pattern is very important to maximize the probability of detection in the shortest possible time window. There are three main groups of search patterns: parallel track search pattern; expanding square search pattern; and sector search pattern. All of them have advantages and disadvantages, so they may be used in different types of scenarios.

The parallel track search pattern is frequently used to search in large areas and when the most probable position of the object is not known. It is an easy pattern that can be divided into several smaller searching areas making it possible to synchronize the searching efforts between various SRUs. The search pattern spacing (S) shown in Figure 12, is defined as two times the distance between the SRU and the target according to the SRU detectability range.

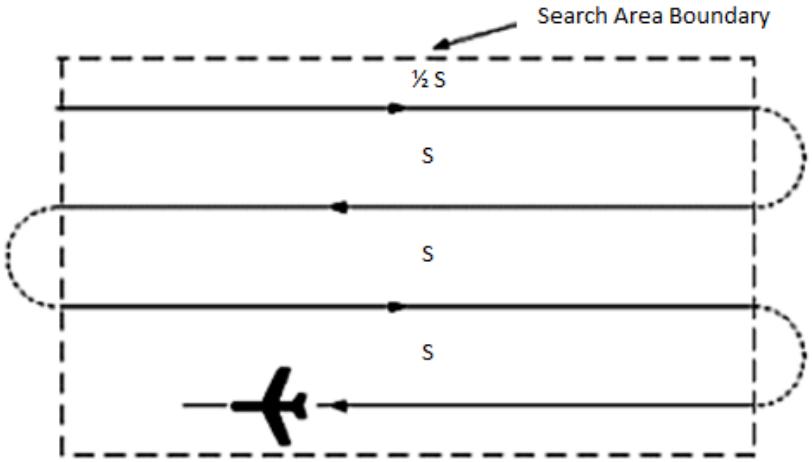

Figure 12 - Parallel track search pattern scheme, taken from Australian National Search Rescue Council (2018)

The expanding square search pattern is used when there is a high accuracy on the most probable location of the missing object, the searching area is small, and a concentrated search is desirable. When used by a vessel, this pattern usually starts against the wind direction to minimize navigational errors

since it is a very precise pattern and requires accurate navigation. The turns are made to the starboard side. An example scheme of this type of pattern is shown in Figure 13.

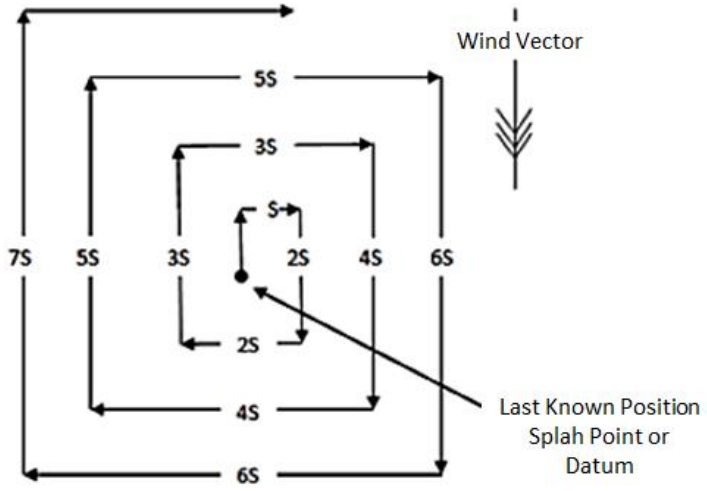

Figure 13 - Expanding square search pattern scheme,
taken from Australian National Search Rescue Council (2018)

The sector search pattern is often used in small search areas to find small floating objects difficult to detect such as a PIW. To use this pattern is necessary to have an accurate prediction of the most probable location of the object because the SRU will repeatedly pass on that point, greatly improving the probability of finding the object in that area. The search starts in the Commence Search Point (CSP) on the border of the searching area. Figure 14 represents the schematics of a sector search pattern.

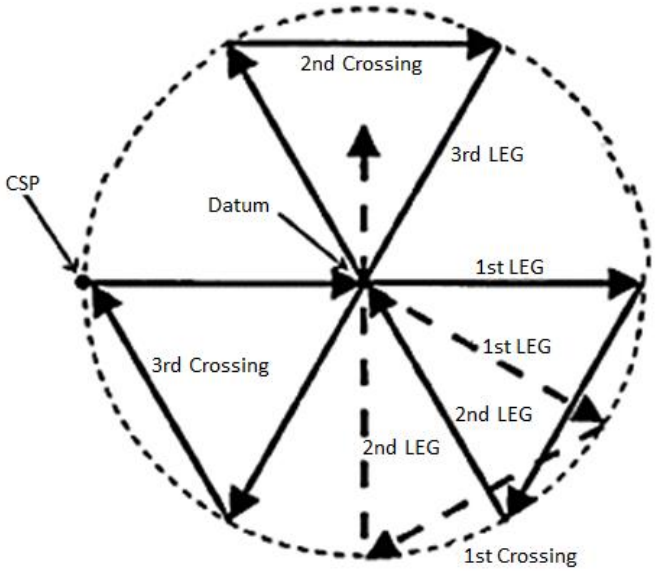

Figure 14 - Sector search pattern scheme,
taken from Australian National Search Rescue Council (2018)

4. Implementation of a Basic Drifting Model

This Chapter describes the implementation of a basic drifting model in a tool developed to obtain the probability distribution maps of the object using MCS, taking in consideration the uncertainties in the process. The formulation described in Section 3.1. is the basis of all the calculations used by the tool and the type of objects presented in Section 3.2. are considered by the tool. The results of the tool developed, are presented and compared with the predictions of the *Opendrift* software in Chapter 6, for different scenarios described in Chapter 5.

This tool is based in two distinct methodologies. In the first and more manual one, it is possible to define every variable mean and standard deviation values, based on normal distributions, by hand for a more personalized input range, and in the second one all variable uncertainties are integrated in the object leeway variables as done by *Opendrift*. The second methodology is used to compare to the *Opendrift* software because it uses the same object associated uncertainties.

The first methodology of the developed tool has the following input variables:

- Initial object location latitude coordinate value, Lat_i [deg];
- Initial object location longitude coordinate value, Lon_i [deg];
- Initial object location X coordinate upper value of probability interval, c_{Xi} [NM];
- Probability of value X being inside the probability interval, $P_{Xi}(-c_{Xi} \leq X \leq c_{Xi})$;
- Initial object location Y coordinate upper value of probability interval, c_{Yi} [NM];
- Probability of value Y being inside the probability interval, $P_{Yi}(-c_{Yi} \leq Y \leq c_{Yi})$;
- Time of the initial location, t_i [d];
- Time of the final location, t_f [d];
- Wind velocity mean value, μ_{V_w} [kt];
- Wind gusts velocity (upper value of probability interval), c_{V_w} [kt];
- Probability of wind velocity value being inside the probability interval, $P_{V_w}(\mu_{V_w} - c_{V_w} \leq V_w \leq \mu_{V_w} + c_{V_w})$;
- Wind direction mean value, μ_{α_w} [deg];
- Wind direction upper value of probability interval, c_{α_w} [deg];
- Probability of wind direction value being inside the probability interval, $P_{\alpha_w}(\mu_{\alpha_w} - c_{\alpha_w} \leq \alpha_w \leq \mu_{\alpha_w} + c_{\alpha_w})$;
- Current velocity mean value, μ_{V_c} [kt];
- Current velocity upper value of probability interval, c_{V_c} [kt];
- Probability of current velocity value being inside the probability interval, $P_{V_c}(\mu_{V_c} - c_{V_c} \leq V_c \leq \mu_{V_c} + c_{V_c})$;
- Current direction mean value, μ_{α_c} [deg];
- Current direction upper value of probability interval, c_{α_c} [deg];

- Probability of current direction value being inside the probability interval, $P_{\alpha_c}(\mu_{\alpha_c} - c_{\alpha_c} \leq \alpha_c \leq \mu_{\alpha_c} + c_{\alpha_c})$;
- Probability of initial position of object being to the right (receiving the wind from starboard side);
- Probability of jibing after one hour of drifting;
- Object Leeway Slope;
- Object Leeway Y-intersect;
- Object Leeway angle, L_α [deg].

The second methodology considers that all uncertainties related to the drifting motion are included into the object type input variables from the list of objects as done by Opendrift. For that reason, instead of having 23 input variables, there are only 15, as follows:

- Initial location latitude coordinate value, Lat_i [deg];
- Initial location longitude coordinate value, Lon_i [deg];
- Initial location X coordinate upper value of probability interval, c_{Xi} [NM];
- Probability of value X being inside the probability interval, $P_{Xi}(-c_{Xi} \leq X \leq c_{Xi})$;
- Initial location Y coordinate upper value of probability interval, c_{Yi} [NM];
- Probability of value Y being inside the probability interval, $P_{Yi}(-c_{Yi} \leq Y \leq c_{Yi})$;
- Time of the initial location, t_i [d];
- Time of the final location, t_f [d];
- Wind velocity value, V_w[kt];
- Wind direction value, α_w[deg];
- Current velocity value, V_c [kt];
- Current direction value, α_c [deg];
- Object type;
- Probability of initial position of object being to the right (receiving the wind from starboard side);
- Probability of jibing after one hour of drifting.

Note that the last two input variables are kept constant across all four scenarios described in the next chapter.

The output variables of the tool are:

- Final location latitude coordinate values, Lat_f [deg]
- Final location longitude coordinate values, Lon_f [deg]

Based on all these input and output variables listed above, the tool calculates the final location of an object drifting on the ocean surface, taking in consideration the wind and current vectors, according to the object's characteristics.

The initial location, the wind velocity and direction and the current velocity and direction in the first methodology are generated via MCS, from normal distributions since they are not always the same and

tend to vary even under the same conditions. However, in the second methodology, the MCS is applied to the initial location, DWL and CWL variables. The DWL and CWL variables already incorporate the uncertainties on the object leeway itself and of the wind and current velocities and directions. Random numbers are generated according to the probabilistic characteristics of the variables to conduct 1000 simulations of the drifting model. The simulation creates a sample of 1000 values of the final location of the object as well as, of its trajectory along the time. That sample of points is the basis for probabilistic modeling of the object location and for planning the search.

The initial location of an object drifting at sea, usually defined as the last known position (LKP), is based on human information such as a sighted incident, a radio communication from someone close by, a supposition from the route the craft was doing, etc. However, LKP can also be a location provided by a Global Positioning System (GPS) tracker or some other technology that is available on the craft lost at sea. This means that the LKP can be more accurate in some situations than others based on the intel provider, this is why the standard deviation of the LKP can be changed in the tool developed, both in X and Y directions. The mean value of the initial location is considered (0, 0) in (x, y) coordinates. So, the normal random variables for X and Y coordinates of the initial location can be represented by equations 13 and 14, respectively:

$$X_i \sim N(0,\ {\sigma_{Xi}}^2) \tag{13}$$

$$Y_i \sim N(0,\ {\sigma_{Yi}}^2) \tag{14}$$

The Inverse Transformation Method is then used to generate samples of X_i and Y_i using the Inverse Normal Cumulative Distribution Function of random numbers between 0 and 1, as represented by equations 15 and 16, respectively:

$$X_{i_j} = F_N^{-1}\left(random_j; 0; \sigma_{Xi}\right) \quad , \quad j = 1, 2, 3, \dots, 1000 \tag{15}$$

$$Y_{i_k} = F_N^{-1}(random_k; 0; \sigma_{Yi}) \quad , \quad k = 1, 2, 3, \dots, 1000 \tag{16}$$

The wind velocity, V_w, and direction, α_w, and the current velocity, V_c, and direction, α_c, values are also generated in the same way in the first methodology for each of the 1000 samples, with a new random number for each variable, as presented in equations 17, 18, 19 and 20.

$$V_{w_l} = F_N^{-1}\left(random_l; \mu_{V_w}; \sigma_{V_w}\right) \quad , \quad l = 1, 2, 3, \dots, 1000 \tag{17}$$

$$\alpha_{w_m} = F_N^{-1}\left(random_m; \mu_{\alpha_w}; \sigma_{\alpha_w}\right) \quad , \quad m = 1, 2, 3, \dots, 1000 \tag{18}$$

$$V_{c_n} = F_N^{-1}\left(random_n; \mu_{V_c}; \sigma_{V_c}\right) \quad , \quad n = 1, 2, 3, \dots, 1000 \tag{19}$$

$$\alpha_{c_o} = F_N^{-1}\left(random_o; \mu_{\alpha_c}; \sigma_{\alpha_c}\right) \quad , \quad o = 1, 2, 3, \dots, 1000 \tag{20}$$

All calculations of the last location coordinates start from the values of these 6 variables (X_i, Y_i, V_w, α_w, V_c, α_c).

Note that every time an angle is defined by the Greek letter α, like α_w and α_c, the directions are defined in degrees, starting as 0° for North direction and growing in clockwise direction: $\alpha \in [0°; 360°[$. When using these direction values in the calculations, they will need to be converted into "trigonometry friendly angles", represented by the Greek letter θ, starting as 0° in East Direction growing in counter-clockwise direction up to 180° and decreasing as negative values in the clockwise direction down to -180°: $\theta \in]-180°; 180°]$. The two-way conversion is represented by equations 21 and 22.

$$\theta\ [deg] = \begin{cases} 90 - \alpha, & if\ \alpha \in [0°; 270°[\\ 450 - \alpha, & if\ \alpha \in [270°; 360°[\end{cases} \tag{21}$$

$$\alpha\ [deg] = \begin{cases} 90 - \theta, & if\ \theta \in]-180°; 90°] \\ 450 - \theta, & if\ \theta \in]90°; 180°] \end{cases} \tag{22}$$

The standard deviation values for each variable depend on the variables' probability interval, but they are all calculated using the equation 23:

$$\sigma = \frac{c - \mu}{\Phi^{-1}[P(X \leq \mu + c)]} = \frac{c - \mu}{\Phi^{-1}\left[1 - \frac{1 - P(\mu - c \leq X \leq \mu + c)}{2}\right]} \tag{23}$$

Where, σ is the standard deviation; c is the upper limit value of the probability interval; μ is the mean value; Φ^{-1} is the Inverse of the Standard Normal Cumulative Distribution Function; P the probability of a given event with a value between 0 and 1.

This means that the standard deviation is calculated from the variables:

- c;
- μ;
- $P(\mu - c \leq X \leq \mu + c)$.

if considering the standard deviation of the initial location in the X direction, σ_{Xi}, depending on the way this location is detected. For example, in scenario 1, it is considered that the one side interval is 0.2 nautical miles with 80% probability because the object initial location is predicted by the someone who knew the the fishing vessel route, meaning $c = 0.2\ [NM]$ and $P(\mu - c \leq X \leq \mu + c) = 0.8$. If the location is provided by a GPS signal, the interval would be smaller, and the interval probability would be higher.

The same type of approach is used for the other variables. For wind velocity the interval is defined as the difference between the wind gusts velocity and the mean wind velocity with a interval probability of 95%.

For σ_{Xi} and σ_{Yi} the value c and the probability $P(\mu - c \leq X \leq \mu + c)$ depends on the information available about the LKP. For σ_{V_w} the value c is the wind gusts velocity which is an information available in most weather websites and the probability used is $P(\mu - c \leq X \leq \mu + c) = 0.9$. For σ_{V_c} the value c is considered by default as being half the smallest scale division from the information used ($c = 0.05\ kts$); for the wind direction, σ_{α_w}, the value of $c = 10\ [deg]$ is defined as default for all simulations for a probability, $P(\mu - c \leq X \leq \mu + c) = 0.9$, meaning 90% of the time the wind direction is inside the interval $[\mu - 10; \mu + 10]$ [deg]. The current direction is usually steadier due to the higher density of the water when compared to the air density, so the values used are $c = 5\ [deg]$ and $P(\mu - c \leq X \leq \mu + c) = 0.9$.

The first step after having values for these 6 variables is to determine the relative wind velocity module, $V_{w_{rel}}$, and direction, $\alpha_{w_{rel}}$. The relative wind speed is the wind measured having the current velocity as refference. It is different from the original wind if the object is moving, i.e., if the current velocity is not zero. So, the relative wind velocity vector can be written, as shown in equation 24, as the difference between the true wind velocity vector and the current velocity vector:

$$\overrightarrow{V_{w_{rel}}} = \overrightarrow{V_w} - \overrightarrow{V_c} \tag{24}$$

Splitting both wind and current velocity vectors into their X and Y components like in equations 25 and 26, the equation 24 turns into equation 27.

$$\overrightarrow{V_w} = (V_{w_x}, V_{w_y}) = (V_w \,.\cos\theta_w\,, V_w \,.\sin\theta_w) \tag{25}$$

$$\overrightarrow{V_c} = (V_{c_x}, V_{c_y}) = (V_c \,.\cos\theta_c\,, V_c \,.\sin\theta_c) \tag{26}$$

$$\begin{aligned}\overrightarrow{V_{w_{rel}}} = \left(V_{w_{rel_x}}, V_{w_{rel_y}}\right) &= \left(V_{w_x} - V_{c_x}, V_{w_y} - V_{c_y}\right) \\ &= (V_w \,.\cos\theta_w - V_c \,.\cos\theta_c\,, V_w \,.\sin\theta_w - V_c \,.\sin\theta_c)\end{aligned} \tag{27}$$

The relative wind velocity vector is defined as a module and a direction by equations 28 and 29, respectively:

$$|\overrightarrow{V_{w_{rel}}}| = V_{w_{rel}} = \sqrt{{V_{w_{rel_x}}}^2 + {V_{w_{rel_y}}}^2} = \sqrt{\left(V_{w_x} - V_{c_x}\right)^2 + \left(V_{w_y} - V_{c_y}\right)^2} = \sqrt{(V_w.\cos\theta_w - V_c.\cos\theta_c)^2 + (V_w.\sin\theta_w - V_c.\sin\theta_c)^2} \quad (28)$$

$$\theta_{w_{rel}} = \tan^{-1}\left(\frac{V_{w_{rel_y}}}{V_{w_{rel_x}}}\right) = \tan^{-1}\left(\frac{V_w.\sin\theta_w - V_c.\sin\theta_c}{V_w.\cos\theta_w - V_c.\cos\theta_c}\right) \quad (29)$$

Changing the reference of the angle using equation 30, it is possible to calculate the alpha of the angle according to the references explained previously.

$$\alpha_{w_{rel}} = \begin{cases} 90 - \theta_{w_{rel}}, & if\ \theta\ \epsilon\ ]-180°; 90°] \\ 450 - \theta_{w_{rel}}, & if\ \theta\ \epsilon\ ]90°; 180°] \end{cases} \quad (30)$$

Taking in consideration the type of object being studied, the object will drift to right or left sides of the relative wind vector, $\overrightarrow{W_{rel}}$, due to its position. The shape of the object will dictate the intensity of the side drift. A positive Leeway angle, L_α, will introduce a drift to the right and a negative angle will produce a drift to the left side of the relative wind direction. A scheme with the Leeway vector, L, decomposition is shown in Figure 15. The Leeway vector can be reduced, as presented in equation 31, to the sum of DWL and CWL vectors:

$$\vec{L} = \overrightarrow{DWL} + \overrightarrow{CWL} \quad (31)$$

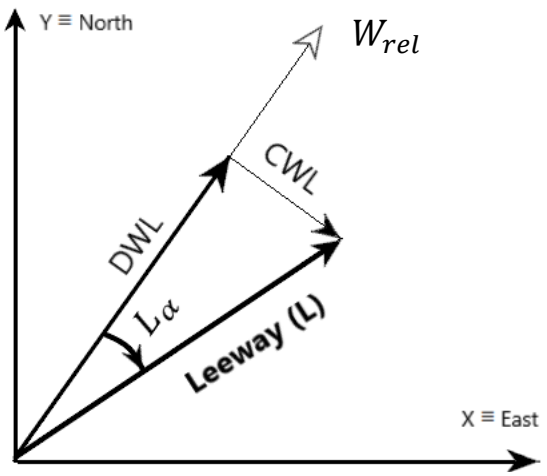

Figure 15 - Leeway Vector Decomposition, taken from Allen and Plourde (1999)

The Leeway angle, L_α, or as sometimes called divergence angle, has a specific value depending on the type of object floating, as well as the slope [%] and the Y-intercept [cm/s] coefficients that define the linear function that calculates the Leeway Velocity vector, V_L, from the relative wind velocity vector as in equation 32:

$$V_L\,[kt] = \left(\frac{Slope\ [\%]}{100} \times V_{w_{rel}}[kt]\right) + Yintercept\ [cm/s] \times \frac{60 * 60}{100 * 1852} \tag{32}$$

Using the second methodology of the tool, the values introduced by the object choice are the nine values listed in Section 3.2. collected from the object list of Breivik et al. (2011). According to this work, the downwind leeway velocity, L_d, and the right crosswind leeway, L_{c+}, and left crosswind leeway, L_{c-}, can be defined by equations 33, 34 and 35, respectively:

$$L_d[m/s] = a_d \times V_{w_{rel}}[m/s] + b_d[m/s] \tag{33}$$

$$L_{c+}[m/s] = a_{c+} \times V_{w_{rel}}[m/s] + b_{c+}[m/s] \tag{34}$$

$$L_{c-}[m/s] = a_{c-} \times V_{w_{rel}}[m/s] + b_{c-}[m/s] \tag{35}$$

Where a_n and b_n are calculated according to equations 36 and 37:

$$a_n = \frac{slope[\%]}{100} + \frac{\varepsilon_n}{20} \tag{36}$$

$$b_n = \frac{offset[cm/s]}{100} + \frac{\varepsilon_n}{2} \tag{37}$$

The variable ε_n is a random variable with a zero mean and standard deviation of the object in study depending on n. The n subscript can be changed by d, $c+$ or $c-$ for downwind leeway, right crosswind leeway or left crosswind leeway, respectively. Each ε_n standard deviation is given by one of the nine object parameters. For example, $\varepsilon_d = F_N^{-1}(rnd; 0; Downwind\ std)$, where rnd is a random number between 0 and 1 and $Downwind\ std$ is a parameter that depends on the object type and can be found in the object table in Annex B. Using the same approach, the left crosswind standard deviation and the

right crosswind standard deviation can also be found in the same table, in order to calculate the ε_{c-} and the ε_{c+}, respectively.

Using equation 31 divided by the time interval, the Leeway Velocity can be represented by equation 38 as:

$$\overrightarrow{V_L}[m/s] = \begin{cases} \overrightarrow{L_d}[m/s] + \overrightarrow{L_{c+}}[m/s], & if\ right \\ \overrightarrow{L_d}[m/s] + \overrightarrow{L_{c-}}[m/s], & if\ left \end{cases} \quad (38)$$

The Leeway vector, $\vec{L}$, translates the influence of the wind in the floating object, but to obtain the total drift vector, $\vec{D}$, that links the initial location (X_i, Y_i) to the final location (X_f, Y_f), it is necessary to add up the current vector, $\vec{C}$, which is the displacement of the floating object by the influence of the current of the sea surface, like shown in equation 39.

$$\vec{D} = \vec{L} + \vec{C} \quad (39)$$

To determine the Leeway vector, it is necessary to multiply the Leeway velocity calculated in equation 29 by the time spent by the object drifting in the water (equations 40 and 41).

$$\vec{L} = \Delta t\ .\overrightarrow{V_L} \quad (40)$$

$$\vec{L} = (L_x, L_y) = \Delta t\ .[V_L.\cos(\theta_W - L_\alpha)\ , V_L.\sin(\theta_W - L_\alpha)] \quad (41)$$

Just like for the Leeway vector, the current vector is calculated from a velocity multiplied by the time of the drift. In this case the velocity used for the calculations is the current velocity, as seen in equation 42 which is decomposed in its respective X and Y components in equation 43.

$$\vec{C} = \Delta t\ .\overrightarrow{V_C} \quad (42)$$

$$\vec{C} = (C_x, C_y) = \Delta t\ .(V_C.\cos\theta_C\ , V_C.\sin\theta_C) \quad (43)$$

From equation 39, the total drift vector can be written as shown in equation 44:

$$\vec{D} = (D_x, D_y) = (L_x + C_x, L_y + C_y) \quad (44)$$

Now the drift vector, $\vec{D}$, is used to determine the final location of the drifting object, knowing the initial location, given by equations 45 and 46.

$$(X_f, Y_f) = (X_i, Y_i) + \vec{D} = (X_i + D_x, Y_i + D_y) \tag{45}$$

$$\begin{cases} X_f = X_i + \Delta t.[V_L.\cos(\theta_W - L_\alpha) + V_C.\cos(\theta_c)] \\ Y_f = Y_i + \Delta t.[V_L.\sin(\theta_W - L_\alpha) + V_C.\sin(\theta_c)] \end{cases} \tag{46}$$

This is the main formulation used to develop the tool for trajectory and final location prediction of an object drifting on the ocean surface subjected to wind and current forces. It should be noticed that a few more details need to be provided. The first one is the transformation of these final X and Y coordinates in final Latitudes and Longitudes in order to represent them over an Earth map and use the output of the simulation to search for the missing object. Another aspect that has been considered in the developed tool is the adding of a random initial drift either to the right or left sides since it is almost impossible to know the initial position of a drifting object. A probability of jibing of the object during the time of drift is also considered to get a simulation closer to reality where the waves or some random wind and current forces make the object rotate and change the side facing the wind and, consequently, create a different trajectory. Finally, some plots are created to provide a better understanding of the trajectories and final locations of the object calculated by the simulation.

To transform the final X and Y coordinates of the object location in Latitude and Longitude, the Haversine Formula (Veness, 2018) is used, which provides the final location from a distance and bearing from a starting point. To calculate the final Latitude and Longitude (Lat_f, Lon_f) the inputs are: the initial Latitude and Longitude (Lat_i, Lon_i), the initial location (X_i, Y_i) and the final location (X_f, Y_f) as given by equation 47.

$$\begin{cases} Lat_f = \sin^{-1}(\sin(Lat_i) \times \cos(\delta) + \cos(Lat_i) \times \sin(\delta) \times \cos(\alpha_b)) \\ Lon_f = Lon_i + atan2\big(\cos(\delta) - \sin(Lat_i) \times \sin\big(Lat_f\big), \sin(\alpha_b) \times \sin(\delta) \times \cos(Lat_i)\big) \end{cases} \tag{47}$$

Where δ is the angular distance and α_b is the bearing angle (clockwise from the North).

Note that $atan2(X,Y)$ is the arctangent of a point with X and Y coordinates instead of the conventional arctangent of a single number $\mathrm{atan}(num)$. It is also important to say that the $atan2$ function is used in many programs with X and Y parameters the other way around, as so: $atan2(\mathrm{Y},\mathrm{X})$.

Equation 48 shows the way of calculating the angular distance of a point.

$$\delta = \frac{d}{R} \tag{48}$$

Where d is the distance between the initial and final locations and R is the Earth radius used as 6371 km.

The distance between the initial and final locations of a drifting object can be described by equation 49:

$$d = \sqrt{\left(Y_f - Y_i\right)^2 + \left(X_f - X_i\right)^2} \tag{49}$$

It is important to note that the Haversine Formula used is a simplified calculation that uses the Earth as a sphere with the same radius R all around, but as it is known, the planet has an ellipsoid shape, meaning this approximation will create an error associated of around 0.3% according to Veness (2018), which is good enough for the purposes of this work due to the unpredictability of factors as the wind and current.

Since it is almost impossible to know the position of a missing object relative to the wind direction, a fifty-fifty probability is introduced to the object start drifting being to right or left side of the relative wind vector (check Figure 11), meaning a positive or negative leeway angle.

To improve the developed tool, at the end of every hour of drift, a 4% probability of jibing is introduced (Allen, 2005) in order to simulate the hypothesis of the object to rotate due to waves or some other force acting on it that will invert the leeway angle and, consequently, changing its course over time. Note that both these probabilities can be changed as an input depending on the information available from the object.

The jibing likelihood has been considered to occur every span of one hour to get some detail in the trajectory of the object overtime. This time interval can be reduced, but that would increase the complexity of the simulation process and so its computational time. So, the time of one hour has been adopted given the balance detail-complexity of the tool developed.

Since the probability of jibing is introduced every one hour of simulation, the random numbers associated with the wind and current velocities and directions, following normal distributions, are also generated at

the end of every hour with the objective of introducing slight changes to the wind and current velocity vectors that in real conditions may change over time.

After all the calculations conducted by the tool, it is necessary to present the results into a more user-friendly way. For this purpose, several graphics have been created. The first one shows the trajectory of each sample element with a different color to have an idea of the trajectory possibilities of the object. Defining each sample element as having a point of double coordinates (X, Y) every hour, each sample element has its own scatter graph series. The software used has a limitation on the number of series used in each graphic (255 series), so it is not possible to represent all the 1000 sample trajectories in the same graphic. However, 255 trajectories are more than enough to have a representative view of the possible trajectories of an object. The second graphic created is a scatter plot with only two series of X and Y coordinates: initial location and final location of the objects at the end of the entire simulation. Each series has 1000 points representing the entire sample simulated.

The object final location coordinates are then further analyzed using *Matlab*. The *Matlab* scripts are available in Annexes H and I. First of all, a histogram analysis is performed in both X and Y directions to determine what would be the best probability model that fits the simulation results. Since the final location points are spread over an area where there is one or more maximum probability locations and the number of points decreases away from those locations, the histograms will tell whether the best model is a single or a combination of several normal distributions, i.e. by a Gaussian Mixture Model (GMM).

After determining the number of normal distributions of the GMM, an estimate of the bivariate normal distribution is calculated and its probability density function (pdf) is drawn in a three-dimensional surface plot. The GMM is then intersected by horizontal planes of different heights to obtain the POC of an object. In particular, the 95% POC curve for every scenario is derived for comparing the different scenarios analyzed.

Additionally, on top of the sample points and the POC curves, the circular search areas following the Datum method proposed by the Australian National SAR Manual (2018) are drawn. These areas are compared to the areas of the POC curves.

5. Simulation of different scenarios

An analysis of different scenarios of drifting objects is taken in consideration with the objective of comparing the tool, developed from the basic formulations of the forces applied to an object floating on the sea surface described in detail in the previous chapter, with the *Opendrift* software. The results of the simulation of these scenarios are presented and analyzed in detail in Chapter 6.

The scenarios selected represent typical wind and current conditions at some specific locations important to study along the Portuguese coast.

5.1. Scenario 1 (Location 1, Object 1)

The first scenario takes place around 50 nautical miles off the Cabo da Roca and has the typical Summer conditions in Portugal with strong Northern winds, and the object lost at sea is a Person in Water (1. PIW). This is a situation that unfortunately occurs many times, usually being fishermen that fall from fishing vessels. Someone that knows the place the fishing vessel is supposed to be fishing at 09:00 in the morning on the 9th of May 2018 informed the authorities. The object drifts for 8 hours in scenario 1. Figure 16 and Figure 17 represent the wind direction and velocity and the current direction and velocity for scenario 1 taken from the Windy website (Lukačovič, 2018).

In case the object drifts to the shore line, which is not the case for scenario 1, the *Opendrift* can act like there is no shoreline, which means some particles can continue floating inland like there was no shore, or the Opendrift script can be edited in order to create an interaction between the object and the shoreline, either to get stranded and not move anymore or if the drift pushes the object offshore again, it gets back to the ocean after hitting land. The script for scenario 1 *Opendrift* prediction is available in Annex D.

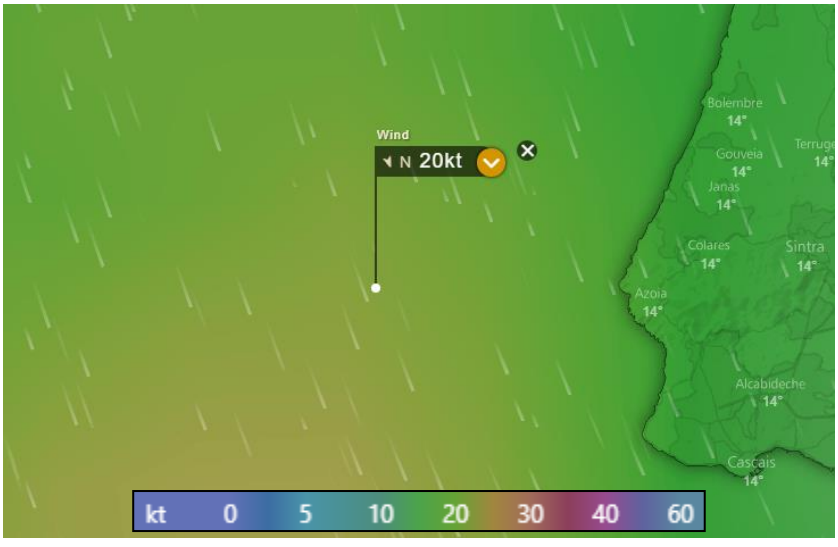

Figure 16 - Scenario 1 wind direction and velocity, taken from Lukačovič (2018)

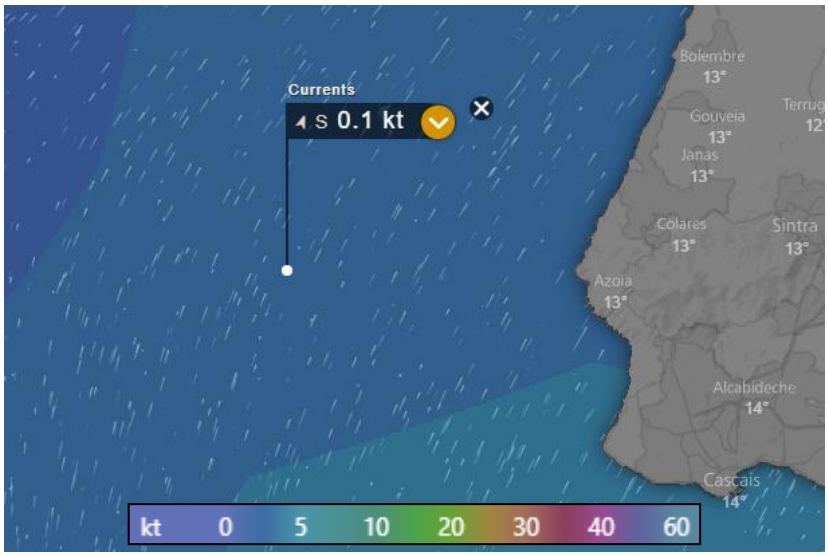

Figure 17 - Scenario 1 current direction and velocity, taken from Lukačovič (2018)

List of Inputs:

- Initial location latitude coordinate value, $Lat_i = 38.780753$ [deg];
- Initial location longitude coordinate value, $Lon_i = -10.521936$ [deg];
- Time of the initial location, $t_i = 09{:}00, 9^{th}\ of\ May\ 2018$ [d];
- Time of the final location, $t_f = 17{:}00, 9^{th}\ of\ May\ 2018$ [d];
- Wind velocity value, $V_w = 20$ [kt];
- Wind direction value, $\alpha_w = 165$ [deg];
- Current velocity value, $V_c = 0.1$ [kt];
- Current direction value, $\alpha_c = 30$ [deg];
- Object type =1 -> PIW-1: Person-in-water (PIW), unknown state (mean values);
- Initial location X coordinate upper value of probability interval, $c_{Xi} = 0.2$ [NM];
- Probability of value X being inside the probability interval, $P_{Xi}(-c_{Xi} \leq X \leq c_{Xi}) = 0.8$;
- Initial location Y coordinate upper value of probability interval, $c_{Yi} = 0.2$ [NM];
- Probability of value Y being inside the probability interval, $P_{Yi}(-c_{Yi} \leq Y \leq c_{Yi}) = 0.8$;

5.2. Scenario 2 (Location 2, Object 2)

The second scenario takes place around half way between Porto and Azores islands in a day with calm weather conditions. The object lost at sea is a mono-hull sailing vessel with fin keel and shallow draft. The vessel communicated their location via GPS at 18:00 on the 10th of May 2018 and said they had no means of propulsion. The object drifts for 40 hours for the scenarios 2, 3 and 4. Figure 18 and Figure 19 represent the wind direction and velocity and the current direction and velocity for scenarios 2, 3 and 4. The *Opendrift* script for scenario 2 is available in Annex E.

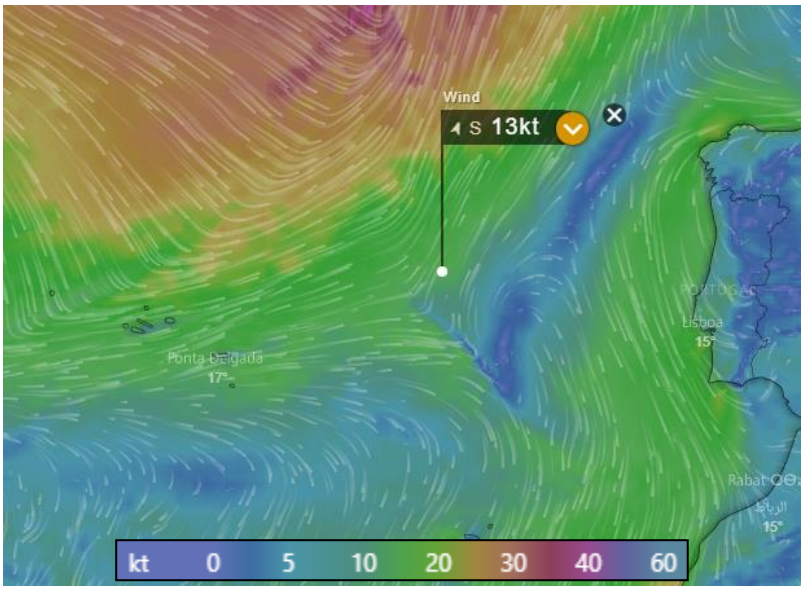

Figure 18 - Scenario 2, 3 and 4 wind direction and velocity, taken from Lukačovič (2018)

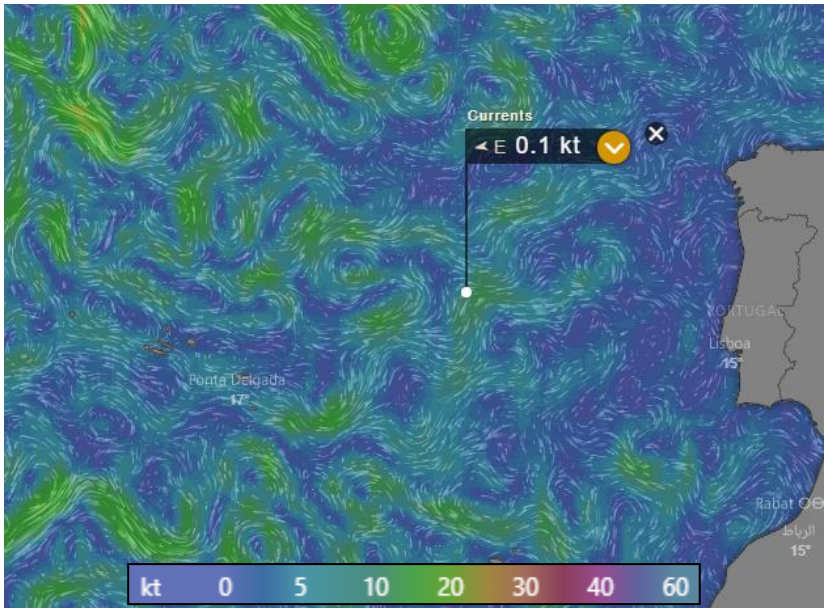

Figure 19 - Scenario 2,3 and 4 current direction and velocity, taken from Lukačovič (2018)

List of Inputs:

- Initial location latitude coordinate value, $Lat_i = 40.000$ [deg];
- Initial location longitude coordinate value, $Lon_i = -18.000$ [deg];
- Time of the initial location, $t_i = 18{:}00, 10^{th}\ of\ May\ 2018$;
- Time of the final location, $t_f = 10{:}00, 12^{th}\ of\ May\ 2018$;
- Wind velocity value, $V_w = 13$ [kt];
- Wind direction value, $\alpha_w = 20$ [deg];
- Current velocity value, $V_c = 0.1$ [kt];

- Current direction value, $\alpha_c = 260$ [deg];
- Object type = 64 -> SAILBOAT-7: Sailboat Mono-hull, fin keel, shallow draft;
- Initial location X coordinate upper value of probability interval, $c_{Xi} = 0.05$ [NM];
- Probability of value X being inside the probability interval, $P_{Xi}(-c_{Xi} \leq X \leq c_{Xi}) = 0.9$;
- Initial location Y coordinate upper value of probability interval, $c_{Yi} = 0.05$ [NM];
- Probability of value Y being inside the probability interval, $P_{Yi}(-c_{Yi} \leq Y \leq c_{Yi}) = 0.9$;

5.3. Scenario 3 (Location 2, Object 3)

Scenario 3 is identical to scenario 2, the only difference is the type of object missing, now being a person in a survival suit with the face up. The *Opendrift* script for scenario 3 is available in Annex F.

List of Inputs:

- Initial location latitude coordinate value, $Lat_i = 40.000$ [deg];
- Initial location longitude coordinate value, $Lon_i = -18.000$ [deg];
- Time of the initial location, $t_i = 18{:}00, 10^{th}\ of\ May\ 2018$;
- Time of the final location, $t_f = 10{:}00, 12^{th}\ of\ May\ 2018$;
- Wind velocity value, $V_w = 13$ [kt];
- Wind direction value, $\alpha_w = 20$ [deg];
- Current velocity value, $V_c = 0.1$ [kt];
- Current direction value, $\alpha_c = 260$ [deg];
- Object type =4 -> PIW-4: PIW, survival suit (face up);
- Initial location X coordinate upper value of probability interval, $c_{Xi} = 0.05$ [NM];
- Probability of value X being inside the probability interval, $P_{Xi}(-c_{Xi} \leq X \leq c_{Xi}) = 0.9$;
- Initial location Y coordinate upper value of probability interval, $c_{Yi} = 0.05$ [NM];
- Probability of value Y being inside the probability interval, $P_{Yi}(-c_{Yi} \leq Y \leq c_{Yi}) = 0.9$;

5.4. Scenario 4 (Location 2, Object 4)

Scenario 4 has all the same inputs as scenario 2 and 3 but the type of object missing is now the object is a light loading life raft with capacity for 4 to 14 people, a deep ballast system, canopy and drogue. The *Opendrift* script for scenario 4 is available in Annex G.

List of Inputs:

- Initial location latitude coordinate value, $Lat_i = 40.000$ [deg];
- Initial location longitude coordinate value, $Lon_i = -18.000$ [deg];
- Time of the initial location, $t_i = 18{:}00, 10^{th}\ of\ May\ 2018$;
- Time of the final location, $t_f = 10{:}00, 12^{th}\ of\ May\ 2018$;
- Wind velocity value, $V_w = 13$ [kt];
- Wind direction value, $\alpha_w = 20$ [deg];

- Current velocity value, $V_c = 0.1$ [kt];
- Current direction value, $\alpha_c = 260$ [deg];
- Object type = 13 -> LIFE-RAFT-DB-16: 4-14 people capacity, deep ballast system, canopy, with drogue, light loading;
- Initial location X coordinate upper value of probability interval, $c_{Xi} = 0.05$ [NM];
- Probability of value X being inside the probability interval, $P_{Xi}(-c_{Xi} \leq X \leq c_{Xi}) = 0.9$;
- Initial location Y coordinate upper value of probability interval, $c_{Yi} = 0.05$ [NM];
- Probability of value Y being inside the probability interval, $P_{Yi}(-c_{Yi} \leq Y \leq c_{Yi}) = 0.9$;

6. Results and analysis

For each scenario plots of the objects' trajectories, initial and final locations are also created using *Opendrift*. These results are then compared with the trajectories and the initial and final locations of the objects calculated using the tool developed. After the comparison, the sample of the final locations of the object is used to define a bivariate GMM in order to obtain the closed curve that represents the 95% probability area. This area is then compared to the area defined by an empirical method proposed in the Australian SAR Manual (Australian National Search Rescue Council, 2018).

6.1. Scenario 1

Scenario 1 has the shortest simulation time of all scenarios, 8 hours. Figure 20 shows in green the initial locations of the 1000 particles and in blue their final locations predicted by *Opendrift*.

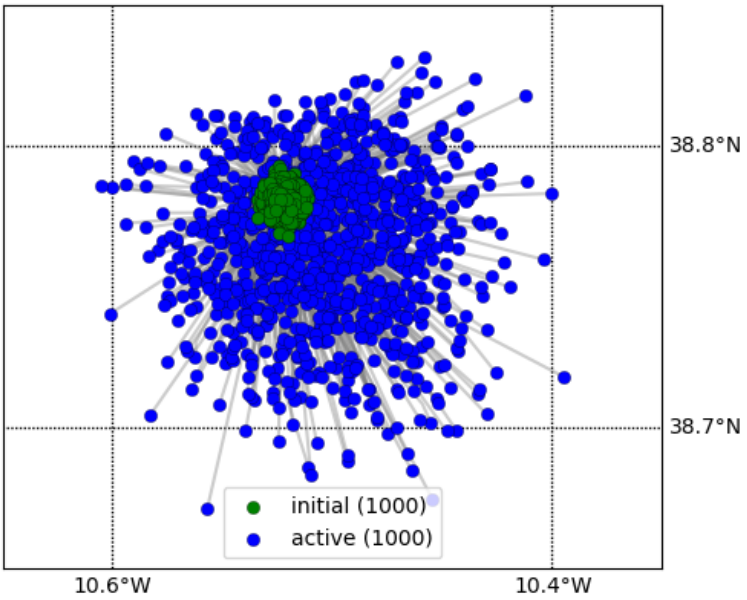

Figure 20 - Trajectories with initial and final object locations simulated using *Opendrift* for scenario 1

Figure 21 presents the particles' trajectories simulated by the developed tool. Due to a software limitation, only 255 out of 1000 particles are drawn, however, in Figure 22, all particles' initial and final locations are represented.

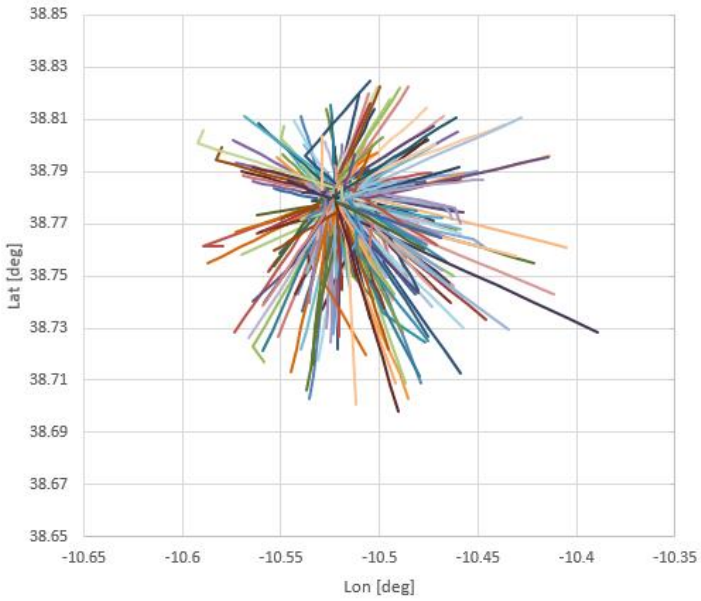

Figure 21 – 255 trajectories simulated using the developed tool for scenario 1

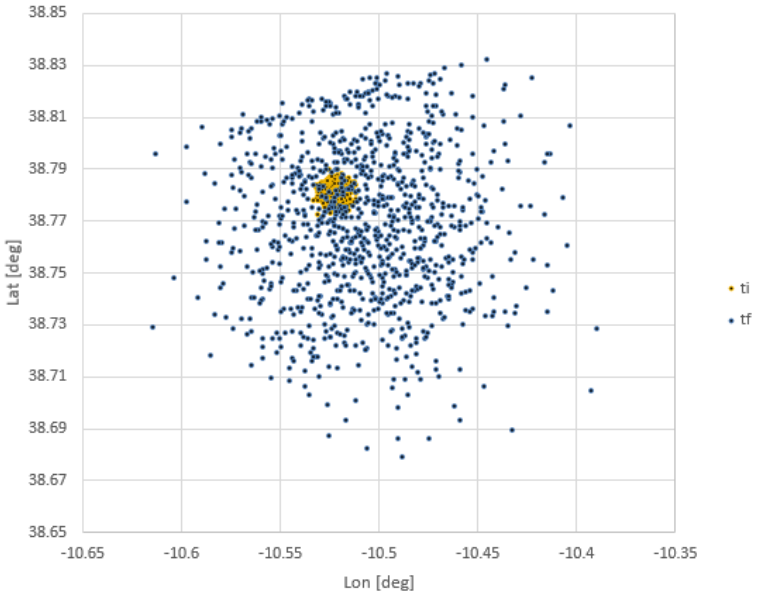

Figure 22 - Initial and final object location of 1000 simulations using the developed tool for scenario 1

Comparing Figure 20 and Figure 22, although the points are not exactly in the same place because in both cases they are generated randomly, from a normal distribution in both downwind and crosswind directions, it is easy to see that the dispersion of points is similar. In this case scenario, the particles spread in all directions, because of the current direction and because the object type is a general PIW, which means the standard deviations for both DWL and CWL are large in relation to better defined objects. A PIW is one of the object types that can have larger differences (tall person, small person, heavy person, light person, adult, children, swimming, quiet…), which contributes to a high value of standard deviation of the object trajectory.

Having as the basis the final locations of the particles in scenario 1 predicted by the tool developed, it is possible to derive the pdf of the points in order to obtain the 95% probability area in which the object can be. To find the adequate distribution, it is necessary to draw a histogram of the final locations in X and Y directions in order to determine if in each direction the histogram would be better represented by one or by a mixture of several normal distributions.

Figure 23 and Figure 24, show one peak in each direction and therefore the best fit for scenario 1 would be a bivariate normal distribution (X and Y) with only one normal pdf in each direction. This means the joint pdf for scenario 1 has only one maximum. The joint pdf can be observed in Figure 25.

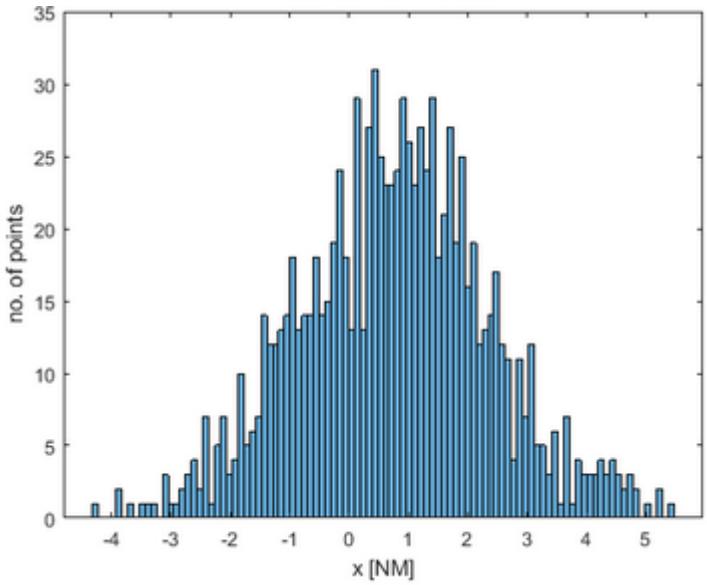

Figure 23 - Histogram of the object final locations in the X direction for scenario 1

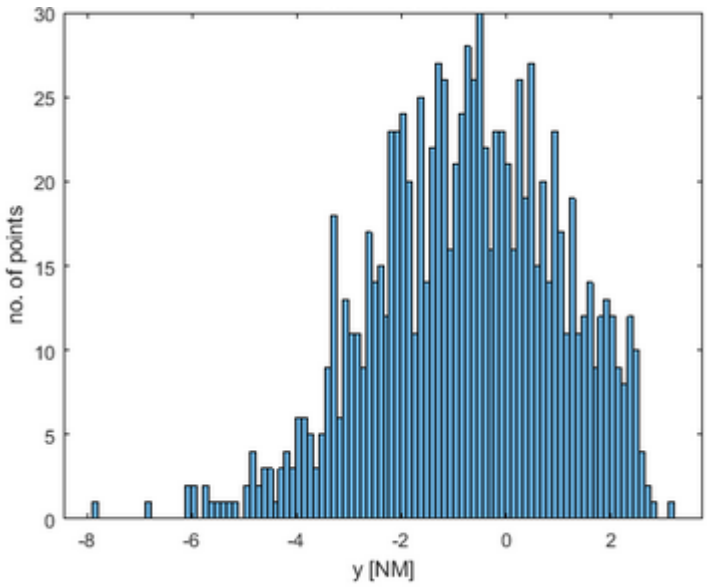

Figure 24 - Histogram of the object final locations in the Y direction for scenario 1

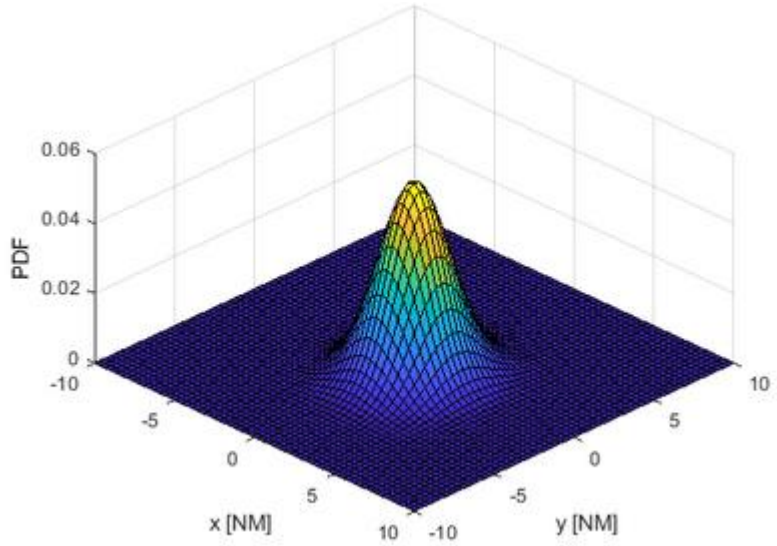

Figure 25 – Joint pdf of the object final locations for scenario 1

The volume under the joint pdf is always equal to one. If a horizontal plane cuts that volume a closed curve is obtained. As the normal distributions in *X* and *Y* directions have different standard deviations, the curve obtained is necessarily an ellipse. That ellipse defines the 95% probability of an object being in its area. The probability associated to the ellipse area depends on the height of the horizontal cutting plane. The volume corresponds to the space under the pdf surface that is inside the ellipse contour.

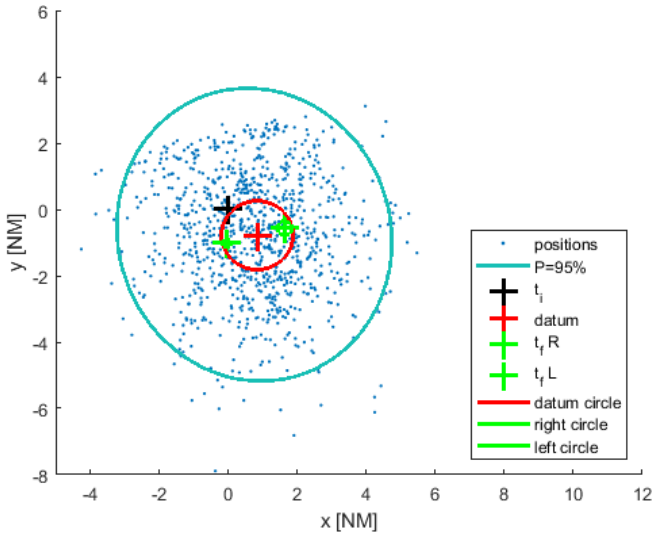

Figure 26 – Simulated object final locations, 95% probability area and datum circle for scenario 1

Figure 26 shows the simulated final locations of the object and the ellipse corresponding to the 95% probability area in blue (“P=95%”). Figure 26 also shows the empirical searching area suggested by the Australian National Search Rescue Council (2018) in red that is also called drift error circle or *datum circle*. In order to get the *datum circle*, it is necessary to add to the LKP point (t_i) the current vector and the leeway vector for both right and left drifts. Adding both vectors to the t_i location point,

the green points, $t_f R$ and $t_f L$, are obtained for the right and left drifts, respectively, representing the final locations of the object. To get an area is necessary to have some kind of error associated, otherwise the graphic would only represent these two final location points. Because of that, a circle is drawn around each green point with the radius of 12.5% of the distance between the LKP and the respective final location point, *right circle* and *left circle*. The *datum circle* is the smallest circle containing both the right and left circles. The radius of the datum circle in red is the drift error itself. The center of the circle is called datum point and it is in line with the right and left points.

Analyzing the 95% probability areas calculated by the developed tool and the drift area calculated from the empirical formulae suggested by the Australian National Search Rescue Council (2018), one can see a large difference between them. This can be explained by the fact that the empirical formulas always use the 12.5% of the distance from the LKP for the radius of the right and left circles. This value is equal for every type of object but in *Opendrift* software and in the tool developed, each type has its own standard deviations and consequently the area is influenced by that. In this scenario the standard deviations are quite large, so the dispersion of the points is also larger than the datum circle area. Another factor that makes the ellipse even larger than the datum circle is the fact that the LKP in *Opendrift* and in the developed tool, also follows a normal distribution, so every particle starts its motion from a different location, contrasting with the empirical formulation where the LKP is a fixed point. Note that there is a large difference between the values of the areas from the developed tool and the empirical formulation meaning that the empirical formulae do not take into account as much uncertainties as the developed tool. The empiric searching area corresponds to a POC of the object of about 17% only, considering the simulation of the object final locations by the developed tool. This means that the empirical formulae are not a good way to define searching areas for short time simulations as in this scenario (8 hours). The fact that the shapes of both areas are different from each other, one being an ellipse and the other being a circle can be important in cases where the leeway angle is quite large, which is not the case because in this scenario 1 the ellipse axis are not very different.

6.2. Scenario 2

This scenario is the first of three with the same inputs of simulation, in which the only difference among them is the type of object drifting. In scenario 2 the object in study is a mono-hull sailboat with fin keel and shallow draft. Figure 27 represents the initial location points, trajectory lines and final object locations obtained by the *Opendrift* simulation.

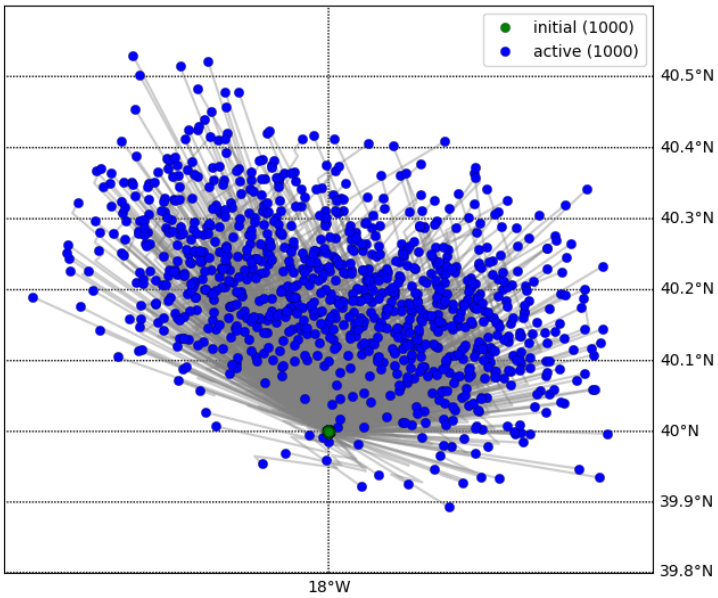

Figure 27 - Trajectories with initial and final object locations simulated using *Opendrift* for scenario 2

Figure 28 and Figure 29 show the same type of results, but obtained using a tool developed specifically in this dissertation. The first one represents the trajectory lines for 255 of the 1000 particles and the second one represents the initial and final locations of all the 1000 particles obtained by MCS.

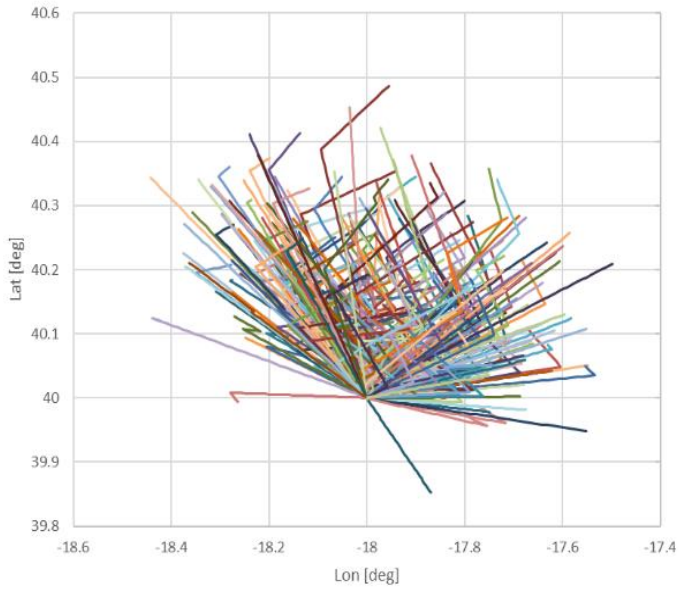

Figure 28 - 255 trajectories simulated using the developed tool for scenario 2

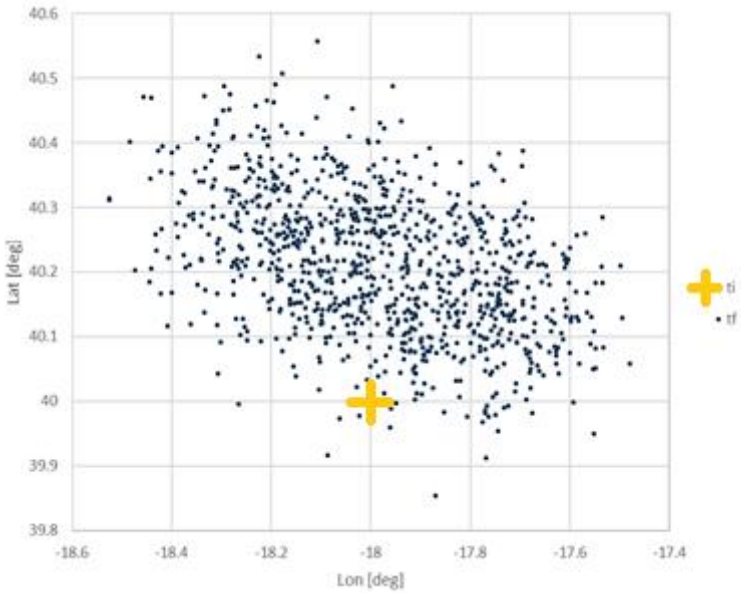

Figure 29 - Initial and final object locations of 1000 simulations using the developed tool for scenario 2

As in scenario 1, the sample of final object locations predicted by the tool is consistent with the one obtained by *Opendrift* in shape and size. In this scenario the shape of the sample of object final locations is more elongated, meaning the CWL has a stronger impact on the trajectory. This phenomenon is a consequence of the sailing boats asymmetry in shape between its bow and stern. Because in this case the time window of simulation is much longer, the final locations of the object are much more spread than in scenario 1.

The histograms of the object final locations for scenario 2, shown in Figure 30 and Figure 31, also indicate that a single bell shape curve would fit them the best, so a bivariate normal distribution is adopted to describe the location uncertainty. The resulting joint pdf is shown in Figure 32. It is perceptible that the surface peak is narrower in the Y direction than in the X direction, just like the histograms shown in Figure 30 and Figure 31.

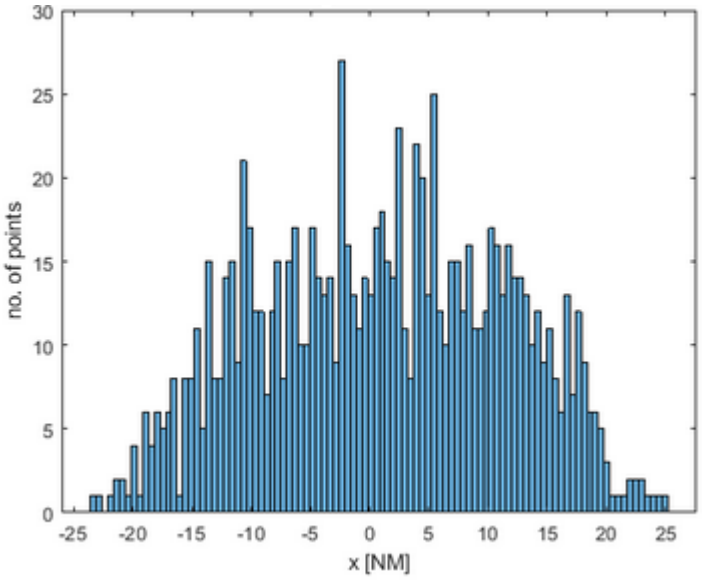

Figure 30 - Histogram of the object final locations in the X direction for scenario 2

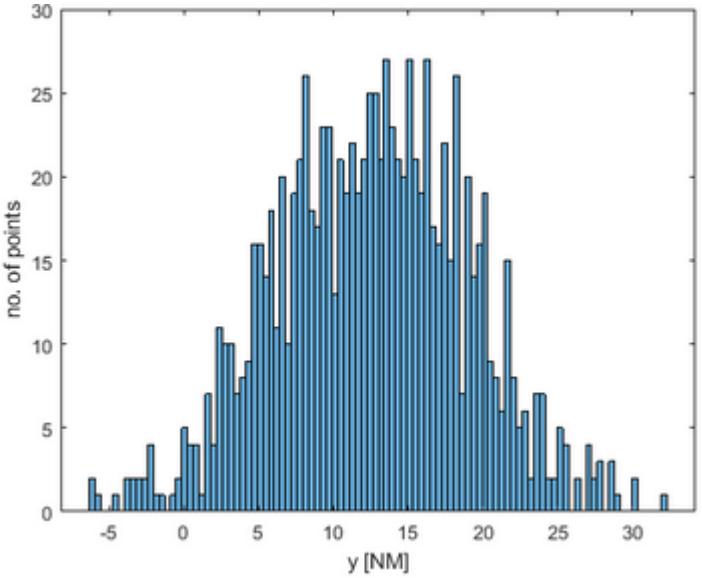

Figure 31 - Histogram of the object final locations in the Y direction for scenario 2

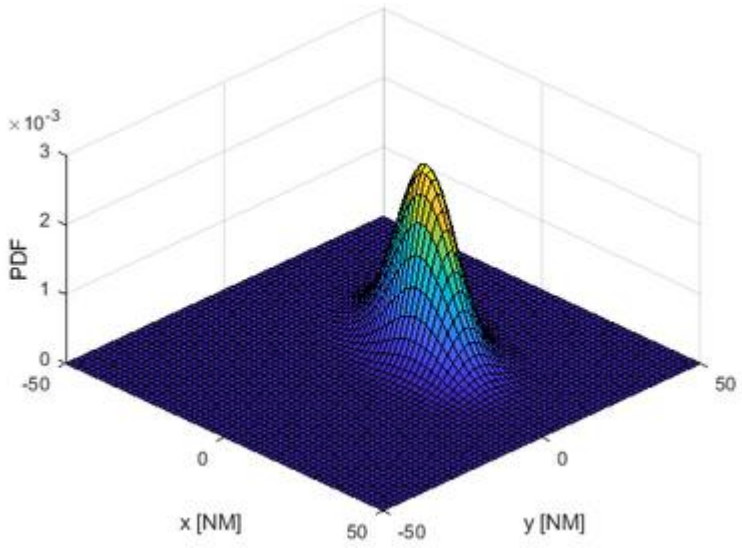

Figure 32 – Joint pdf of the object final locations for scenario 2

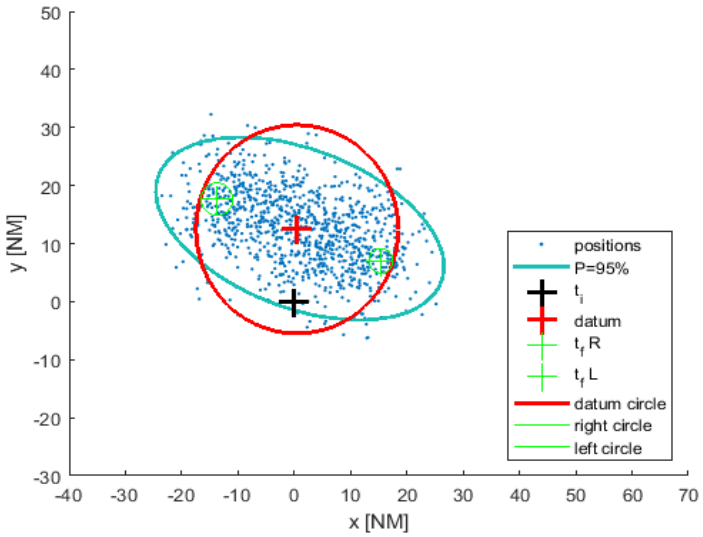

Figure 33 – Simulated object final locations, 95% probability area and datum circle for scenario 2

The results presented in Figure 33 are obtained following the same approach as the one described for scenario 1. As mentioned before, it is now more perceptible the spread of the object final locations. The 95% probability area has a larger ratio between the longer and shorter axis due to that elongation. The drift error, defined by the Australian SAR Manual as the datum circle radius, has a similar value than the ellipse shorter axis and the datum point is really close to the geometric center of the ellipse. The datum circle area is much closer to the ellipse area than in the first scenario and its location and size are more consistent with the ellipse area. The main difference is the fact that the empirical formulae search area does not take into account the greater dispersion perpendicular to the wind speed that is characteristic from asymmetric objects like sailing vessels. The fact that the ellipse has more points inside its perimeter than the datum circle means that if the circle represents a probability value of the object being inside the closed curve, that value would have to be smaller than 95%. Considering the object final locations

obtained by the developed tool, the empirical area corresponds to approximately a 93% POC. This makes the empirical formulation much better for longer simulations like in this scenario (40 hours), than for shorter simulations like in scenario 1 (8 hours).

6.3. Scenario 3

The simulated final object locations in Figure 34 obtained by *Opendrift* look consistent with the ones predicted by the developed tool in Figure 36 and the trajectories are also in line with the initial and final locations. The same graphic scale is used in Figure 29 and Figure 36 to get a better understanding of the differences between objects' drift characteristics. After 40 hours of drifting on the ocean surface, the person in a survival suit with the face up, has a much smaller probability area than the sailing vessel, so it would be less time consuming to search the whole area for the person in a survival suit than for the sailing vessel. However, there are also some other important aspects to take in consideration when searching for a floating object. The size of the object is certainly one of the most important factors since it is much easier to spot a sailing vessel than a person. Another important aspect is the life time of the object. The search for a person in a survival suit is most probably tighter timewise than searching for a sailboat, since the chances of a person surviving many hours in a sailboat should be higher than a person floating just with its survival suit. All these hypotheses assume there is someone onboard the sailing boat. But that is a subject that is not the main focus of this work.

The spread of simulated final locations for this object is more circular shaped than the sailboat sample because the person floating does not have a significant lift force acting on the body, when compared to the sailboats that have a shape designed to achieve that lift force. The lack of that force in this scenario prevents the object to drift long distances in the CWL direction. The fact that the object in this scenario has a smaller projected area subjected to the wind forces is reflected in shorter distances traveled in the DWL direction as well, when compared to scenario 2 object.

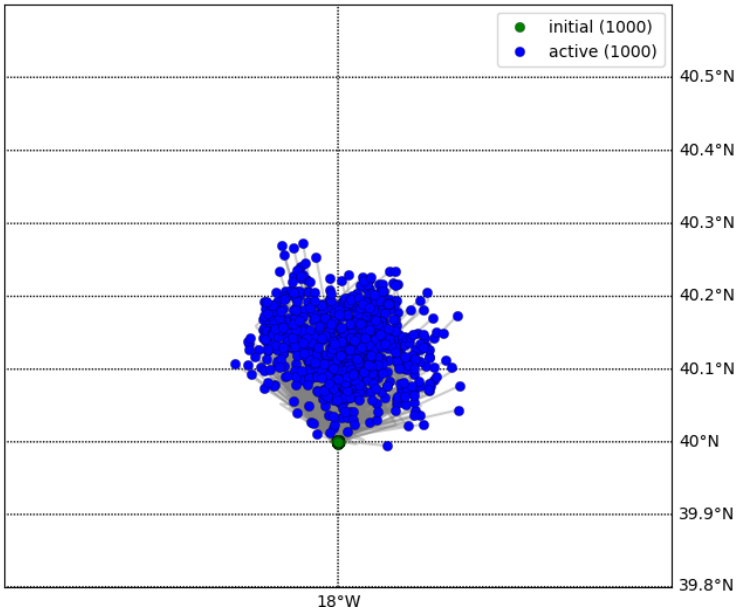

Figure 34 - Trajectories with initial and final object locations simulated using *Opendrift* for scenario 3

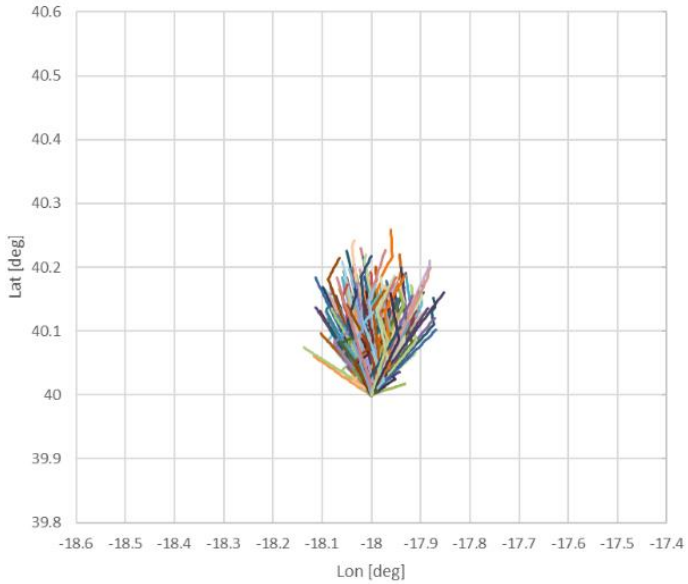

Figure 35 - 255 trajectories simulated using the developed tool for scenario 3

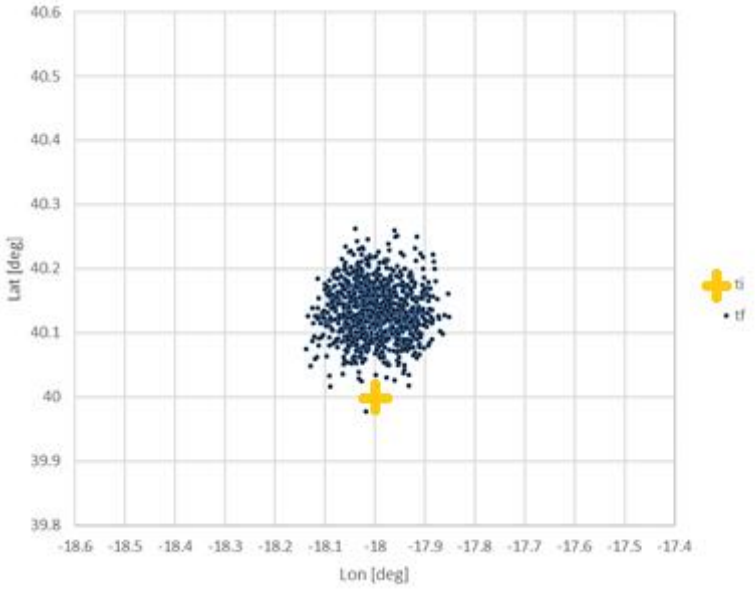

Figure 36 - Initial and final object locations of 1000 simulations using the developed tool for scenario 3

Using the same approach to determine the best pdf fit in the X and Y directions, as in the previous scenarios, the single normal pdfs are the ones giving closer results to the histograms of the object final locations in Figure 37 and Figure 38 for X and Y directions, respectively.

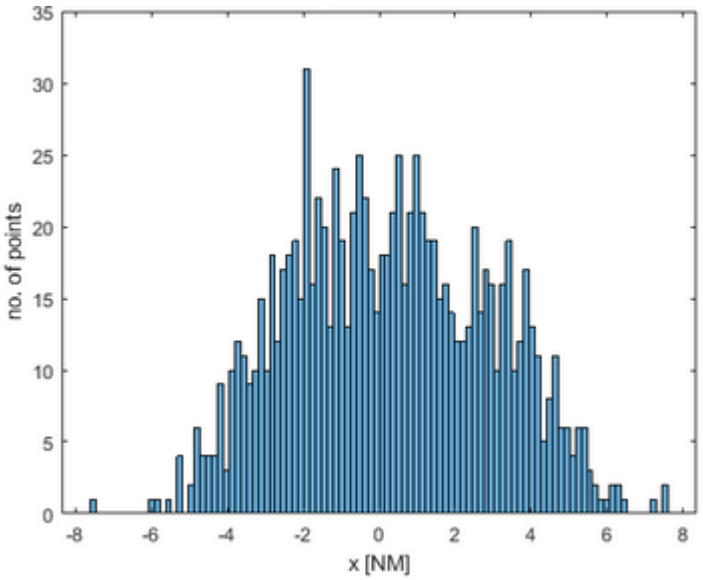

Figure 37 - Histogram of the object final locations in the X direction for scenario 3

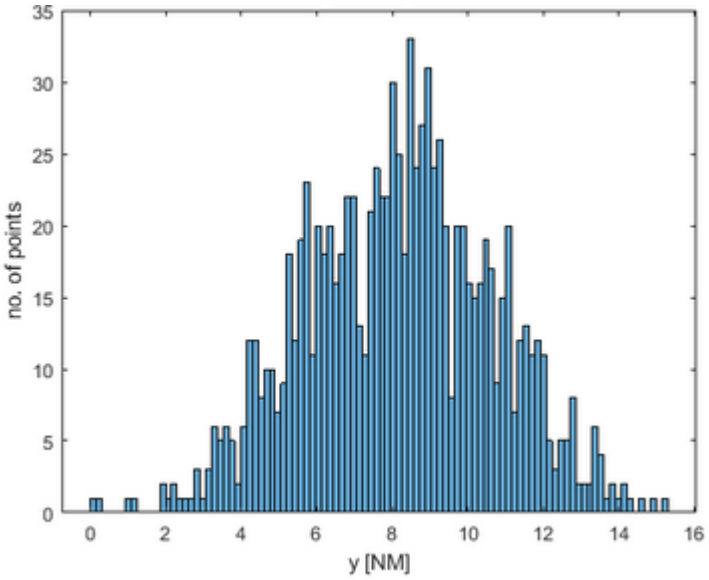

Figure 38 - Histogram of the object final locations in the Y direction for scenario 3

Figure 39 shows the corresponding joint bivariate normal distribution of the object final locations. This shape represents the probability of the object, which started drifting close to the location (0, 0), end up somewhere in the XY plane. The higher the pdf value, the higher the probability of the object location be in that (X, Y) coordinates point. The joint pdf is then used to calculate the 95% probability area represented in blue in Figure 40.

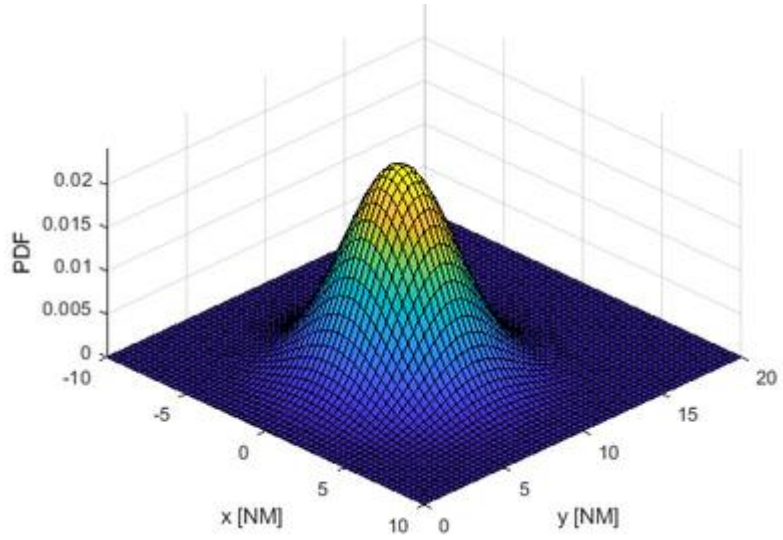

Figure 39 - Joint pdf of the object final locations for scenario 3

As expected from the sample of the object final locations, the ellipse has almost equal values for the long and short axis, giving it a shape close to a circle. The comparison must be done with scenario 1 ellipse because the objects in question have similar characteristics and that can be confirmed by their shape close to a circle. The major difference between the two objects is the standard deviations of the

scenario 1 (PIW) are much larger than the ones from scenario 3 due to the fact that for the general PIW object many characteristics are unknown.

As in Figure 26 and Figure 33, in this scenario the calculated datum circle has a smaller area than the ellipse and, in this case just like in scenario 1, it is totally inside the ellipse. This means that the probability of finding the object within the datum circle is smaller than 95%, as seen in Figure 40. The approximate value for the empirical search area probability of containment is 82%, when considering the object final locations obtained by the developed tool.

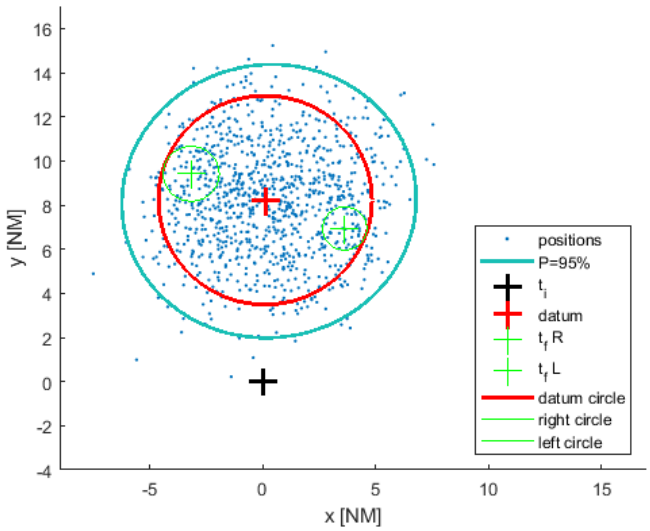

Figure 40 - Simulated object final locations, 95% probability area and datum circle for scenario 3

6.4. Scenario 4

In scenario 4 the output graphics of both *Opendrift* software and the developed tool look really similar to the results of scenario 3. The scenario 4 object is a symmetric raft that has two devices to slow down its drift: deep ballast and a canopy. This means that the sample of the object final locations is quite compact if compared to a simulation of a life raft without those devices. Those devices make the raft move slower and have a behavior close to a PIW. Those devices maintain the search area smaller making it easier to find, in case that information is known by the search planning team. Figure 41 shows the initial and final locations of the object as well as its trajectories for the forty hours' time period, simulated by *Opendrift* software. Figure 42 and Figure 43 show the same information but now from the developed tool simulation. The first one shows the trajectories of 255 of 1000 particles due to a software limitation and the second figure represents the initial and final locations of the floating object.

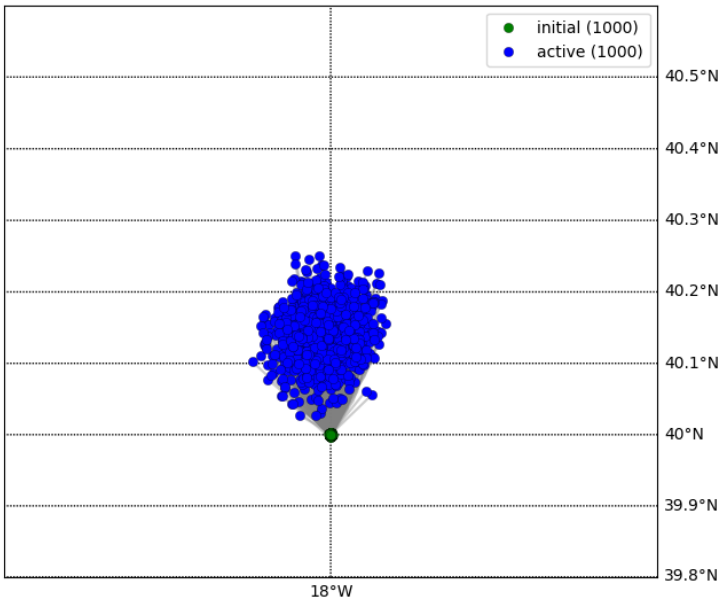

Figure 41 - Trajectories with initial and final object locations simulated using *Opendrift* for scenario 4

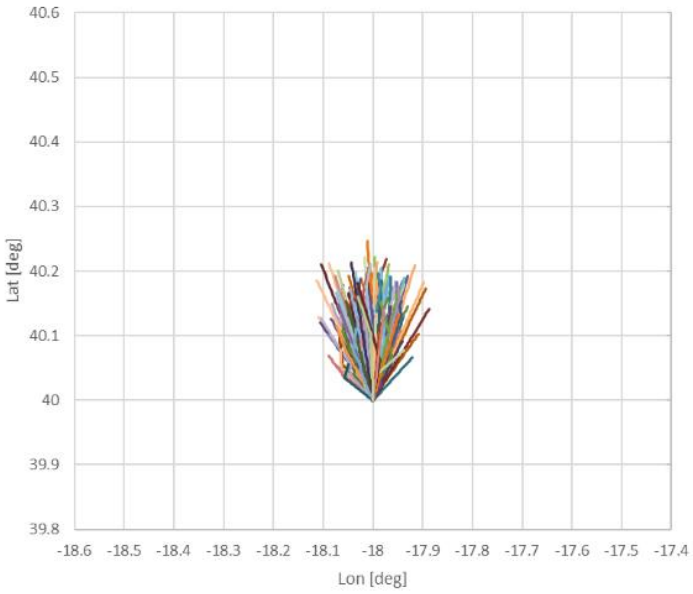

Figure 42 - 255 trajectories simulated using the developed tool for scenario 4

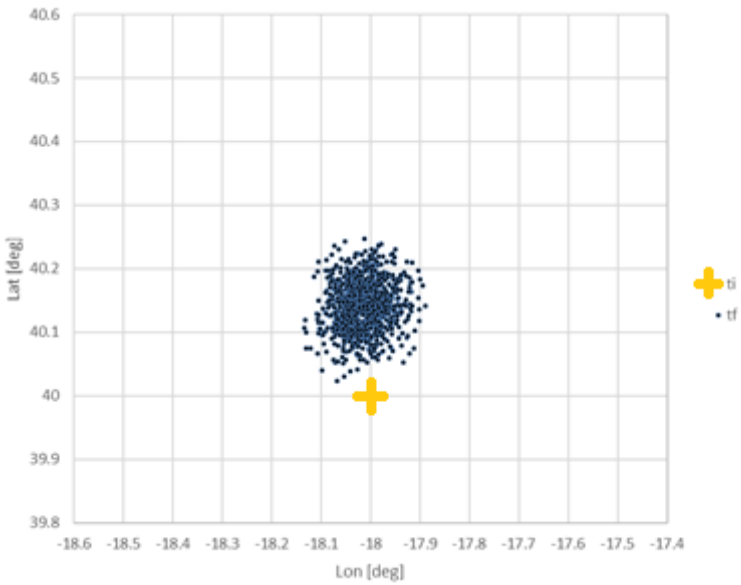

Figure 43 - Initial and final object locations of 1000 simulations using the developed tool for scenario 4

Histograms of the object final locations for axis X and Y are represented in Figure 44 and Figure 45, and like in every other scenario the best pdf fit for the histograms is a single normal pdf because of the “bell shape” with only one peak and vanishing smoothly in both directions.

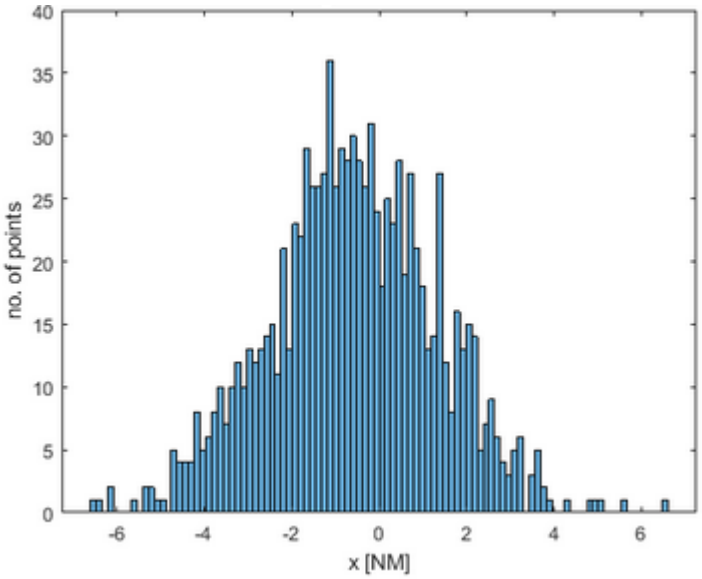

Figure 44 - Histogram of the object final locations in the X direction for scenario 4

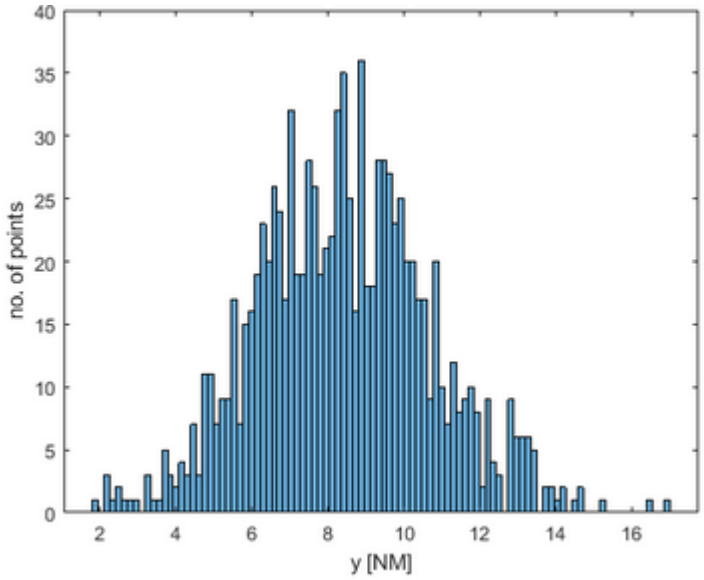

Figure 45 - Histogram of the object final locations in the Y direction for scenario 4

The bivariate normal pdf of the object final locations generated by the developed tool is represented in Figure 46. Unmistakably a one peaked surface is visible as predicted from the histograms' shapes.

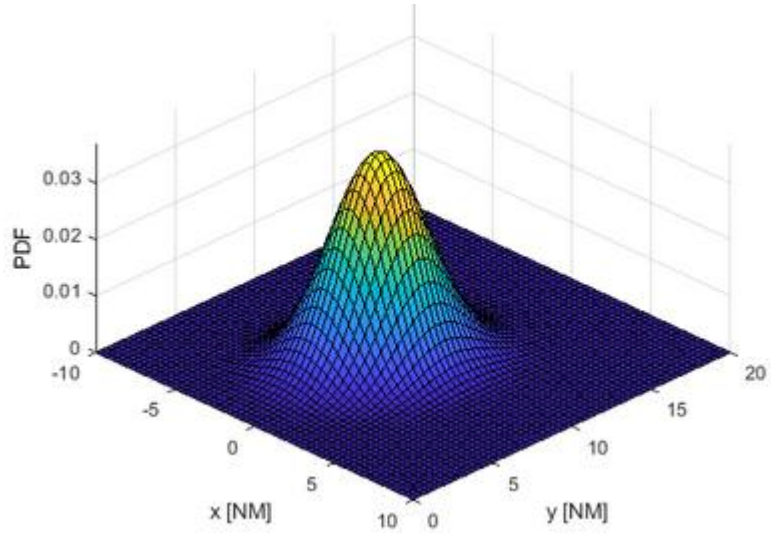

Figure 46 - Joint pdf of the object final locations for scenario 4

Cutting the surface horizontally and calculating a volume of 0.95, produced an ellipse shaped curve shown in blue ("P=95%") in Figure 47. The ellipse is narrower than the one in scenario 3 in the CWL direction due to the object shape symmetry. As well as the ellipse and the sample of the object final locations, the datum point and the circle centered in it are also shown in Figure 47. That circle follows the same pattern in all scenarios, being always inferior than the 95% ellipse area. In this case, the empirical search area corresponds to approximately a 69% POC, considering the object final locations simulated by the developed tool. The approximate POC values for the empirical search areas

considering the object final locations developed by the developed tool are 17%, 93%, 82% and 69% for scenarios 1, 2, 3 and 4, respectively. This means that the developed tool takes in consideration more uncertainties than the empirical formulation, especially in shorter simulations (as in scenario 1). It is also interesting to note that between scenarios 2, 3 and 4, the one with the larger values of crosswind leeway is the second, followed by the third and finally the fourth, which means the empirical search area is closer to the developed tool 95% POC area in size when the crosswind leeway is larger.

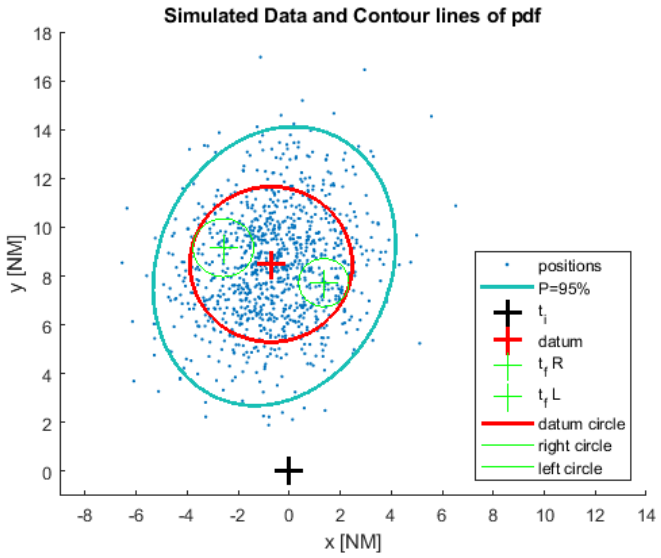

Figure 47 - Simulated object final locations, 95% probability area and datum circle for scenario 4

6.5. Comparisons

Although a bivariate single normal distribution has been the best option for the scenarios analyzed, in some cases the Gaussian mixture model (GMM) is more adequate to represent the uncertainty on the object final location. For example, when the object does not jibe during the simulation time, two separate areas of final locations of the object are obtained, depending on the starting position of the objective relative to the wind direction. Considering the example from scenario 2 but with the probability of jibing equal to zero, the two samples of the object final locations create histograms with two peaks instead of one at least in one of the directions as clearly shown in Figure 48 and Figure 49.

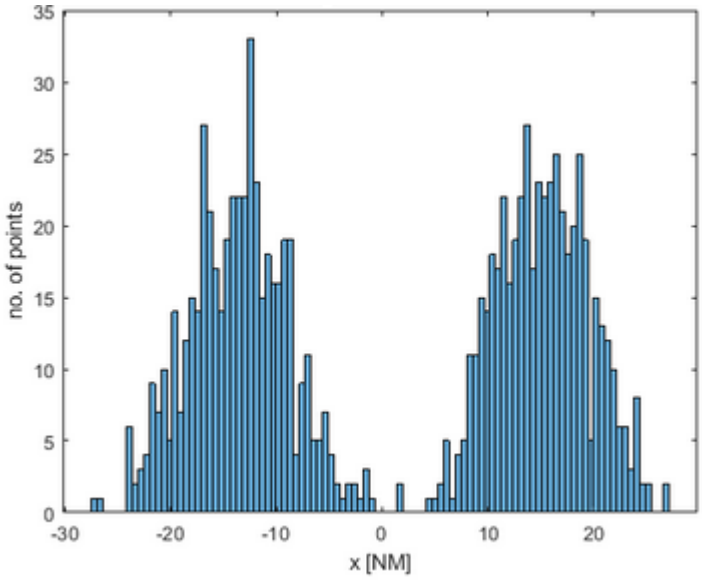

Figure 48 - Histogram of the object final locations in the X direction for scenario 2 without jibing

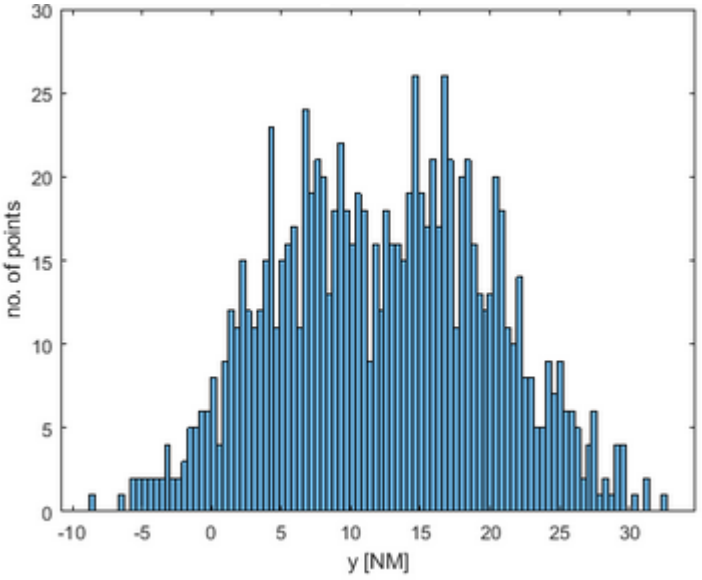

Figure 49 - Histogram of the object final locations in the Y direction for scenario 2 without jibing

The double peak shape in the histograms originates a bivariate GMM pdf surface with two maximums as shown in Figure 50.

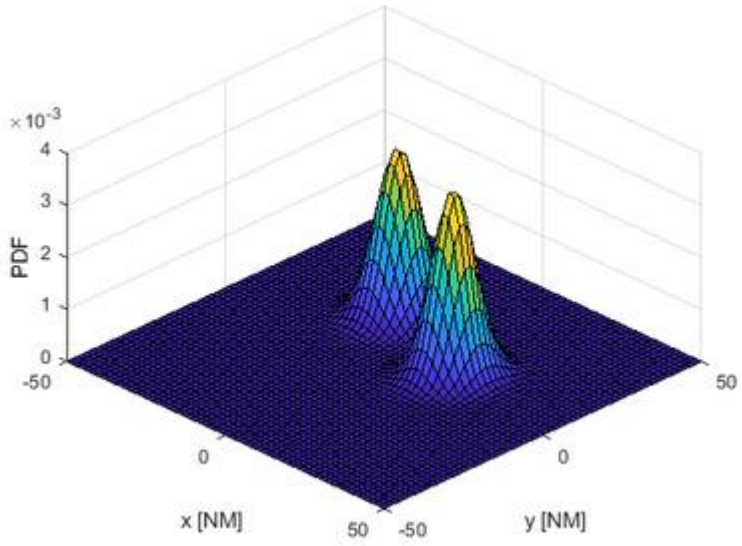

Figure 50 - Joint pdf of the object final locations for scenario 2 without jibing

This distribution causes Figure 51 to show two ellipses instead of one, for the right and left drifts separately. So, there is approximately 95% chances of the object location be inside one of the two ellipses. However, it is not possible to change the jibing probability in the empirical formulae, so the circle obtained is exactly the same as in scenario 2. If the empirical formulae considered the same uncertainties than the developed tool, the datum circle should contain both ellipses and be tangent to both of them.

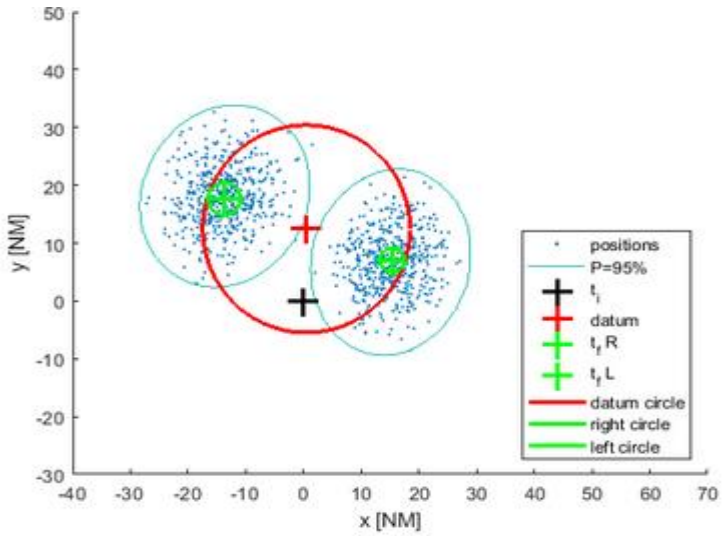

Figure 51 - Simulated object final locations, 95% probability area and datum circle for scenario 2 without jibing

An interesting study is the superposition of the searching areas from scenarios 2, 3 and 4 since all of them have the same inputs with exception to the type of object. The graphic shown in Figure 52 provides a comparison between the 95% probability areas from scenarios 2, 3 and 4. The larger area represents the sailboat simulated locations, the middle one represents the PIW in a survival suit and the smallest

area represents the simulated locations of the life raft. There is a large difference between the sailboat area and the two other object areas given the influence of the wind in the sailboat in comparison to the PIW and the raft.

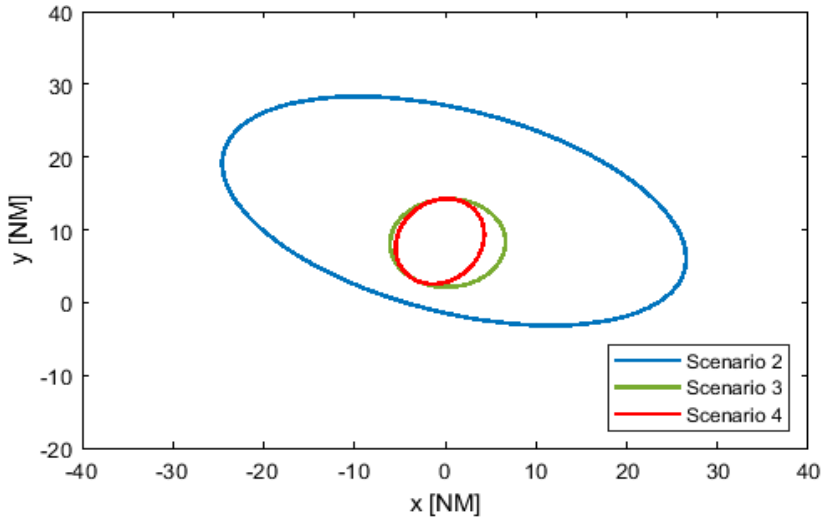

Figure 52 - 95% probability areas for scenarios 2, 3 and 4

The areas represented in the graphic are 1125.375 NM^2, 122.750 NM^2 and 79.750 NM^2, for scenarios 2, 3 and 4 respectively. The fact that the sailboat searching area is about 9 and 14 times larger than the PIW and life raft areas respectively, it does not mean it is harder to find the sailing vessel. The sailboat can be spotted from a longer distance because of its dimensions. So, the area must always be compared taking in consideration the degree of difficulty to spot the object, either because of its size, color or shape, as mentioned before in Chapter 3 when discussing the POS.

7. Conclusions

In this dissertation a basic drifting model has been implemented to simulate the trajectories of drifting objects at sea using MCS, taking in consideration the uncertainties associated to the process.

The dissertation has presented an overview of the maritime SAR operations structure in Portuguese waters and an analysis of the casualties and incidents, which has shown that the fishing and cargo vessels are the ones requiring more SAR operations and that most of the accidents in Portuguese waters take place within 12 miles from shore.

Four different scenarios have been defined and analyzed using the developed tool and compared to *Opendrift* predictions. The trajectories of the objects obtained by the developed tool are in line with the ones provided by the *Opendrift* software, validating the tool developed.

A bivariate GMM has been proposed to describe the uncertainty on the object final location and to derive the 95% probability area of object containment to support search and rescue operations. In all four scenarios the probability model of the object final location consists on a bivariate single normal distribution model and, therefore, the searching areas obtained are single ellipses. The 95% probability curves (POC) obtained for the four different scenarios are consistent with the sample of the object final locations, showing more spread out areas when the crosswind leeway vector has higher values, as in the second scenario.

Search areas calculated according to an empirical formulation proposed by the Australian National Search Rescue Council (2018) have been plotted on top of the POC curves and the sample of object final locations. The resulting empirical areas are smaller than the POC curves obtained by the developed tool, particularly in the first scenario. The approximate POC values for the empirical search areas considering the object final locations resultant from the developed tool are 17%, 93%, 82% and 69% for scenarios 1, 2, 3 and 4, respectively. This means that the developed tool takes in consideration more uncertainties than the empirical formulation, especially in shorter simulations (as in scenario 1). It is also interesting to note that between scenarios 2, 3 and 4, the one with the larger values of crosswind leeway is the second, followed by the third and finally the fourth, which means the empirical search area is closer to the developed tool 95% POC area in size when the crosswind leeway is larger. The simple and empirical method adopts always a circular searching area that does not account for the asymmetrical characteristics of the sample of the object final locations, as clearly shown in scenario 2. All this together shows that the empirical formulation has limitations and does not account properly for the uncertainty on the drifting of the object, which is reflected on the size and shape of the searching area.

The influence of jibing on the trajectories and on the final location of the object has been illustrated by analyzing the second scenario with a probability of jibing of 0%. In this case if the object started drifting right it would keep drifting right and if it started drifting left it would keep drifting left until the end of the simulation. This created a sample of object final locations divided in two high-density areas that were

well represented by a GMM and therefore the 95% POC area is described by two ellipses instead of only one.

Analyzing all the points mentioned above, it is reasonable to conclude that all the initial proposed and defined objectives for this Naval Architecture and Ocean Engineering Master Thesis have been achieved, introducing a new topic with room for future deeper developments.

This work can be further improved with a more detailed analysis of targets drifting at sea, taking in consideration the probability of surviving time of people onboard different objects. A study on the different communication methods for the determination of the LKP radius could be developed, defining a different standard deviation for the initial location of the drift according to the detection method. There is the possibility of further developing this model with the input of wind and current vector grids in real-time. It would be also interesting to use real known scenarios to compare to the predictions of the developed tool in order to validate it more consistently. As final suggestion, it would be interesting to simulate different search patterns for different scenarios to assess the best option in terms of time and probability of finding the missing object.

References

Afonso, R., 2008. Contributos para o Plano Integrado de Busca e Salvamento Marítimo Nacional. Instituto de Estudos Superiores Militares.

AGCS, 2017. Safety and Shipping Review 2017, Allianz Global Corporate & Specialty (AGCS). Fritz-Schaeffer-Strasse 9, 81737 Munich, Germany.

Allen, A., Plourde, J., 1999. Review of Leeway: Field Experiments and Implementation, Technical Report No. CG-D-08-99, US Coast Guard Research and Development Center. 1082 Shennecossett Road, Groton, CT, USA.

Allen, A.A., 2005. Leeway divergence, Technical Report No. CG-D-05-05, U.S. Coast Guard Research and Development Center. 1082 Shennecossett Road, Groton, CT, USA.

Australian National Search Rescue Council, 2018. National Search and Rescue Manual. Camberra ACT 2601, Australia.

Autoridade Marítima Nacional, 2018. Estações Salva-vidas e Dispositivo [WWW Document]. URL https://www.amn.pt/ISN/Paginas/Estacoes.aspx (accessed 8.13.18).

Breivik, Ø., 2008. Leeway model documentation v2.5. Available at: http://www.ifremer.fr/sar-drift/exchange-repository/leeway_documentation_v2.5.pdf.

Breivik, Ø., Allen, A.A., 2008. An operational search and rescue model for the Norwegian Sea and the North Sea. J. Mar. Syst. 69, 99–113. https://doi.org/10.1016/j.jmarsys.2007.02.010

Breivik, Ø., Allen, A.A., Maisondieu, C., Roth, J.C., 2011. Wind-induced drift of objects at sea: The leeway field method. Appl. Ocean Res. 33, 100–109. https://doi.org/10.1016/j.apor.2011.01.005

Dagestad, K.F., Röhrs, J., Breivik, Ø., Ådlandsvik, B., 2018. OpenDrift v1.0: A generic framework for trajectory modelling. Geosci. Model Dev. 11, 1405–1420. https://doi.org/10.5194/gmd-11-1405-2018

EMSA, 2017. Annual overview of marine casualties and incidents 2017, European Maritime Safety Agency (EMSA). Praça Europa 4, Lisboa, Portugal.

Fitzgerald, B., R., Finlayson, D., Cross, J.F., Allen, A.A., 1993. Drift of Common Search and Rescue Objects, Phase II. Montreal.

GAMA, 2017. Investigação de acidentes marítimos Sumário da Atividade 2017, Gabinete de Investigação de Acidentes Marítimos e da Autoridade para a Meteorologia Aeronáutica (GAMA). Rua C do Aeroporto, Lisboa, Portugal.

Guedes Soares, C., Teixeira, A.P., 2001. Risk assessment in maritime transportation. Reliab. Eng. Syst. Saf. 74, 299–309. https://doi.org/10.1016/S0951-8320(01)00104-1

Hodgins, D.O., Mak, R.Y., 1995. Leeway dynamic study, phase I : development and verification of a mathematical drift model for four-person liferafts. Transportation Development Centre, Montreal, Canada.

IMO, ICAO, 1998. International Aeronautical and Maritime Search and Rescue Manual, 1st ed.

Kratzke, T.M., Stone, L.D., Frost, J.R., 2010. Search and Rescue Optimal Planning System. Inf. Fusion (FUSION), 2010 13th Conf.

Lukačovič, I., 2018. Windy [WWW Document]. URL https://www.windy.com/ (accessed 5.9.18).

Ni, Z., Qiu, Z., Su, T.C., 2010. On predicting boat drift for search and rescue 37, 1169–1179. https://doi.org/10.1016/j.oceaneng.2010.05.009

Portuguese Government, 1999. Decreto Lei 399/99. Diário da República 6912–6913.

Portuguese Government, 1994. Decreto Lei 15/94. Diário da República 322–326.

Portuguese Government, 1985. Decreto Lei 32/85. Diário da República 2618–2643.

Portuguese Navy, 2018. A Marinha: Busca e Salvamento [WWW Document]. URL http://www.marinha.pt/pt-pt/marinha/busca-e-salvamento/Paginas/default.aspx (accessed 4.4.18).

Richardson, P.L., 1997. Drifting in the wind: Leeway error in shipdrift data. Deep. Res. Part I Oceanogr. Res. Pap. 44, 1877–1903. https://doi.org/10.1016/S0967-0637(97)00059-9

Sebastião, P., Guedes Soares, C., 2007. Uncertainty in predictions of oil spill trajectories in open sea. Ocean Eng. 34, 576–584. https://doi.org/10.1016/j.oceaneng.2006.01.014

Sebastião, P., Guedes Soares, C., 2006. Uncertainty in predictions of oil spill trajectories in a coastal zone. J. Mar. Syst. 63, 257–269. https://doi.org/10.1016/j.jmarsys.2006.06.002

Sebastião, P., Guedes Soares, C., 1995. Modeling the fate of oil spills at sea. Spill Sci. Technol. Bull. 2, 121–131. https://doi.org/10.1016/S1353-2561(96)00009-6

Silveira, P.A.M., Teixeira, A.P., Guedes Soares, C., 2013. Use of AIS data to characterise marine traffic patterns and ship collision risk off the coast of Portugal. J. Navig. 66, 879–898. https://doi.org/10.1017/S0373463313000519

Veness, C., 2018. Calculate distance, bearing and more between Latitude/Longitude points [WWW Document]. URL https://www.movable-type.co.uk/scripts/latlong.html (accessed 4.4.18).

Vettor, R., Guedes Soares, C., 2015. Computational System for Planning Search and Rescue Operations at Sea. Procedia Comput. Sci. 51, 2848–2853. https://doi.org/10.1016/j.procs.2015.05.446

Zhang, D., Yan, X.P., Yang, Z.L., Wall, A., Wang, J., 2013. Incorporation of formal safety assessment and Bayesian network in navigational risk estimation of the Yangtze River. Reliab. Eng. Syst. Saf. 118, 93–105. https://doi.org/10.1016/J.RESS.2013.04.006

Zhang, J., Teixeira, A.P., Guedes Soares, C., Yan, X., 2017. Probabilistic modelling of the drifting trajectory of an object under the effect of wind and current for maritime search and rescue. Ocean Eng. 129, 253–264. https://doi.org/10.1016/j.oceaneng.2016.11.002

Zhang, J.F., Teixeira, A.P., Guedes Soares, C., 2016. Study on path planning strategies for search and rescue, in: Guedes Soares & Santos, Ed. Maritime Technology and Engineering 3. Taylor & Francis Group, London, pp. 937–942.

Annexes

Annex A – Object table with 3 parameters from Allen and Plourde (1999) in the format used by the developed tool following the first methodology.

	Slope	Y-intercept	Lα
1. PIW	1.1	3.5	40
1.1. PIW / Vertical	0.5	3.8	24
1.2. PIW / Sitting	1.2	0.2	24
1.3.1.1. PIW / Horizontal / Survival Suit / face up	1.4	5.3	40
1.3.2.1. PIW / Horizontal / Scuba Suit / face up	0.7	4.3	40
1.3.3.1. PIW / Horizontal / Deceased / face down	1.5	4	40
2.1.1. Survival Craft / Maritime Life Rafts / No Ballast Systems	4.2	1.6	38
2.1.1.1. Survival Craft / Maritime Life Rafts / No Ballast Systems / no canopy, no drogue	5.7	10.9	32
2.1.1.2. Survival Craft / Maritime Life Rafts / No Ballast Systems / no canopy, with drogue	4.4	-10.3	38
2.1.1.3. Survival Craft / Maritime Life Rafts / No Ballast Systems / canopy, no drogue	3.7	5.7	32
2.1.1.4. Survival Craft / Maritime Life Rafts / No Ballast Systems / canopy, with drogue	3	0	38
2.1.2. Survival Craft / Maritime Life Rafts / Shallow Ballast Systems and Canopy	2.9	-0.2	30
2.1.2.1. Survival Craft / Maritime Life Rafts / Shallow Ballast Systems and Canopy / no drogue	3.2	-1	30
2.1.2.2. Survival Craft / Maritime Life Rafts / Shallow Ballast Systems and Canopy / with drogue	2.5	0.7	30
2.1.2.3. Survival Craft / Maritime Life Rafts / Shallow Ballast Systems and Canopy / capsized	1.7	-5.2	11
2.1.3. Survival Craft / Maritime Life Rafts / Deep Ballast Systems & Canopies	3	0.8	18
2.1.3.1. Survival Craft / Maritime Life Rafts / Deep Ballast Systems & Canopies / 4-6 person capacity	2.9	2	20
2.1.3.1.1. Survival Craft / Maritime Life Rafts / Deep Ballast Systems & Canopies / 4-6 person capacity / without drogue	3.8	-2.1	20
2.1.3.1.1.1. Survival Craft / Maritime Life Rafts / Deep Ballast Systems & Canopies / 4-6 person capacity / without drogue / light loading	3.8	-2.1	20
2.1.3.1.1.2. Survival Craft / Maritime Life Rafts / Deep Ballast Systems & Canopies / 4-6 person capacity / without drogue / heavy loading	3.6	-1.5	20
2.1.3.1.2. Survival Craft / Maritime Life Rafts / Deep Ballast Systems & Canopies / 4-6 person capacity / with drogue	1.8	1.4	16
2.1.3.1.2.1. Survival Craft / Maritime Life Rafts / Deep Ballast Systems & Canopies / 4-6 person capacity / with drogue / light loading	1.6	2.7	32
2.1.3.1.2.2. Survival Craft / Maritime Life Rafts / Deep Ballast Systems & Canopies / 4-6 person capacity / with drogue / heavy loading	2.1	0	27
2.1.3.2. Survival Craft / Maritime Life Rafts / Deep Ballast Systems & Canopies / 15-25 person capacity	3.6	-4.4	14
2.1.3.2.1.1. Survival Craft / Maritime Life Rafts / Deep Ballast Systems & Canopies / 15-25 person capacity / without drogue / light loading	3.9	-3.1	12
2.1.3.2.2.1. Survival Craft / Maritime Life Rafts / Deep Ballast Systems & Canopies / 15-25 person capacity / with drogue / heavy loading	3.1	-3.6	12
2.1.3.3. Survival Craft / Maritime Life Rafts / Deep Ballast Systems & Canopies / Capsized	0.9	0	16
2.1.3.4. Survival Craft / Maritime Life Rafts / Deep Ballast Systems & Canopies / Swamped	1	-2.2	11
2.2.1. Survival Craft / Other Maritime Survival Craft / life capsule	3.8	-4.1	30
2.2.2. Survival Craft / Other Maritime Survival Craft / USCG Sea Rescue Kit	2.5	-2.1	10
2.3.1.1. Survival Craft / Aviation Life Rafts / no ballast, with canopy / 4-6 person, without drogue	3.7	5.7	32
2.3.2.1. Survival Craft / Aviation Life Rafts / Evacuation Slide / 46-person	2.8	-0.6	20
3.1.1.1. Person-Powered Craft / Sea Kayak / with Person on / aft deck	1.1	12.5	20
3.2.1. Person-Powered Craft / Surf board / with person	2	0	20
3.3.1.1. Person-Powered Craft / Windsurfer / with person and mast / & sail in water	2.3	5.2	16
4.1.1.1. Sailing Vessels / Mono-hull / Full Keel, Deep Draft	3	0	65
4.1.2.1. Sailing Vessels / Mono-hull / Fin Keel, Shoal Draft	4	0	65
5.1.1.1. Power Vessels / Skiffs / Flat Bottom / Boston whaler	3.4	2.1	30

5.1.2.1. Power Vessels / Skiffs / V-hull / Std. Conf.	3	3.9	20
5.1.2.2. Power Vessels / Skiffs / V-hull / Swamped	1.7	0	20
5.2.1.1. Power Vessels / Sport Boats, Cuddy Cabin, Modified V-hull	6.9	-4.1	25
5.3.1.1. Power Vessels / Sport Fisher, Center Consol, Open cockpit	6	-4.6	30
5.4. Power Vessels / Commercial Fishing Vessels	3.7	1	65
5.4.1.1. Power Vessels / Commercial Fishing Vessels / Sampans / Hawaiian	4	0	65
5.4.2.1. Power Vessels / Commercial Fishing Vessels / Side-stern Troller / Japanese	4.2	0	65
5.4.3.1. Power Vessels / Commercial Fishing Vessels / Longliners / Japanese	3.7	0	65
5.4.4.1. Power Vessels / Commercial Fishing Vessels /Junk / Korean	2.7	4.9	65
5.4.5.1. Power Vessels / Commercial Fishing Vessels / Gill-netter / with rear reel	4	0.3	45
5.5. Power Vessels / Coastal Freighter	2.8	0	65
6.1. Boating Debris / F/V debris	2	0	14
6.2. Boating Debris / Bait/wharf box holds a cubic meter of ice	1.3	13.8	42
6.2.1. Boating Debris / Bait/wharf box holds a cubic meter of ice / lightly loaded	2.6	9.2	20
6.2.2. Boating Debris / Bait/wharf box holds a cubic meter of ice / full loaded	1.6	8	44
7.1.1.1. Non-SAR Objects / Immigration Vessel, Cuban refugee raft / without sail	1.5	8.7	23
7.1.1.2. Non-SAR Objects / Immigration Vessel, Cuban refugee raft / with sail	7.9	-8.9	45
7.2.1. Non-SAR Objects / Sewage Floatables, Tampoon Applicators	1.8	0	7
7.3. Non-SAR Objects / Medical Waste	2.8	0	14
7.3.1. Non-SAR Objects / Medical Waste / Vials	3.7	0	14
7.3.1.1. Non-SAR Objects / Medical Waste / Vials / Large	4.4	0	13
7.3.1.2. Non-SAR Objects / Medical Waste / Vials / Small	3	0	14
7.3.2. Non-SAR Objects / Medical Waste / Syringes	1.8	0	7
7.3.2.1. Non-SAR Objects / Medical Waste / Syringes / Large	1.8	0	7
7.3.2.2. Non-SAR Objects / Medical Waste / Syringes / Small	1.8	0	7

Annex B – Object table with 9 parameters from Breivik et al. (2011) in the format used by the developed tool following the second methodology and by *Opendrift*.

No.	Name	Description	downwind slope [%]	downwind offset [cm/s]	downwind std dev [cm/s]	right slope [%]	right offset [cm/s]	right std dev [cm/s]	left slope [%]	left offset [cm/s]	left std dev [cm/s]
1	PIW-1	Person-in-water (PIW), unknown state (mean values)	0.96	0.00	12.00	0.54	0.00	9.40	-0.54	0.00	9.40
2	PIW-2	>PIW, vertical PFD type III conscious	0.48	0.00	8.30	0.15	0.00	6.70	-0.15	0.00	6.70
3	PIW-3	>PIW, sitting, PFD type I or II	1.60	-3.98	2.42	0.13	0.33	2.11	-0.13	-0.33	2.11
4	PIW-4	>PIW, survival suit (face up)	1.71	1.12	3.93	1.36	-3.30	1.71	-0.13	-2.65	1.62
5	PIW-5	>PIW, scuba suit (face up)	0.63	0.00	5.30	0.31	0.00	4.50	-0.31	0.00	4.50
6	PIW-6	>PIW, deceased (face down)	1.117	10.20	3.04	0.04	3.90	4.05	-0.04	-3.90	4.05
7	LIFE-RAFT-DB-10	Life raft, deep ballast (DB) system, general, unknown capacity and loading (mean values)	3.52	-2.50	6.10	0.62	-3.00	3.50	-0.45	-0.20	3.60
8	LIFE-RAFT-DB-11	>4-14 person capacity, deep ballast system, canopy (average)	3.50	-1.80	6.40	0.78	-3.60	3.60	-0.47	-0.10	3.90
9	LIFE-RAFT-DB-12	>>4-14 person capacity, deep ballast system, no drogue	3.75	-2.30	4.40	0.78	-3.60	3.60	-0.47	-0.10	3.90

10	LIFE-RAFT-DB-13	>>>4-14 person capacity, deep ballast system, canopy, no drogue, light loading	3.75	-2.32	4.51	1.00	-5.31	3.91	-0.47	-0.14	3.91
11	LIFE-RAFT-DB-14	>>>4-14 person capacity, deep ballast system, no drogue, heavy loading	3.59	-1.92	2.56	0.48	-0.16	2.17	-0.48	0.16	2.17
12	LIFE-RAFT-DB-15	>>4-14 person capacity, deep ballast system, canopy, with drogue (average)	1.91	0.90	1.60	0.78	-3.60	3.60	-0.47	-0.10	3.90
13	LIFE-RAFT-DB-16	>>>4-14 person capacity, deep ballast system, canopy, with drogue, light loading	1.95	-0.53	3.59	0.21	1.29	2.15	-0.21	-1.29	2.15
14	LIFE-RAFT-DB-17	>>>4-14 person capacity, deep ballast system, canopy, with drogue, heavy loading	2.19	-0.96	1.01	1.39	-7.90	1.46	-1.39	7.90	1.46
15	LIFE-RAFT-DB-18	>15-50 person capacity, deep ballast system, canopy, general (mean values)	3.68	-4.96	5.37	0.34	-1.85	2.50	-0.49	1.58	2.63
16	LIFE-RAFT-DB-19	>>15-50 person capacity, deep ballast system, canopy, no drogue, light loading	3.93	-3.30	3.01	0.38	-3.33	2.16	-0.59	1.59	2.28
17	LIFE-RAFT-DB-20	>>15-50 person capacity, deep ballast system, canopy, with drogue, heavy loading	3.15	-4.49	3.35	0.39	-1.80	2.50	-0.38	2.98	1.64
18	LIFE-RAFT-DB-21	Deep ballast system, general (mean values), capsized	0.88	0.00	2.50	0.18	0.00	2.40	-0.18	0.00	2.40
19	LIFE-RAFT-DB-22	Deep ballast system, general (mean values), swamped	0.99	0.00	2.40	0.14	0.00	2.30	-0.14	0.00	2.30
20	LIFE-RAFT-SB-6	Life-raft, shallow ballast (SB) system AND canopy, general (mean values)	2.68	0.00	12.00	1.10	0.00	9.40	-1.10	0.00	9.40
21	LIFE-RAFT-SB-7	>Life-raft, shallow ballast system, canopy, no drogue	2.96	0.00	1.50	1.21	0.00	1.70	-1.21	0.00	1.70
22	LIFE-RAFT-SB-8	>Life-raft, shallow ballast system AND canopy, with drogue	2.31	0.00	4.00	0.95	0.00	3.50	-0.95	0.00	3.50
23	LIFE-RAFT-SB-9	Life-raft, shallow ballast system AND canopy, capsized	1.68	0.00	2.40	0.24	0.00	2.40	-0.24	0.00	2.40
24	LIFE-RAFT-SB-10	Life Raft - Shallow ballast, canopy, Navy Sub Escape (SEIE) 1-man raft, NO drogue	3.30	-3.90	4.20	0.50	7.0	5.7	0.1	-6.2	3.6
25	LIFE-RAFT-SB-11	Life Raft - Shallow ballast, canopy, Navy Sub Escape (SEIE) 1-man raft, with drogue	1.7	-3.90	4.20	0.00	5.7	3.3	0.0	-3.4	2.2
26	LIFE-RAFT-NB-1	Life-raft, no ballast (NB) system, general (mean values)	3.70	0.00	12.00	1.98	0.00	9.40	-1.98	0.00	9.40
27	LIFE-RAFT-NB-2	>Life-raft, no ballast system, no canopy, no drogue	5.34	9.91	9.82	2.26	1.04	9.08	-2.26	-1.04	9.08
28	LIFE-RAFT-NB-3	>Life-raft, no ballast system, no canopy, with drogue	3.15	-4.47	4.00	1.51	0.00	5.00	-1.51	0.00	5.00
29	LIFE-RAFT-NB-4	>Life-raft, no ballast system, with canopy, no drogue	3.39	0.00	2.40	1.49	0.00	2.40	-1.49	0.00	2.40
30	LIFE-RAFT-NB-5	>Life-raft, no ballast system, with canopy, with drogue	1.21	0.00	12.00	0.92	0.00	9.40	-0.92	0.00	9.40
31	USCG-RESCUE	Survival Craft - USCG Sea Rescue Kit - 3 ballasted life rafts and 300 meter of line	2.48	0.00	3.80	0.32	0.00	3.40	-0.32	0.00	3.40
32	AVIATION-1	Life-raft, 4-6 person capacity, no ballast, with canopy, no drogue	3.39	0.00	2.40	1.49	0.00	2.40	-1.49	0.00	2.40
33	AVIATION-2	Evacuation slide with life-raft, 46 person capacity	2.71	0.00	3.80	0.72	0.00	3.40	-0.72	0.00	3.40
34	LIFE-CAPSULE	Survival Craft - SOLAS Hard Shell Life Capsule, 22 man	3.52	0.00	1.90	1.44	0.00	2.00	-1.44	0.00	2.00
35	OVATEK-CRAFT-1	Survival Craft - Ovatek Hard Shell Life Raft, 4 and 7-man, lightly loaded, no drogue (average)	3.51	3.49	5.66	1.08	-1.24	5.35	-1.721	4.67	6.24
36	OVATEK-CRAFT-2	>Survival Craft - Ovatek Hard Shell Life Raft, 4 man, lightly loaded, no drogue	3.86	0.01	2.75	0.32	1.31	2.62	-0.19	-2.67	2.81

37	OVATEK-CRAFT-3	>Survival Craft - Ovatek Hard Shell Life Raft, 7 man, lightly loaded, no drogue	3.26	6.16	6.65	2.32	-7.33	4.77	-2.10	6.02	5.35
38	OVATEK-CRAFT-4	Survival Craft - Ovatek Hard Shell Life Raft, 4 and 7-man, fully loaded, drogued (average)	1.04	2.99	2.13	0.034	1.57	1.30	-0.02	-0.96	1.17
39	OVATEK-CRAFT-5	>Survival Craft - Ovatek Hard Shell Life Raft, 4 man, fully loaded, drogued	1.09	2.31	1.59	0.027	0.95	0.99	-0.07	-0.79	1.31
40	OVATEK-CRAFT-6	>Survival Craft - Ovatek Hard Shell Life Raft, 7 man, fully loaded, drogued	0.995	3.46	2.34	0.023	-1.86	1.32	-0.005	-0.95	0.88
41	PERSON-POWERED-VESSEL-1	Sea Kayak with person on aft deck	1.16	11.12	4.12	0.41	0.00	4.39	-0.41	0.00	4.39
42	PERSON-POWERED-VESSEL-2	Surf board with person	1.93	0.00	8.30	0.51	0.00	6.70	-0.51	0.00	6.70
43	PERSON-POWERED-VESSEL-3	Windsurfer with mast and sail in water	2.25	5.03	2.50	0.69	-1.30	2.96	-0.69	1.30	2.96
44	SKIFF-1	Skiff - modified-v, cathedral-hull, runabout outboard powerboat	3.15	0.00	2.20	1.29	0.00	2.20	-1.29	0.00	2.20
45	SKIFF-2	Skiff, V-hull	2.87	3.98	3.33	0.32	-2.93	2.53	-0.62	1.03	3.05
46	SKIFF-3	Skiffs, swamped and capsized	1.65	0.00	3.10	0.39	0.00	2.90	-0.39	0.00	2.90
47	SKIFF-4	Skiff - v-hull bow to stern (aluminum, Norway)	2.52	13.37	3.87	1.07	-3.58	5.82	-1.07	3.58	5.82
48	SPORT-BOAT	Sport boat, no canvas, modified V-hull	6.54	0.00	3.00	2.19	0.00	2.80	-2.19	0.00	2.80
49	SPORT-FISHER	Sport fisher, center console, open cockpit	5.55	0.00	3.30	2.27	0.00	3.00	-2.27	0.00	3.00
50	FISHING-VESSEL-1	Fishing vessel, general (mean values)	2.47	0.00	12.00	2.76	0.00	9.40	-2.76	0.00	9.40
51	FISHING-VESSEL-2	Fishing vessel, Hawaiian Sampan	2.67	0.00	8.30	2.98	0.00	6.70	-2.98	0.00	6.70
52	FISHING-VESSEL-3	>Fishing vessel, Japanese side-stern trawler	2.80	0.00	8.30	3.13	0.00	6.70	-3.13	0.00	6.70
53	FISHING-VESSEL-4	>Fishing vessel, Japanese Longliner	2.47	0.00	8.30	2.76	0.00	6.70	-2.76	0.00	6.70
54	FISHING-VESSEL-5	>Fishing vessel, Korean fishing vessel	1.80	0.00	3.79	2.01	0.00	3.30	-2.01	0.00	3.30
55	FISHING-VESSEL-6	>Fishing vessel, Gill-netter with rear reel	3.72	-0.87	3.33	1.41	2.00	3.36	-1.41	-2.00	3.36
56	COASTAL-FREIGHTER	Coastal freighter.	1.87	0.00	8.30	2.09	0.00	6.70	-2.09	0.00	6.70
57	SAILBOAT-1	Sailboat Mono-hull (Average)	4.5	0.0	19.4	4.95	0.0	18.42	-2.82	0.0	24.95
58	SAILBOAT-2	>Sailboat Mono-hull (Dismasted, Average)	3.94	0.0	19.62	3.98	0.0	12.6788	-0.79	0.0	2.13
59	SAILBOAT-3	>>Sailboat Mono-hull (Dismasted - rudder amidships)	6.27	0.0	9.22	4.01	0.0	12.34	-4.01	0.0	12.34
60	SAILBOAT-4	>>Sailboat Mono-hull (Dismasted - rudder missing)	2.42	0.0	1.29	0.79	0.0	2.17	-0.79	0.0	2.13
61	SAILBOAT-5	>Sailboat Mono-hull (Bare-masted, Average)	5.23	0.0	18.52	5.89	0.0	18.87	-6.09	0.0	18.58
62	SAILBOAT-6	>>Sailboat Mono-hull (Bare-masted, rudder amidships)	6.66	0.0	16.56	7.36	0.0	15.15	-7.53	0.0	16.69
63	SAILBOAT-6	>>Sailboat Mono-hull (Bare-masted, rudder hove-to)	2.69	0.0	10.48	2.81	0.0	11.14	-4.01	0.0	13.6608
64	SAILBOAT-7	Sailboat Mono-hull, fin keel, shallow draft (was SAILBOAT-2)	2.67	0.00	8.30	2.98	0.00	6.70	-2.98	0.00	6.70
65	SAILBOAT-8	Sunfish sailing dingy - Bare-masted, rudder missing	1.79	3.09	4.04	0.1	3.53	4.05	-0.1	-3.53	4.05
66	FV-DEBRIS	Fishing vessel debris	1.97	0.00	8.30	0.36	0.00	6.70	-0.36	0.00	6.70
67	SLDMB	Self-locating datum marker buoy - no windage	0.00	0.00	0.00	0.00	0.00	0.00	0.00	0.00	0.00
68	SEPIRB	Navy Submarine EPIRB (SEPIRB)	0.4	-1.8	6.0	0.0	6.1	4.6	0.0	-4.6	4.6

69	BAIT-BOX-1	Bait/wharf box, holds a cubic metre of ice, mean values	0.72	15.18	5.59	1.86	-5.26	4.20	-1.86	5.26	4.20
70	BAIT-BOX-2	Bait/wharf box, holds a cubic metre of ice, lightly loaded	2.53	9.01	3.05	1.09	-2.76	4.14	-1.09	2.76	4.14
71	BAIT-BOX-3	>Bait/wharf box, holds a cubic metre of ice, full loaded	1.15	7.94	3.17	1.48	-0.32	2.99	-1.48	0.32	2.99
72	OIL-DRUM	55-gallon (220 l) Oil Drum	0.75	2.66	2.83	0.48	2.88	3.92	-0.45	-1.46	4.59
73	CONTAINER-1	Scaled down (13) 40-ft Container (70% submerged)	1.78	1.44	2.99	0.27	-2.44	2.31	-0.27	2.44	2.31
74	CONTAINER-2	20-ft Container (80% submerged)	1.25	3.96	2.81	0.19	1.14	4.36	-0.19	-1.14	4.36
75	MINE	WWII L-MK2 mine	1.07	4.47	6.55	0.41	1.15	4.13	-0.41	-1.15	4.13
76	REFUGEE-RAFT-1	Immigration vessel, Cuban refugee-raft, no sail	1.56	8.30	1.53	0.078	2.70	1.52	-0.078	-2.70	1.52
77	REFUGEE-RAFT-2	Immigration vessel, Cuban refugee-raft, with sail	6.43	-3.47	3.63	2.22	0.00	7.12	-2.22	0.00	7.12
78	SEWAGE	Sewage floatables, tampon applicator	1.79	0.00	3.10	0.16	0.00	2.90	-0.16	0.00	2.90
79	MED-WASTE-1	Medical waste (mean values)	2.75	0.00	12.00	0.50	0.00	9.40	-0.50	0.00	9.40
80	MED-WASTE-2	>Medical waste, vials	3.64	0.00	12.00	0.67	0.00	9.40	-0.67	0.00	9.40
81	MED-WASTE-3	>>Medical waste, vials, large	4.34	0.00	3.10	0.74	0.00	2.90	-0.74	0.00	2.90
82	MED-WASTE-4	>>Medical waste, vials, small	2.95	0.00	5.40	0.54	0.00	4.50	-0.54	0.00	4.50
83	MED-WASTE-5	>Medical waste, syringes	1.79	0.00	12.00	0.16	0.00	9.40	-0.16	0.00	9.40
84	MED-WASTE-6	>>Medical waste, syringes, large	1.79	0.00	3.10	0.16	0.00	2.90	-0.16	0.00	2.90
85	MED-WASTE-7	>>Medical waste, syringes, small	1.79	0.00	2.40	0.16	0.00	2.30	-0.16	0.00	2.30

Annex C – Short tutorial for *Opendrift* installing and running in *Python*

-Download Miniconda 2 (Python 2) for Windows from *conda* website [https://conda.io/miniconda.html]

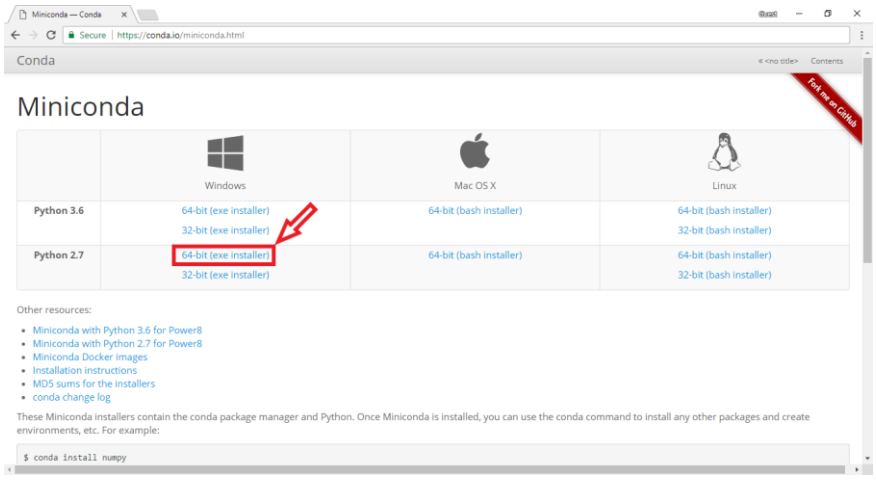

-Install Miniconda 2 [C:/Programs/Miniconda2]

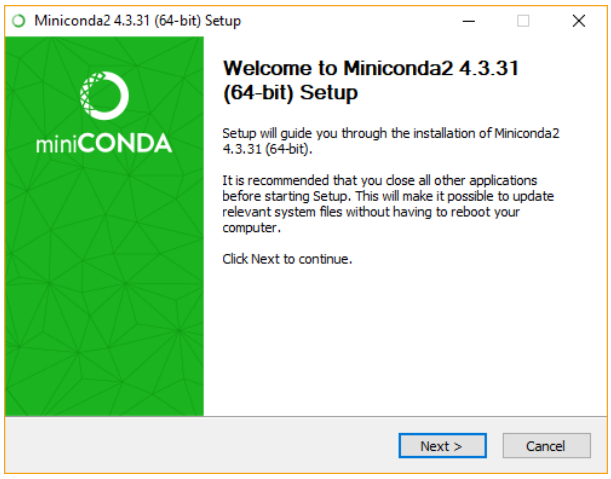

-Open Anaconda Command Prompt

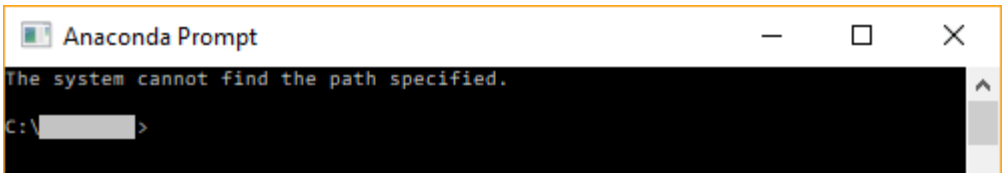

-Install the packages needed for Opendrift, this might take several minutes:

>>conda install --yes hdf4 numpy scipy matplotlib basemap netcdf4 configobj pillow gdal

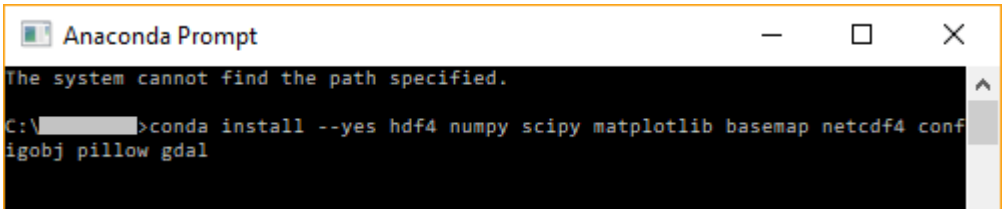

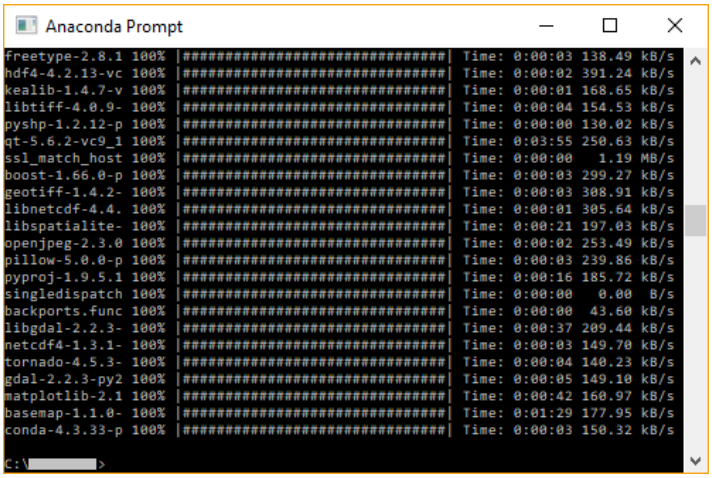

-Install the packages needed for the OilLibrary:

>>conda install --yes setuptools sqlalchemy transaction zope.sqlalchemy awesome-slugify unit_conversion pytest

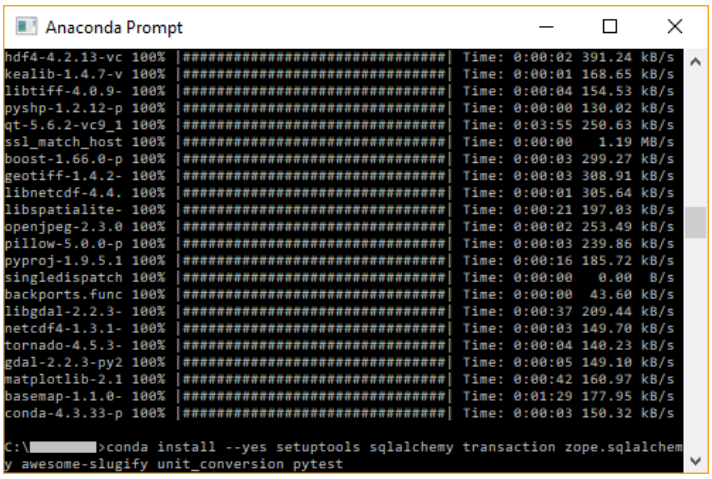

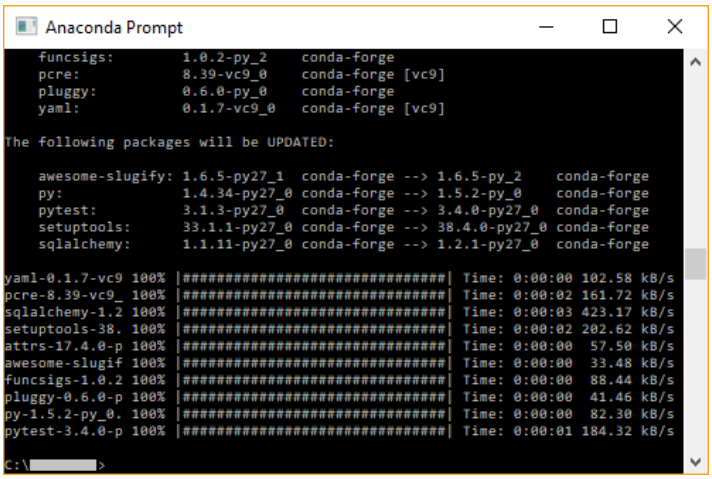

-Download OilLibrary-master zipped folder from [https://github.com/NOAA-ORR-ERD/OilLibrary] and extract it. In this example it is extracted directly to the Desktop.

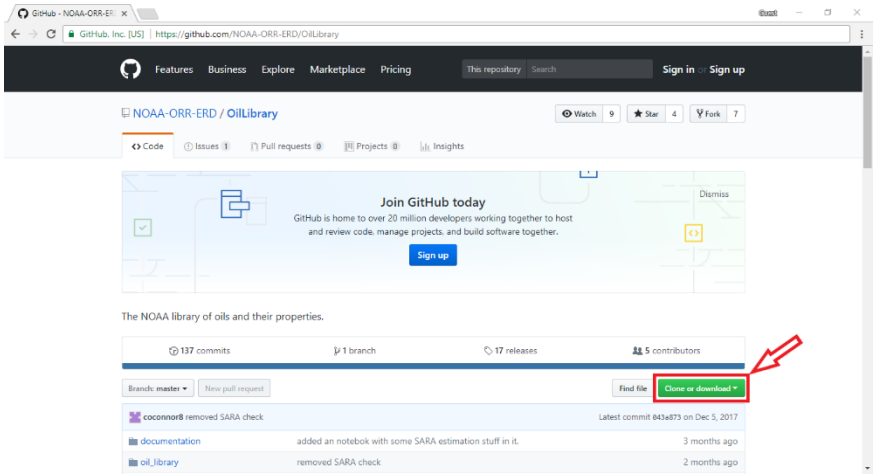

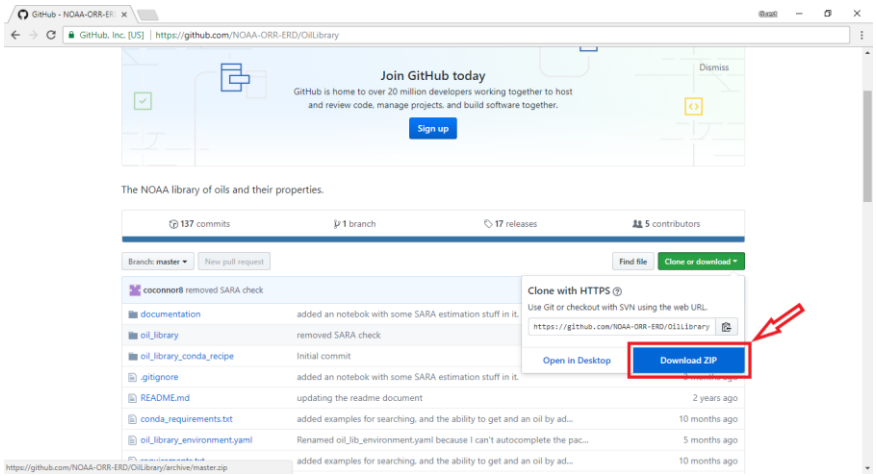

-Install OilLibrary

>>cd C:/…/Desktop/OilLibrary-master

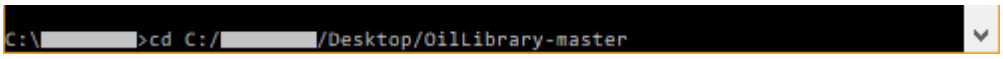

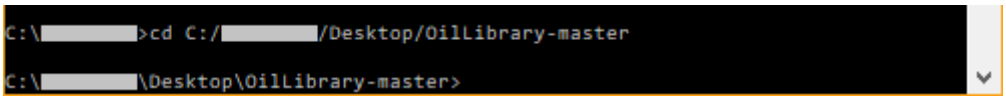

>>python setup.py develop

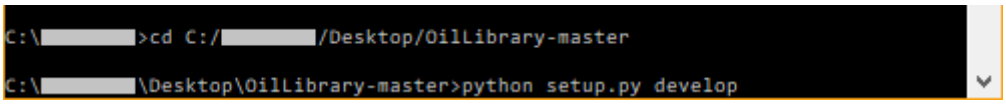

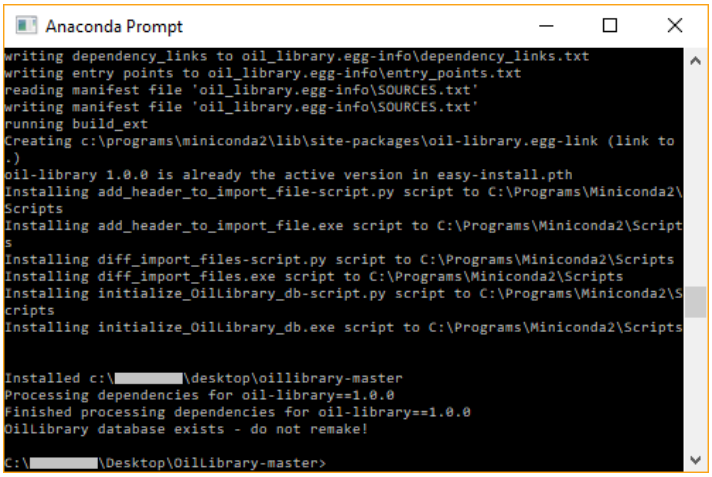

-Download opendrift-master zipped folder from [https://github.com/OpenDrift/opendrift/archive/master.zip] and unzip it. In this case it is unzipped directly in the Desktop.

-Install Opendrift

>>cd C:/…/Desktop/opendrift-master

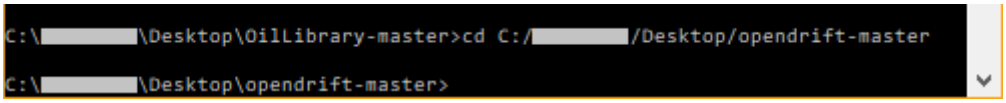

>>python setup.py develop

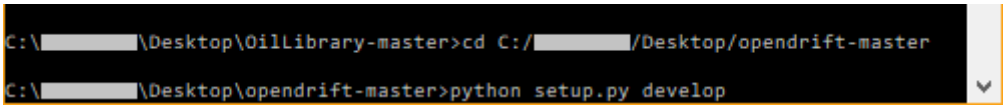

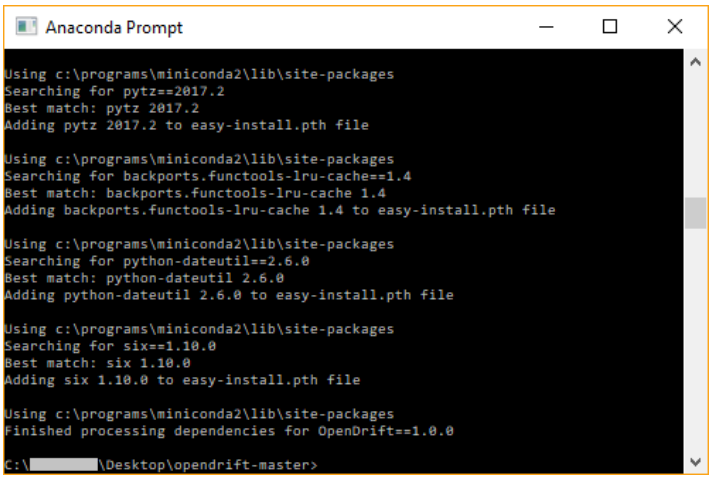

Opendrift is now installed in the computer. To explain how to run an *opendrift* file, the directory of the Anaconda Prompt is changed again as shown in the following image, in this case to the *examples* folder available inside the *opendrift-master* folder.

>>cd C:/…/Desktop/opendrift-master/examples

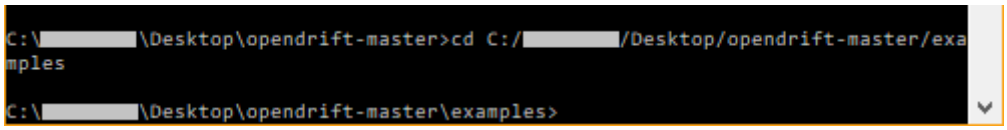

Then just run the file wanted with python using a command like:

>>python example_leeway.py

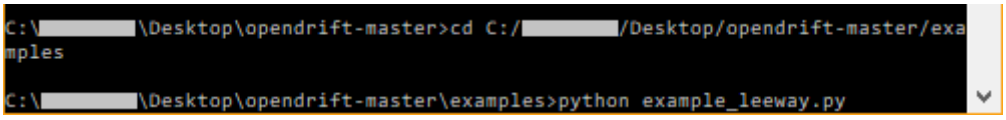

When the ENTER key is pressed, the script runs and after some time a new window pops up with a moving image with the appearance of the frame below.

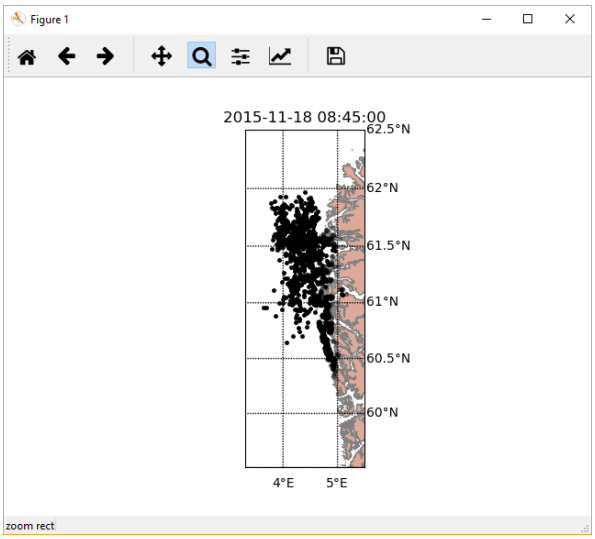

When you close this window shown above, a new window pops up, this time with a static plot like the one following.

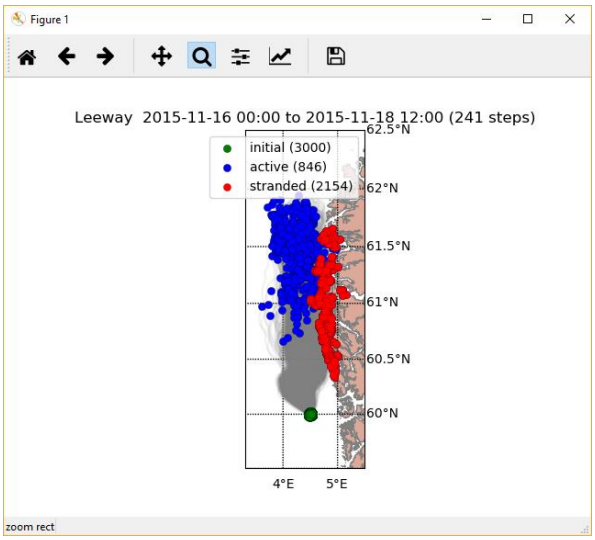

Finally, when you close this last window, the *Anaconda Command Prompt* finishes running and makes itself available for new commands:

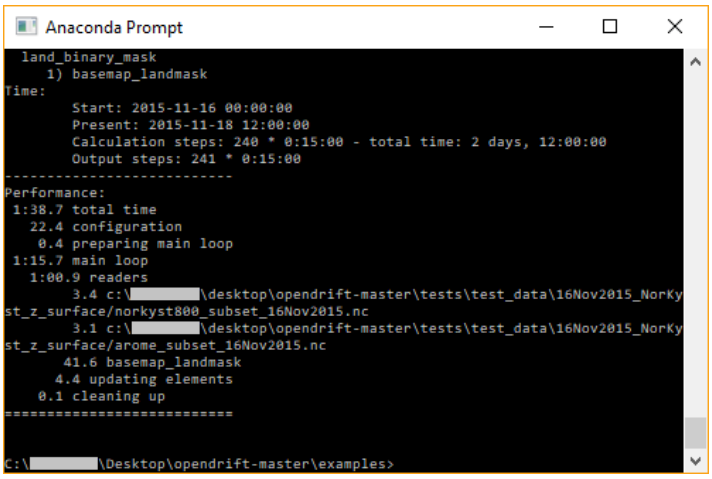

Running the scripts this way makes editing very easy. The easiest way to make a personal script is start from an example file and edit it the way that suits the user's needs. The other way would be writing a script from scratch, but that would require much more knowledge of the *Opendrift* modules and more knowledge of programming in *Python*.

The easiest and most intuitive way to run the program would be using the GUI file available, although it is not a very flexible tool:

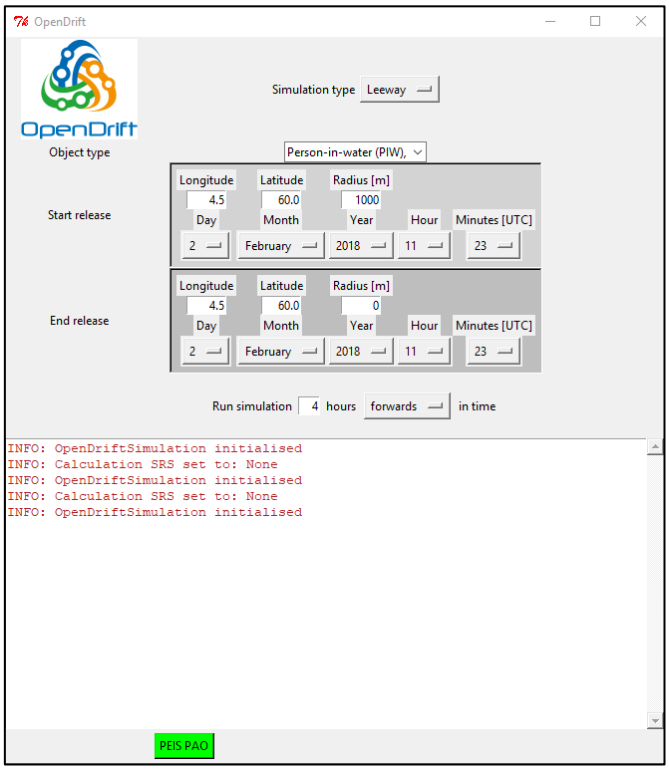

With this tool you can select the type of simulation needed and a limited number of other inputs and afterwards need to press the PEIS PAO green button on the bottom to run the simulation. Note: In order to see the button, in some cases is necessary to move the *Windows* taskbar to the side because the window is too long for the screen.

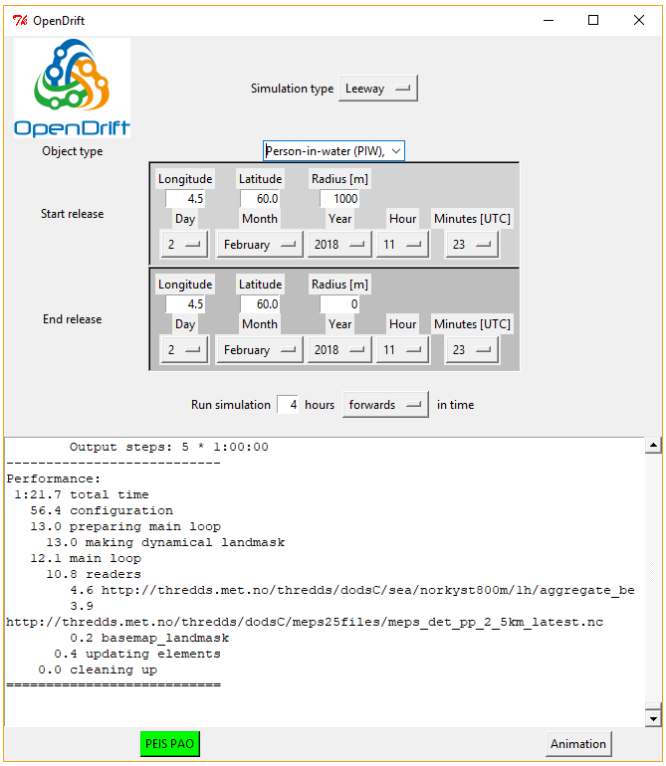

After running the simulation, a new button appears on the bottom right where is written *Animation*. If this button is pressed, an animation of the simulation is shown, as in the image bellow.

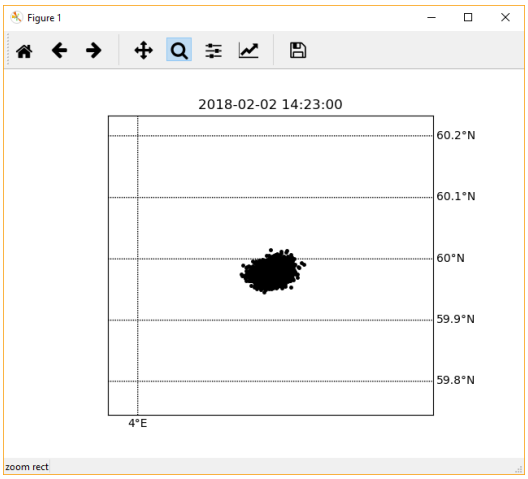

Annex D – *Opendrift* file script in *python* format *.py* for scenario 1

```
#!/usr/bin/env python
from opendrift.readers import reader_basemap_landmask
from opendrift.models.leeway import Leeway
from datetime import datetime
lw = Leeway(loglevel=0)  # Set loglevel to 0 for debug information
#Current and wind speeds
lw.fallback_values['x_sea_water_velocity'] = 0.02572222222
lw.fallback_values['y_sea_water_velocity'] = 0.04455219577
lw.fallback_values['x_wind'] = 2.662960397
lw.fallback_values['y_wind'] = -9.938303502
```

```
# Landmask (Basemap)
reader_basemap = reader_basemap_landmask.Reader(
                    llcrnrlon=-10.65, llcrnrlat=38.65,
                    urcrnrlon=-10.35, urcrnrlat=38.85, resolution='h',
                    projection='merc')
lw.add_reader(reader_basemap,
              variables=['land_binary_mask'])
lw.set_config('general:coastline_action', 'none')
# Seeding some particles.
lon = -10.521936; lat = 38.780753; # Scenario 1
# Seed leeway elements at defined position and time
objType = 1  # 1 = PIW
lw.seed_elements(lon, lat, radius=370.4, number=1000,
                 time=datetime(2018,5,9,9,0,0), objectType=objType)
lw.set_projection('+proj=merc')
# Running model (time of simulation)
simulation_hours=8
simulation_seconds=simulation_hours*3600
steps_=60*4
t_step=simulation_seconds/steps_
lw.run(steps=steps_, time_step=t_step, outfile='scenario1_output')
# Print and plot results
print lw
lw.animation()
lw.plot()
```

Annex E – *Opendrift* file script in *python* format *.py* for scenario 2

```
#!/usr/bin/env python
from opendrift.readers import reader_basemap_landmask
from opendrift.models.leeway import Leeway
from datetime import datetime
lw = Leeway(loglevel=0)  # Set loglevel to 0 for debug information
#Current and wind speeds
lw.fallback_values['x_sea_water_velocity'] = -0.05066288774
lw.fallback_values['y_sea_water_velocity'] = -0.008933234029
lw.fallback_values['x_wind'] = 2.287354714
lw.fallback_values['y_wind'] = 6.284455427
# Landmask (Basemap)
reader_basemap = reader_basemap_landmask.Reader(
                    llcrnrlon=-18.6, llcrnrlat=39.8,
                    urcrnrlon=-17.4, urcrnrlat=40.6, resolution='h',
                    projection='merc')
lw.add_reader(reader_basemap,
              variables=['land_binary_mask'])
lw.set_config('general:coastline_action', 'none')
# Seeding some particles
lon = -18.000000; lat = 40.000000; # Scenario 2
# Seed leeway elements at defined position and time
objType = 64  # 64 = SAILBOAT-7 : Sailboat Mono-hull, fin keel, shallow draft (was
SAILBOAT-2)
lw.seed_elements(lon, lat, radius=92.6, number=1000,
                 time=datetime(2018,5,10,18,0,0), objectType=objType)
lw.set_projection('+proj=merc')
# Running model (time of simulation)
simulation_hours=40
```

```
simulation_seconds=simulation_hours*3600
steps_=60*4
t_step=simulation_seconds/steps_
lw.run(steps=steps_, time_step=t_step, outfile='scenario2_output')
# Print and plot results
print lw
lw.animation()
lw.plot()
```

Annex F – *Opendrift* file script in *python* format *.py* for scenario 3

```
#!/usr/bin/env python
from opendrift.readers import reader_basemap_landmask
from opendrift.models.leeway import Leeway
from datetime import datetime
lw = Leeway(loglevel=0)  # Set loglevel to 0 for debug information
#Current and wind speeds
lw.fallback_values['x_sea_water_velocity'] = -0.05066288774
lw.fallback_values['y_sea_water_velocity'] = -0.008933234029
lw.fallback_values['x_wind'] = 2.287354714
lw.fallback_values['y_wind'] = 6.284455427
# Landmask (Basemap)
reader_basemap = reader_basemap_landmask.Reader(
                    llcrnrlon=-18.6, llcrnrlat=39.8,
                    urcrnrlon=-17.4, urcrnrlat=40.6, resolution='h',
                    projection='merc')
lw.add_reader(reader_basemap,
              variables=['land_binary_mask'])
lw.set_config('general:coastline_action', 'none')
# Seeding some particles
lon = -18.000000; lat = 40.000000; # Scenario 3
# Seed leeway elements at defined position and time
objType = 4  # 4 = PIW-4 : PIW, survival suit (face up)
lw.seed_elements(lon, lat, radius=92.6, number=1000,
                 time=datetime(2018,5,10,18,0,0), objectType=objType)
lw.set_projection('+proj=merc')
# Running model (time of simulation)
simulation_hours=40
simulation_seconds=simulation_hours*3600
steps_=60*4
t_step=simulation_seconds/steps_
lw.run(steps=steps_, time_step=t_step, outfile='scenario3_output')
# Print and plot results
print lw
lw.animation()
lw.plot()
```

Annex G – *Opendrift* file script in *python* format *.py* for scenario 4

```
#!/usr/bin/env python
from opendrift.readers import reader_basemap_landmask
from opendrift.models.leeway import Leeway
from datetime import datetime
lw = Leeway(loglevel=0)  # Set loglevel to 0 for debug information
#Current and wind speeds
```

```
lw.fallback_values['x_sea_water_velocity'] = -0.05066288774
lw.fallback_values['y_sea_water_velocity'] = -0.008933234029
lw.fallback_values['x_wind'] = 2.287354714
lw.fallback_values['y_wind'] = 6.284455427
# Landmask (Basemap)
reader_basemap = reader_basemap_landmask.Reader(
                    llcrnrlon=-18.6, llcrnrlat=39.8,
                    urcrnrlon=-17.4, urcrnrlat=40.6, resolution='h',
                    projection='merc')
lw.add_reader(reader_basemap,
              variables=['land_binary_mask'])
lw.set_config('general:coastline_action', 'none')
# Seeding some particles
lon = -18.000000; lat = 40.000000; # Scenario 4
# Seed leeway elements at defined position and time
objType = 13  # 13 = LIFE-RAFT-DB-16 : 4-14 person capacity, deep ballast system, canopy,
with drogue, light loading
lw.seed_elements(lon, lat, radius=92.6, number=1000,
                 time=datetime(2018,5,10,18,0,0), objectType=objType)
lw.set_projection('+proj=merc')
# Running model (time of simulation)
simulation_hours=40
simulation_seconds=simulation_hours*3600
steps_=60*4
t_step=simulation_seconds/steps_
lw.run(steps=steps_, time_step=t_step, outfile='scenario4_output')
# Print and plot results
print lw
lw.animation()
lw.plot()
```

Annex H – *Matlab* script for result analysis in *.m* format for each scenario

```
clc
clear all;
close all;

fileID = fopen('S1.txt');

%read headers
A_text = textscan(fileID,'%s %s',1);

%read numbers
A_data = textscan(fileID,'%f %f',1000);
A = cell2mat(A_data);

%histograms
figure1 = figure('Color',[1 1 1]);
histogram(A(:,1),100);
title('Histogram of x values')
xlabel('x [NM]');
ylabel('no. of points');

figure2 = figure('Color',[1 1 1]);
histogram(A(:,2),100);
title('Histogram of y values')
xlabel('y [NM]');
ylabel('no. of points');

% Scatter plot with points of size 25
```

```
figure3 = figure('Color',[1 1 1]);
scatter(A(:,1),A(:,2),25,'.')
title('Simulated Data')

%fit a 1 curve Gaussian Mixture Model (GMM)
options = statset('Display','final');
gm = fitgmdist(A,1,'Options',options);

%Probability Density Function (PDF) of the GMM
gmPDF = @(x,y)pdf(gm,[x y]);

%pdf matrix (X,Y,Z)
[X,Y] = ndgrid(-10:0.1:10,-10:0.1:10);
Z = arrayfun (@(x,y)pdf(gm,[x y]),X,Y);

%pdf matrix (X,Y,Z-lvl)
lvl = 0;
Z2 = Z-lvl;
Z2(Z2<0)=0;

% calculate lvl for vol=0.95
x = -10:0.1:10;
y = x;
vol = trapz(y,trapz(x,Z2,2),1);
while vol > 0.95
    lvl = lvl+0.00001;
    Z2 = Z-lvl;
    Z2(Z2<0)=0;
    x = -10:0.1:10;
    y = x;
    vol = trapz(y,trapz(x,Z2,2),1);

    %% Volume Correction
    Check = 0; % Variable created to ease the determination of the left extremity
of the ellipse
    j = 1; % Index variable for the calculation of the area
    clear var a b G_x_Small G_x_Big G_Var_x G_y G_Var_y Area Soma_A
    for k = 1 : 1 : length(Z2(:,1)) % Cycle along all the Z2 lines
        %The area of the ellipse only needs to be calculated for the values
        % of Z2 that are nonzero.
        % This line of code determines if a column has any non-zero value
        Dif_Zero = find((Z2(:,k) ~= 0) == 1);

        % If there are non-zero values than we need to determine the column
        % where that occurs
        if ~isempty(Dif_Zero)
            if Check == 0
                Col = k; % First column were the values are non-zero
                Check = 1; % So that the cycle doesnt keep changing the value of
Col, this variable was created
            end


            a(j) = min(Dif_Zero); % As shown in the Excel, this variable determines
the line of the upper perimeter of the ellise
            b(j) = max(Dif_Zero); % As shown in the Excel, this variable determines
the line of the the lower perimeter of the ellise

            G_x_Small(j) = X(a(j),k); % The value of the upper perimeter of the
ellipse
            G_x_Big(j) = X(b(j),k); % The value of the lower perimeter of the
ellipse

            G_Var_x(j) = G_x_Big(j) - G_x_Small(j); % Width of the ellipse

            G_y(j) = Y(a(j),k); % The y value of the ellipse

            if j > 1
```

```
                %% Cálculo da área usando trapézios

                G_Var_y(j-1) = abs(G_y(j)-G_y(j-1)); % 'Altura'
                % (('Base menor' + 'Base maior')/2) * 'altura'
                Area(j-1) = ( (G_Var_x(j) + G_Var_x(j-1)) / 2 ) * (G_Var_y(j-1));
            end
            j = j + 1;
        end
    end
    Check = 0;
    Soma_A = sum(Area);
    vol = vol + Soma_A*lvl;
end

%Plot PDF contour for P=95%
hold on
plot1 = ezcontour(gmPDF,[-5 12],[-8 6]);
plot1.LevelList = [lvl];
title('Simulated Data and Contour lines of pdf');
set(plot1,'LineWidth', 2)

%plot the datum circles and line
%
hold on
%values from excel
x_r = -0.037013861;
y_r = -1.014461401;
x_l = 1.632105967;
y_l = -0.567222091;
rad_r = 0.126892053;
rad_l = 0.215982884;
rad = 1.035437468;
%discover the center coordinates
m = (y_l-y_r)/(x_l-x_r);
b = y_r-x_r*m;
x3 = 1/(2*(m^2+1))*((2*x_r-2*b*m+2*y_r*m)+sqrt((-2*x_r+2*b*m-2*y_r*m)^2-
4*(m^2+1)*(x_r^2+b^2-2*b*y_r+y_r^2-rad_r^2)));
y3 = m*x3+b;
x4 = 1/(2*(m^2+1))*((2*x_r-2*b*m+2*y_r*m)-sqrt((-2*x_r+2*b*m-2*y_r*m)^2-
4*(m^2+1)*(x_r^2+b^2-2*b*y_r+y_r^2-rad_r^2)));
y4 = m*x4+b;
d3 = sqrt((x3-x_l)^2+(y3-y_l)^2);
d4 = sqrt((x4-x_l)^2+(y4-y_l)^2);
x5 = 1/(2*(m^2+1))*((2*x_l-2*b*m+2*y_l*m)+sqrt((-2*x_l+2*b*m-2*y_l*m)^2-
4*(m^2+1)*(x_l^2+b^2-2*b*y_l+y_l^2-rad_l^2)));
y5 = m*x5+b;
x6 = 1/(2*(m^2+1))*((2*x_l-2*b*m+2*y_l*m)-sqrt((-2*x_l+2*b*m-2*y_l*m)^2-
4*(m^2+1)*(x_l^2+b^2-2*b*y_l+y_l^2-rad_l^2)));
y6 = m*x6+b;
d5 = sqrt((x5-x_r)^2+(y5-y_r)^2);
d6 = sqrt((x6-x_r)^2+(y6-y_r)^2);
if (d3>d4) && (d5>d6)
    center_x = (x3+x5)/2;
    center_y = (y3+y5)/2;
elseif (d4>d3) && (d5>d6)
    center_x = (x4+x5)/2;
    center_y = (y4+y5)/2;
elseif (d3>d4) && (d6>d5)
    center_x = (x3+x6)/2;
    center_y = (y3+y6)/2;
elseif (d4>d3) && (d6>d5)
    center_x = (x4+x6)/2;
    center_y = (y4+y6)/2;
end
theta = 0 : 0.01 : 2*pi;
circle_x = rad * cos(theta) + center_x;
circle_y = rad * sin(theta) + center_y;
circler_x = rad_r * cos(theta) + x_r;
```

```
circler_y = rad_r * sin(theta) + y_r;
circlel_x = rad_l * cos(theta) + x_l;
circlel_y = rad_l * sin(theta) + y_l;
% Plot crosses at circle the centers
plot(0, 0, 'k+', 'MarkerSize', 15, 'LineWidth', 2);
plot(center_x, center_y, 'r+', 'MarkerSize', 15, 'LineWidth', 2);
plot(x_r, y_r, 'g+', 'MarkerSize', 15, 'LineWidth', 2);
plot(x_l, y_l, 'g+', 'MarkerSize', 15, 'LineWidth', 2);
hold on;
% Plot circles around the centers
plot(circle_x, circle_y, 'r-', 'LineWidth', 2);
plot(circler_x, circler_y, 'g-', 'LineWidth', 2);
plot(circlel_x, circlel_y, 'g-', 'LineWidth', 2);
legend('positions','P=95%','t_i','datum','t_f R','t_f L','datum circle','right
circle','left circle','Location','southeast');
xlabel('x [NM]')
ylabel('y [NM]')

%plot the PDF of GMM in 3D
figure4 = figure('Color',[1 1 1]);
hold off
plot2 = ezsurf(gmPDF,[-10 10],[-10 10]);
view(45,45)
zlabel('PDF')
xlabel('x [NM]')
ylabel('y [NM]')

%show the ellipse area value
fprintf('\n\nEllipse Area = %.3f [NM^2]\n',Soma_A);

%show the red circle area value
emp_area = rad^2 * pi;
fprintf('Empirical Area = %.3f [NM^2]\n',emp_area);
```

Annex I – *Matlab* script for result analysis in *.m* format for comparison between scenarios

```
clc
clear all;
close all;

fileID_2 = fopen('S2.txt');

%read headers
A_text = textscan(fileID_2,'%s %s',1);

%read numbers
A_data = textscan(fileID_2,'%f %f',1000);
A = cell2mat(A_data);

%fit a 1 curve Gaussian Mixture Model (GMM)
options_2 = statset('Display','final');
gm_2 = fitgmdist(A,1,'Options',options_2);

%Probability Density Function (PDF) of the GMM
gmPDF_2 = @(x,y)pdf(gm_2,[x y]);

%pdf matrix (X,Y,Z)
[X,Y] = ndgrid(-50:0.5:50,-50:0.5:50);
Z_2 = arrayfun (@(x,y)pdf(gm_2,[x y]),X,Y);

%pdf matrix (X,Y,Z-lvl)
lvl_2 = 0;
Z2_2 = Z_2-lvl_2;
Z2_2(Z2_2<0)=0;

% calculate lvl for vol=0.95
```

```
x = -50:0.5:50;
y = x;
vol = trapz(y,trapz(x,Z2_2,2),1);
while vol > 0.95
    lvl_2 = lvl_2+0.00001;
    Z2_2 = Z_2-lvl_2;
    Z2_2(Z2_2<0)=0;
    x = -50:0.5:50;
    y = x;
    vol = trapz(y,trapz(x,Z2_2,2),1);

    %% Volume Correction
    Check = 0; % Variable created to ease the determination of the left extremity
of the ellipse
    j = 1; % Index variable for the calculation of the area
    clear var a b G_x_Small G_x_Big G_Var_x G_y G_Var_y Area Soma_A
    for k = 1 : 1 : length(Z2_2(:,1)) % Cycle along all the Z2 lines
        %The area of the ellipse only needs to be calculated for the values
        % of Z2 that are nonzero.
        % This line of code determines if a column has any non-zero value
        Dif_Zero = find((Z2_2(:,k) ~= 0) == 1);

        % If there are non-zero values than we need to determine the column
        % where that occurs
        if ~isempty(Dif_Zero)
            if Check == 0
                Col = k; % First column were the values are non-zero
                Check = 1; % So that the cycle doesnt keep changing the value of
Col, this variable was created
            end


            a(j) = min(Dif_Zero); % As shown in the Excel, this variable determines
the line of the upper perimeter of the ellise
            b(j) = max(Dif_Zero); % As shown in the Excel, this variable determines
the line of the the lower perimeter of the ellise

            G_x_Small(j) = X(a(j),k); % The value of the upper perimeter of the
ellipse
            G_x_Big(j) = X(b(j),k); % The value of the lower perimeter of the
ellipse

            G_Var_x(j) = G_x_Big(j) - G_x_Small(j); % Width of the ellipse

            G_y(j) = Y(a(j),k); % The y value of the ellipse

            if j > 1
                %% Cálculo da área usando trapézios

                G_Var_y(j-1) = abs(G_y(j)-G_y(j-1)); % 'Altura'
                % (('Base menor' + 'Base maior')/2) * 'altura'
                Area(j-1) = ( (G_Var_x(j) + G_Var_x(j-1)) / 2 ) * (G_Var_y(j-1));
            end
            j = j + 1;
        end
    end
    Check = 0;
    Soma_A_2 = sum(Area);
    vol = vol + Soma_A_2*lvl_2;
end

%%%%%%%%%%%%%%%%%%%%%%%%%%%%%%%%%%%%%%%%%%%%%%%%%%%%%%%%%%%%%%%%%%%%%%%

fileID_3 = fopen('S3.txt');

%read headers
B_text = textscan(fileID_3,'%s %s',1);
```

```
%read numbers
B_data = textscan(fileID_3,'%f %f',1000);
B = cell2mat(B_data);

%fit a 1 curve Gaussian Mixture Model (GMM)
options_3 = statset('Display','final');
gm_3 = fitgmdist(B,1,'Options',options_3);

%Probability Density Function (PDF) of the GMM
gmPDF_3 = @(x,y)pdf(gm_3,[x y]);

%pdf matrix (X,Y,Z)
Z_3 = arrayfun (@(x,y)pdf(gm_3,[x y]),X,Y);

%pdf matrix (X,Y,Z-lvl)
lvl_3 = 0;
Z2_3 = Z_3-lvl_3;
Z2_3(Z2_3<0)=0;

% calculate lvl for vol=0.95
x = -50:0.5:50;
y = x;
vol = trapz(y,trapz(x,Z2_3,2),1);
while vol > 0.95
    lvl_3 = lvl_3+0.00001;
    Z2_3 = Z_3-lvl_3;
    Z2_3(Z2_3<0)=0;
    x = -50:0.5:50;
    y = x;
    vol = trapz(y,trapz(x,Z2_3,2),1);

    %% Volume Correction
    Check = 0; % Variable created to ease the determination of the left extremity
of the ellipse
    j = 1; % Index variable for the calculation of the area
    clear var a b G_x_Small G_x_Big G_Var_x G_y G_Var_y Area Soma_A
    for k = 1 : 1 : length(Z2_3(:,1)) % Cycle along all the Z2 lines
        %The area of the ellipse only needs to be calculated for the values
        % of Z2 that are nonzero.
        % This line of code determines if a column has any non-zero value
        Dif_Zero = find((Z2_3(:,k) ~= 0) == 1);

        % If there are non-zero values than we need to determine the column
        % where that occurs
        if ~isempty(Dif_Zero)
            if Check == 0
                Col = k; % First column were the values are non-zero
                Check = 1; % So that the cycle doesnt keep changing the value of
Col, this variable was created
            end


            a(j) = min(Dif_Zero); % As shown in the Excel, this variable determines
the line of the upper perimeter of the ellise
            b(j) = max(Dif_Zero); % As shown in the Excel, this variable determines
the line of the the lower perimeter of the ellise

            G_x_Small(j) = X(a(j),k); % The value of the upper perimeter of the
ellipse
            G_x_Big(j) = X(b(j),k); % The value of the lower perimeter of the
ellipse

            G_Var_x(j) = G_x_Big(j) - G_x_Small(j); % Width of the ellipse

            G_y(j) = Y(a(j),k); % The y value of the ellipse

            if j > 1
                %% Cálculo da área usando trapézios
```

```
                G_Var_y(j-1) = abs(G_y(j)-G_y(j-1)); % 'Altura'
                % (('Base menor' + 'Base maior')/2) * 'altura'
                Area(j-1) = ( (G_Var_x(j) + G_Var_x(j-1)) / 2 ) * (G_Var_y(j-1));
            end
            j = j + 1;
        end
    end
    Check = 0;
    Soma_A_3 = sum(Area);
    vol = vol + Soma_A_3*lvl_3;
end

%%%%%%%%%%%%%%%%%%%%%%%%%%%%%%%%%%%%%%%%%%%%%%%%%%%%%%%%%%%%%%%%

fileID_4 = fopen('S4.txt');

%read headers
C_text = textscan(fileID_4,'%s %s',1);

%read numbers
C_data = textscan(fileID_4,'%f %f',1000);
C = cell2mat(C_data);

%fit a 1 curve Gaussian Mixture Model (GMM)
options_4 = statset('Display','final');
gm_4 = fitgmdist(C,1,'Options',options_4);

%Probability Density Function (PDF) of the GMM
gmPDF_4 = @(x,y)pdf(gm_4,[x y]);

%pdf matrix (X,Y,Z)
Z_4 = arrayfun (@(x,y)pdf(gm_4,[x y]),X,Y);

%pdf matrix (X,Y,Z-lvl)
lvl_4 = 0;
Z2_4 = Z_4-lvl_4;
Z2_4(Z2_4<0)=0;

% calculate lvl for vol=0.95
x = -50:0.5:50;
y = x;
vol = trapz(y,trapz(x,Z2_4,2),1);
while vol > 0.95
    lvl_4 = lvl_4+0.00001;
    Z2_4 = Z_4-lvl_4;
    Z2_4(Z2_4<0)=0;
    x = -50:0.5:50;
    y = x;
    vol = trapz(y,trapz(x,Z2_4,2),1);

    %% Volume Correction
    Check = 0; % Variable created to ease the determination of the left extremity
of the ellipse
    j = 1; % Index variable for the calculation of the area
    clear var a b G_x_Small G_x_Big G_Var_x G_y G_Var_y Area Soma_A
    for k = 1 : 1 : length(Z2_4(:,1)) % Cycle along all the Z2 lines
        %The area of the ellipse only needs to be calculated for the values
        % of Z2 that are nonzero.
        % This line of code determines if a column has any non-zero value
        Dif_Zero = find((Z2_4(:,k) ~= 0) == 1);

        % If there are non-zero values than we need to determine the column
        % where that occurs
        if ~isempty(Dif_Zero)
            if Check == 0
                Col = k; % First column were the values are non-zero
```

```
                Check = 1; % So that the cycle doesnt keep changing the value of
Col, this variable was created
            end


            a(j) = min(Dif_Zero); % As shown in the Excel, this variable determines
the line of the upper perimeter of the ellise
            b(j) = max(Dif_Zero); % As shown in the Excel, this variable determines
the line of the the lower perimeter of the ellise

            G_x_Small(j) = X(a(j),k); % The value of the upper perimeter of the
ellipse
            G_x_Big(j) = X(b(j),k); % The value of the lower perimeter of the
ellipse

            G_Var_x(j) = G_x_Big(j) - G_x_Small(j); % Width of the ellipse

            G_y(j) = Y(a(j),k); % The y value of the ellipse

            if j > 1
                %% Cálculo da área usando trapézios

                G_Var_y(j-1) = abs(G_y(j)-G_y(j-1)); % 'Altura'
                % (('Base menor' + 'Base maior')/2) * 'altura'
                Area(j-1) = ( (G_Var_x(j) + G_Var_x(j-1)) / 2 ) * (G_Var_y(j-1));
            end
            j = j + 1;
        end
    end
    Check = 0;
    Soma_A_4 = sum(Area);
    vol = vol + Soma_A_4*lvl_4;
end

%%%%%%%%%%%%%%%%%%%%%%%%%%%%%%%%%%%%%%%%%%%%%%%%%%%%%%%%%%%%%%%%%%%%%%%%

%Plot PDF contours for P=95%
figure1 = figure('Color',[1 1 1]);

axes1 = axes('Position',[0.13 0.285472972972973 0.775 0.639527027027027]);
hold(axes1,'on');

plot2 = ezcontour(gmPDF_2,[-40 40],[-20 40]);
set(plot2,'LineColor',[0 0.450980392156863 0.741176470588235]);
plot2.LevelList = [lvl_2];
set(plot2,'LineWidth', 2);

plot3 = ezcontour(gmPDF_3,[-10 20],[-10 20]);
set(plot3,'LineColor',[0.470588235294118 0.670588235294118 0.188235294117647]);
plot3.LevelList = [lvl_3];
set(plot3,'LineWidth', 2);

plot4 = ezcontour(gmPDF_4,[-10 20],[-10 20]);
set(plot4,'LineColor',[1 0 0]);
plot4.LevelList = [lvl_4];
set(plot4,'LineWidth', 2);

legend('Scenario 2','Scenario 3','Scenario 4','Location','Southeast');
xlabel('x [NM]');
ylabel('y [NM]');
title('{pdf}({gm}_{2},[{x},{y}])');
xlim(axes1,[-40 40]);
ylim(axes1,[-20 40]);
box(axes1,'on');
set(axes1,'BoxStyle','full','CLim',[0.00013 0.00143],'Colormap',...
    [1 0 0;1 1 1;0 0 1;0 0 0;1 0 0;1 1 1;0 0 1;0 0 0;1 0 0;1 1 1;0 0 1;0 0 0;1 0
0;1 1 1;0 0 1;0 0 0;1 0 0;1 1 1;0 0 1;0 0 0;1 0 0;1 1 1;0 0 1;0 0 0;1 0 0;1 1 1;0 0
1;0 0 0;1 0 0;1 1 1;0 0 1;0 0 0;1 0 0;1 1 1;0 0 1;0 0 0;1 0 0;1 1 1;0 0 1;0 0 0;1 0
```

```
0;1 1 1;0 0 1;0 0 0;1 0 0;1 1 1;0 0 1;0 0 0;1 0 0;1 1 1;0 0 1;0 0 0;1 0 0;1 1 1;0 0
1;0 0 0;1 0 0;1 1 1;0 0 1;0 0 0;1 0 0;1 1 1;0 0 1;0 0 0],...
    'Layer','top','XColor',[0 0 0],'YColor',[0 0 0],'ZColor',[0 0 0]);

%show the ellipses area values
fprintf('\n\nScenario 2 - Ellipse Area = %.3f [NM^2]\n',Soma_A_2);
fprintf('Scenario 3 - Ellipse Area = %.3f [NM^2]\n',Soma_A_3);
fprintf('Scenario 4 - Ellipse Area = %.3f [NM^2]\n',Soma_A_4);
```